Journal of Computational Physics 340 (2017) 200–242

Contents lists available at ScienceDirect

Journal of Computational Physics

www.elsevier.com/locate/jcp

# An entropy stable nodal discontinuous Galerkin method for the two dimensional shallow water equations on unstructured curvilinear meshes with discontinuous bathymetry

Niklas Wintermeyer [a], Andrew R. Winters [a,*], Gregor J. Gassner [a], David A. Kopriva [b]

[a] Mathematisches Institut, Universität zu Köln, Weyertal 86-90, 50931 Köln, Germany
[b] Department of Mathematics, The Florida State University, Tallahassee, FL 32306, USA

ARTICLE INFO

*Article history:*
Received 11 September 2015
Received in revised form 6 January 2017
Accepted 18 March 2017
Available online 22 March 2017

*Keywords:*
Shallow water equations
Discontinuous Galerkin spectral element method
Summation-by-parts
Entropy stability
Well-balanced
Discontinuous bathymetry

ABSTRACT

We design an arbitrary high-order accurate nodal discontinuous Galerkin spectral element approximation for the non-linear two dimensional shallow water equations with non-constant, possibly discontinuous, bathymetry on unstructured, possibly curved, quadrilateral meshes. The scheme is derived from an equivalent flux differencing formulation of the split form of the equations. We prove that this discretization exactly preserves the local mass and momentum. Furthermore, combined with a special numerical interface flux function, the method exactly preserves the mathematical entropy, which is the total energy for the shallow water equations. By adding a specific form of interface dissipation to the baseline entropy conserving scheme we create a provably entropy stable scheme. That is, the numerical scheme discretely satisfies the second law of thermodynamics. Finally, with a particular discretization of the bathymetry source term we prove that the numerical approximation is well-balanced. We provide numerical examples that verify the theoretical findings and furthermore provide an application of the scheme for a partial break of a curved dam test problem.

© 2017 Elsevier Inc. All rights reserved.

## 1. Introduction

Fluid flows in lakes, rivers, and near coastlines are of interest in oceanography and climate modeling. For such flows the vertical scales of motion are much smaller than the horizontal scales. From this and the assumption of hydrostatic balance [1], the Euler equations can be simplified to the shallow water equations. If the fluid flows over a non-constant bottom topography the shallow water equations may be written as a hyperbolic system of balance laws

$$\vec{w}_t + \vec{f}_x + \vec{g}_y = \vec{s}. \tag{1.1}$$

It is well-known that solutions of the balance laws (1.1) may develop discontinuities in finite time, independent of the smoothness of the initial data. Hence, we consider solutions of the balance laws (1.1) in a weak sense that are well-defined provided the source term $\vec{s}$ remains uniformly bounded, i.e., weak solutions of (1.1) are well-defined under the assumption that the function used to model the bottom topography is in the space $W^{1,\infty}(\mathbb{R})$, see e.g. [2].

* Corresponding author.
*E-mail address:* awinters@math.uni-koeln.de (A.R. Winters).

http://dx.doi.org/10.1016/j.jcp.2017.03.036
0021-9991/© 2017 Elsevier Inc. All rights reserved.

The design of numerical methods to approximate (1.1) is driven by the need for stable, accurate and robust behaviors. For instance, the preservation of steady state solutions is critical in problems with non-constant bottom topographies. Preserving steady solutions discretely is particularly troublesome for discontinuous bottom topographies where special discretization of the source term are required, e.g. [3,4]. One steady state constraint for the shallow water equations is the "lake at rest" condition [4–6], since the relevant waves in a flow can be viewed as small perturbations of the lake at rest, see [5]. A good numerical method for the shallow water equations should accurately capture both steady states and their small perturbations (quasi-steady flows) so as to diminish the appearance of unphysical waves with magnitude proportional to the mesh size (a so-called "numerical storm" [7]), that are normally present for numerical schemes that cannot preserve the "lake at rest" condition. A numerical method that exactly preserves the "lake at rest" steady state property is said to be *well-balanced*, see e.g. [3,5,6,8].

Another critical requirement of the numerics is the ability of the method to remain stable and accurate. Particularly the removal of aliasing errors that can drive non-linear instabilities, and maintenance of stability if discontinuities develop are key characteristics of a numerical scheme. Recent work has appeared on the use of high-order discontinuous Galerkin (DG) approximations to create numerical methods for the solution of systems of conservation laws that discretely satisfy the second law of thermodynamics, e.g., [8–10]. These high-order DG methods may be derived from the perspective of mathematical entropy conservation, e.g. [9,11,12], or reformulations of the PDE into a split formulation to maintain conservation, e.g. [8,10]. We note that the motivation behind these two approaches are similar [13].

The split form of an equation is found by averaging its conservative and non-conservative advective forms. This is problematic as it is not obvious that discretization of the split form remain conservative. However, conservation is critical for the numerical solution to model the correct shock speeds. Recent success has been had using diagonal norm summation-by-parts (SBP) operators to discretize the spatial derivatives in the split formulation of the equations [8,14–17]. Fisher et al. [14] show that split form operators derived from SBP derivative matrices are consistent and conservative in the Lax–Wendroff sense. There is now a known link between SBP finite difference operators and the discontinuous Galerkin spectral element approximation with Legendre–Gauss–Lobatto points, e.g. [15]. This link was used in [8] to derive an entropy conserving discontinuous Galerkin spectral element method (DGSEM) for the one dimensional shallow water equations. This paper exploits the links further and extends in a non-trivial way the previous work found in [8] to multiple dimensions and possibly discontinuous bottom topographies.

In this paper we present an entropy stable, high-order discontinuous Galerkin spectral element approximation for the shallow water equations with a discontinuous bottom topography for unstructured and curved quadrilateral grids. The DGSEM is naturally discontinuous at element boundaries, so we ensure high-order (spectral) accuracy by placing element boundaries at discontinuities in the bottom topography. The ability to do so allows one to model realistic bottom topographies appearing in oceanography. The scheme presented herein is also well-balanced, an attribute difficult to guarantee in curvilinear coordinates. We find that the numerical satisfaction of the metric identities [18] (referred to in [19] as the geometric conservation law) is critical to prove that the baseline scheme remains entropy conservative and well-balanced on arbitrary meshes.

Our approach is to use results of Fisher [19] and Fisher and Carpenter [20] to derive an entropy conserving approximation, and from that an entropy stable one, which is possible because it is possible to reformulate the spectral element approximation of the split form of the shallow water equations into an equivalent flux differencing structure. We use the flux differencing reformulation to prove the underlying properties of the entropy stable DGSEM, as well as to highlight how an existing DGSEM code can be altered to incorporate entropy stability.

The paper is organized as follows: in Sec. 2 we begin with a brief description of the continuous entropy analysis of the two dimensional shallow water equations. We outline the discontinuous Galerkin spectral element method with the summation-by-parts (SBP) property in Sec. 3. This section also introduces the important reformulation of the DGSEM into an equivalent flux differencing framework. We provide in Sec. 4.1 a discretization of the two dimensional shallow water equations using the flux differencing formulation that is conservative and entropy conservative on curvilinear meshes. We also provide a detailed proof that the approximation remains well-balanced. Then, in Sec. 4.2, additional dissipation is added to the scheme to ensure that the approximation remains valid for flow regimes that may contain discontinuities. Numerical results in Sec. 5 demonstrate and underline our theoretical findings. Our conclusions are presented in Sec. 6. Finally, Appendix D provides algorithms and implementation details of how a standard DGSEM code can be altered to incorporate the newly proposed entropy stable fluxes.

## 2. Shallow water equations

We begin with the balance law form of the two dimensional shallow water equations

$$\begin{aligned} h_t + (hu)_x + (hv)_y &= 0, \\ (hu)_t + (h\,u^2 + g\,h^2/2)_x + (huv)_y &= -g\,h\,b_x, \\ (hv)_t + (huv)_x + (h\,v^2 + g\,h^2/2)_y &= -g\,h\,b_y, \end{aligned} \tag{2.1}$$

which includes the continuity and momentum equations. The quantity $h = h(x, y, t)$ denotes the water height measured from the bottom topography $b = b(x, y)$ with the total height given by $H = h + b$. Additionally the constant $g$ is the gravi-

tational acceleration. The fluid velocities are given by $u = u(x, y, t)$ in the $x$-direction and $v = v(x, y, t)$ in the $y$-direction. The shallow water model (2.1) is compactly written as a system of balance laws (1.1) with $\vec{w} = (h, hu, hv)^T$, the fluxes

$$\vec{f} = (hu, h\,u^2 + g\,h^2/2, huv)^T, \quad \vec{g} = (hv, huv, h\,v^2 + g\,h^2/2)^T, \tag{2.2}$$

and the source term $\vec{s} = (0, -ghb_x, -ghb_y)^T$.

Because the system (2.1) is non-linear, we must define in what sense our numerical approximation will be stable. The extension of the usual $L^2$ stability for linear problems is the so-called *entropy stability* [12], where a (generalized, mathematical) entropy function rather than the $L^2$ norm of the solution is non-increasing in time. To this end we impose the entropy condition as an additional admissibility criterion on the system.

The mathematical entropy condition states that for smooth solutions the entropy of the system is conserved and for discontinuous solutions the entropy decays. Numerical approximations that satisfy the entropy condition discretely are referred to as *entropy stable*. The balance law (2.1) for the shallow water equations is equipped with a strongly convex mathematical entropy function $e = e(\vec{w})$ in the form of the total energy [3]

$$e := \frac{1}{2}h\left(u^2 + v^2\right) + \frac{1}{2}gh^2 + ghb. \tag{2.3}$$

To develop the conservation law for the entropy function $e(\vec{w})$ we define the set of entropy variables, $\vec{q} = (q_1, q_2, q_3)^T$, by

$$\begin{aligned} q_1 &:= \frac{\partial e}{\partial w_1} = g(h + b) - \frac{1}{2}u^2 - \frac{1}{2}v^2, \\ q_2 &:= \frac{\partial e}{\partial w_2} = u, \\ q_3 &:= \frac{\partial e}{\partial w_3} = v. \end{aligned} \tag{2.4}$$

To determine the entropy fluxes, $\mathcal{F}(\vec{w})$ and $\mathcal{G}(\vec{w})$, we use two compatibility relations that must hold between them, the entropy variables and the physical fluxes [12]

$$\mathcal{F}_{\vec{w}} = \vec{q}^{\,T}\vec{f}_{\vec{w}}, \quad \mathcal{G}_{\vec{w}} = \vec{q}^{\,T}\vec{g}_{\vec{w}}. \tag{2.5}$$

We pre-multiply the balance law (1.1) with the entropy variables (2.4) and apply the conditions (2.5) to find the conservation law for the entropy function

$$e_t + \mathcal{F}_x + \mathcal{G}_y = 0. \tag{2.6}$$

Explicitly, the entropy fluxes of the shallow water equations are

$$\begin{aligned} \mathcal{F} &:= \frac{1}{2}(hu^3 + huv^2) + g(hu(h + b)), \\ \mathcal{G} &:= \frac{1}{2}(hv^3 + hu^2v) + g(hv(h + b)). \end{aligned} \tag{2.7}$$

In the presence of discontinuities the entropy conservation law (2.6) becomes the entropy inequality

$$e_t + \mathcal{F}_x + \mathcal{G}_y \leq 0. \tag{2.8}$$

Thus, we define an entropy conserving approximation of the non-linear shallow water equations, (2.1), to be one that discretely satisfies (2.6). Furthermore, a method that satisfies (2.8) is entropy stable [12].

Finally, we note that systems of balance laws have important steady state configurations where the flux and source terms are in balance. For the shallow water equations, one such steady state solution is the "lake at rest" condition defined by

$$\begin{aligned} h + b &= \text{const}, \\ u = v &= 0. \end{aligned} \tag{2.9}$$

A numerical method that preserves the "lake at rest" state is said to be well-balanced. If a method is not well-balanced spurious waves on the order of the mesh size truncation error can be generated and pollute the approximation.

## 3. Nodal discontinuous Galerkin spectral element method

The entropy stable method that we propose is a form of nodal Discontinuous Galerkin Spectral Element Method (DGSEM). In this section, we introduce the basic construction of the DGSEM on curvilinear quadrilateral grids. A more complete

discussion can be found in [18]. Also in this section, we provide details about the relationship of DG methods to summation-by-parts (SBP) operators, which allows us to write the approximation as an equivalent sub-cell flux differencing formulation (FDF) [20]. The FDF is useful for theoretical purposes, particularly the proof of local conservation and satisfaction of the Lax–Wendroff theorem, to demonstrate that the split form DGSEM has local and global conservation. Also, special choices of the flux functions in the FDF generate a DG discretization of a split form of the original PDE. Additionally, if the underlying flux functions in the FDF are two-point entropy conserving fluxes then the FDF remains high-order and entropy conservative [20]. Because of the equivalence between the FDF and the DGSEM with the SBP property this automatically generates an entropy conservative DGSEM.

### 3.1. Conservation law in curvilinear coordinates

The DGSEM approximates the system of conservation laws (1.1) defined on a domain $\Omega$ on an unstructured mesh of quadrilateral elements. To simplify the discussion, we work with the components of the system (2.1) written as

$$(w_k)_t + (f_k(\vec{w}))_x + (g_k(\vec{w}))_y = s_k(w), \quad k = 1, 2, 3, \tag{3.1}$$

where $w_1 = h$, $w_2 = hu$ and $w_3 = hv$.

We decompose $\Omega$ into non-overlapping quadrilateral elements $G$ and map each element to the computational reference element $E = [-1, 1]^2$. A commonly used transformation between the reference square and an arbitrary curve-sided quadrilateral element is transfinite interpolation with linear blending [18]. The mapping between the coordinates of the reference square $(\xi, \eta)$ and the physical coordinates $\vec{x} = (x, y)$ is

$$\begin{aligned}\vec{x}(\xi,\eta) = &\frac{1}{2}\big[(1-\xi)\vec{\Gamma}_4(\eta) + (1+\xi)\vec{\Gamma}_2(\eta) + (1-\eta)\vec{\Gamma}_1(\xi) + (1+\eta)\vec{\Gamma}_3(\xi)\big] \\ &- \frac{1}{4}\big[(1-\xi)\{(1-\eta)\vec{\Gamma}_1(-1) + (1+\eta)\vec{\Gamma}_3(-1)\} + (1+\xi)\{(1-\eta)\vec{\Gamma}_1(1) + (1+\eta)\vec{\Gamma}_3(1)\}\big],\end{aligned} \tag{3.2}$$

where we assume that each convex element is bounded by four curves $\vec{\Gamma}_j$, $j = 1, 2, 3, 4$.

Under the transformation the conservation law on $\Omega$ remains a conservation law on $E$. We transform the two dimensional balance law (3.1) from physical space to the reference space by rewriting derivatives using the chain rules

$$\begin{aligned}\frac{\partial w}{\partial x} &= \frac{\partial w}{\partial \xi}\frac{\partial \xi}{\partial x} + \frac{\partial w}{\partial \eta}\frac{\partial \eta}{\partial x}, \\ \frac{\partial w}{\partial y} &= \frac{\partial w}{\partial \xi}\frac{\partial \xi}{\partial y} + \frac{\partial w}{\partial \eta}\frac{\partial \eta}{\partial y},\end{aligned} \tag{3.3}$$

for some $w(x, y)$. Applying the chain rule (3.3) to (3.1) gives us the transformed conservation law in reference space

$$\mathcal{J}(w_k)_t + (\tilde{f}_k)_\xi + (\tilde{g}_k)_\eta = 0, \tag{3.4}$$

where the element mapping (3.2) is used to compute the Jacobian, $\mathcal{J}$, and the contravariant flux components $\tilde{f}_k$, $\tilde{g}_k$, $k = 1, 2, 3$ according to

$$\begin{aligned}\mathcal{J} &= x_\xi\, y_\eta - x_\eta\, y_\xi, \\ \tilde{f}_k(\vec{w}) &= y_\eta\, f_k(\vec{w}) - x_\eta\, g_k(\vec{w}), \\ \tilde{g}_k(\vec{w}) &= -y_\xi\, f_k(\vec{w}) + x_\xi\, g_k(\vec{w}),\end{aligned} \tag{3.5}$$

for $k = 1, 2, 3$.

### 3.2. Polynomial approximation on the reference element

The DGSEM is constructed by approximating the variables $w_k$ and contravariant fluxes $\tilde{f}_k$, $\tilde{g}_k$ in the reference space by polynomials of degree $N$ in each direction. We use a nodal form of the interpolation with nodes defined at the Legendre–Gauss–Lobatto (LGL) points $\{\xi_i\}_{i=0}^N$ and $\{\eta_j\}_{j=0}^N$ in the reference square $E = [-1, 1]^2$. The Lagrange basis functions for the interpolant are

$$\ell_j(\xi) = \prod_{i=0, i\neq j}^{N} \frac{\xi - \xi_i}{\xi_j - \xi_i}, \qquad j = 0, \ldots, N, \tag{3.6}$$

and satisfy the cardinal property

$$\ell_j(\xi_i) = \delta_{ij}, \qquad i, j = 0, \ldots, N, \tag{3.7}$$

where $\delta_{ij}$ denotes Kronecker's symbol with $\delta_{ij} = 1$ for $i = j$ and $\delta_{ij} = 0$ for $i \neq j$. We write the element-wise polynomial approximation (e.g. for the components of $\vec{w}$) as

$$w_k(x, y, t)\big|_G = w_k(x(\xi, \eta), y(\xi, \eta), t) \approx W_k(\xi, \eta, t) := \sum_{i=0}^{N} \sum_{j=0}^{N} W_k^{i,j}(t)\, \ell_i(\xi)\, \ell_j(\eta), \quad k = 1, 2, 3, \tag{3.8}$$

where $\{W_k^{i,j}(t)\}_{i=0,\, j=0}^{N,N}$ are the time dependent nodal degrees of freedom. The nodal polynomial (3.8) is equivalent to an orthogonal Legendre polynomial expansion used in a modal spectral method, but is more convenient to use in the approximation of non-linear equations like the shallow water equations.

We use the idea of collocation throughout this work to approximate quantities derived from the $W_k$. For instance the velocity $u$ is approximated by a polynomial of degree $N$ in each direction (3.8) as well, where its nodal values are computed as

$$U^{i,j} := \frac{W_2^{i,j}}{W_1^{i,j}}, \quad i, j = 0, \ldots, N. \tag{3.9}$$

This collocation strategy also applies to the contravariant fluxes, where we interpolate the metric terms at the same nodes. For instance

$$\tilde{F}_k^{i,j} = y_\eta(\xi_i, \eta_j)\, F_k(\vec{W}^{i,j}) - x_\eta(\xi_i, \eta_j)\, G_k(\vec{W}^{i,j}), \qquad i, j = 0, \ldots, N, \quad k = 1, 2, 3, \tag{3.10}$$

where $F_k$ and $G_k$ are the polynomial approximations to the three flux components $f_k$ and $g_k$ defined in (2.2). Similarly, the Jacobian of the transformation is approximated by the polynomial of degree $N$ with nodal values $J^{i,j} = \mathcal{J}(\xi_i, \eta_j)$.

For spectral approximations, the derivative is approximated elementwise directly from the derivative of the polynomial approximation, e.g.,

$$\frac{\partial}{\partial \xi} W_k(\xi, \eta, t) = \sum_{i=0}^{N} \sum_{j=0}^{N} W_k^{i,j}(t)\, \frac{\partial}{\partial \xi} \ell_i(\xi)\, \ell_j(\eta), \tag{3.11}$$

where $k = 1, 2, 3$. We introduce the polynomial derivative matrix $\mathbf{D}$ with entries

$$D_{ij} := \left. \frac{\partial \ell_j}{\partial \xi} \right|_{\xi = \xi_i}, \qquad i, j = 0, \ldots, N, \tag{3.12}$$

which is used to calculate the discrete derivative with respect to $\xi$. Since we use the same polynomial ansatz in the $\xi$ and $\eta$ directions, the derivative operator is identical in each spatial direction.

We can reuse the 1D operator (3.12) for the 2D scheme if we store the individual slices of the approximate solution in a 2D array. Entries in one column refer to the nodal values at constant $\eta$, entries in one row refer to a constant $\xi$

$$\mathbf{W}_k := \begin{pmatrix} (W_k)^{\xi=-1,\eta=-1} & \cdots & (W_k)^{\xi=-1,\eta=+1} \\ \textit{sub-cell:} & \ddots & \vdots \\ (W_k)^{\xi=+1,\eta=-1} & \cdots & (W_k)^{\xi=+1,\eta=+1} \end{pmatrix} = \begin{pmatrix} W_k^{0,0} & \cdots & W_k^{0,N} \\ \vdots & \ddots & \vdots \\ W_k^{N,0} & \cdots & W_k^{N,N} \end{pmatrix}. \tag{3.13}$$

By storing the nodal values of variables, fluxes and metric terms in 2D arrays, we can multiply the 1D derivative operator $\mathbf{D}$ from the left to represent taking the $\xi$ derivative at each constant $\eta$. If we multiply with $\mathbf{D}^T$ from the right, we obtain the $\eta$ derivative. This notation allows us to write the scheme in a compact matrix–vector notation while using unmodified 1D derivative operators.

With the notation (3.13), the nodal values of the derivative of a nodal approximation $w$ are given by

$$(\mathbf{W}_k)_\xi = \mathbf{D}\, \mathbf{W}_k \qquad \text{and} \qquad (\mathbf{W}_k)_\eta = \mathbf{W}_k\, \mathbf{D}^T, \tag{3.14}$$

or in index notation

$$(W_k^{i,j})_\xi = \sum_{l=0}^{N} D_{il}\, W_k^{l,j} \qquad \text{and} \qquad (W_k^{i,j})_\eta = \sum_{l=0}^{N} D_{li} W_k^{j,l}, \tag{3.15}$$

where $i, j = 0, \ldots, N$.

We demand that the discretization preserves free-stream solutions, i.e., constant solutions of the balance law (3.4) should remain constant for all times. A necessary and sufficient condition for constant state preservation is that the metric identities

$$\frac{\partial}{\partial \xi}\mathcal{J}\vec{a}^1 + \frac{\partial}{\partial \eta}\mathcal{J}\vec{a}^2 = \vec{0}, \tag{3.16}$$

are satisfied, where the volume weighted contravariant basis vectors, $\mathcal{J}\vec{a}^i$, $i = 1, 2$ are

$$\mathcal{J}\vec{a}^1 = \left(y_\eta, -x_\eta\right)^T, \quad \mathcal{J}\vec{a}^2 = \left(-y_\xi, x_\xi\right)^T. \tag{3.17}$$

The metric identities are not automatically satisfied for the discretization, which, using the array notation (3.13) for the nodal values of the metric terms and (3.14) for the derivative are

$$\begin{aligned} \mathbf{D}\mathbf{y}_\eta - \mathbf{y}_\xi \mathbf{D}^T &= \mathbf{0}, \\ -\mathbf{D}\mathbf{x}_\eta + \mathbf{x}_\xi \mathbf{D}^T &= \mathbf{0}. \end{aligned} \tag{3.18}$$

Kopriva [21] proved that free-stream preservation is guaranteed for the DGSEM when the linear blending formula (3.2) is used and boundaries of the quadrilateral elements are approximated by polynomials with an order equal to (or lower than) the polynomial order of the approximate solution. Thus, we use an isoparametric approximation in which each boundary curve $\vec{\Gamma}_j(\zeta)$, $\zeta \in [-1, 1]$ of an element $G$ is approximated by a polynomial of order $N$. We use the same Lagrange basis functions (3.6) to approximate the boundary curves

$$\vec{\Gamma} = \sum_{j=0}^{N} \vec{\Gamma}(\zeta_j)\ell_j(\zeta), \tag{3.19}$$

where due to their robust interpolation properties [18], the nodes $\{\zeta_j\}_{j=0}^N$ are typically chosen to be the Chebyshev–Gauss–Lobatto or Legendre–Gauss–Lobatto nodes. The polynomial boundary curve approximations (3.19) are used to construct the mapping (3.2) for each element. As the mapping is a polynomial in $\xi$ and $\eta$, the derivatives necessary to obtain the metric terms and the normal vectors are computed directly in the discrete derivative sense (3.14). Further details of the isoparametric polynomial approximation of boundary curves can be found in [18,21].

### 3.3. Discontinuous Galerkin spectral element method (DGSEM)

Following a standard approach we derive a nodal discontinuous Galerkin scheme, e.g. [18] or [22]. We will discuss the specific form of the approximation of the source term in Sec. 4. Omitting the source term, the nodal discontinuous Galerkin method in weak form of the transformed conservation law (3.4) reads

$$\int_{E,N} J\,(W_k)_t\,\varphi\,d\xi d\eta - \int_{E,N} \tilde{F}_k\varphi_\xi\,d\xi d\eta - \int_{E,N} \tilde{G}_k\varphi_\eta\,d\xi d\eta = -\oint_{\partial E,N} \left(\tilde{F}_k^*(\vec{W}^+, \vec{W}^-), \tilde{G}_k^*(\vec{W}^+, \vec{W}^-)\right)\cdot \hat{n}\,\varphi\,dS, \tag{3.20}$$

for $k = 1, 2, 3$ and in the equivalent strong form [23]

$$\int_{E,N} \left(J\,(W_k)_t + (\tilde{F}_k)_\xi + (\tilde{G}_k)_\eta\right)\varphi\,d\xi d\eta = -\oint_{\partial E,N} \left(\tilde{F}_k^*(\vec{W}^+, \vec{W}^-) - \tilde{F}_k, \tilde{G}_k^*(\vec{W}^+, \vec{W}^-) - \tilde{G}_k\right)\cdot \hat{n}\varphi\,dS, \tag{3.21}$$

for $k = 1, 2, 3$, where $\varphi$ is a polynomial of degree $N$ or less in each space direction. We also use the notation $\int_{E,N}$ to represent Legendre–Gauss–Lobatto Quadrature, which is the tensor product of quadrature in one spatial dimension

$$\int_{-1,N}^{1} f(\xi)\,d\xi \approx \sum_{j=0}^{N} f(\xi_j)\omega_j, \tag{3.22}$$

with $\{\omega_j\}_{j=0}^N$ being the LGL quadrature weights. The quadrature is exact if the integrand $f$ is a polynomial of degree $2N-1$ or less. The numerical fluxes $\tilde{F}_k^*$ and $\tilde{G}_k^*$, in the normal direction, couple neighboring elements. We indicate this coupling by the dependence on the "outer" and "inner" values $\vec{W}^+, \vec{W}^-$ along the normal vector $\hat{n}$. The boundary integrals in (3.20) and (3.21) describe the integration along the four edges of the element $E$.

The two forms (3.20) and (3.21) of the DGSEM are algebraically equivalent because the quadrature satisfies a *summation-by-parts* rule [23]. In one space dimension, and for any two polynomials $U(\xi)$ and $V(\xi)$, exactness of the quadrature implies that

$$\sum_{j=0}^{N} U_j V_j' \omega_j = \int_{-1}^{1} U V_\xi d\xi = UV|_{-1}^{1} - \int_{-1}^{1} U_\xi V d\xi = UV|_{-1}^{1} - \sum_{j=0}^{N} U_j' V_j \omega_j. \tag{3.23}$$

In other words,

$$\int_{-1,N}^{1} UV_\xi d\xi = UV|_{-1}^{1} - \int_{-1,N}^{1} U_\xi V d\xi. \tag{3.24}$$

The result extends to two and three space dimensions [23].

The formal statements of the DGSEM, (3.20) and (3.21) can be reduced to a pointwise form [18], which in turn can be represented in a matrix form where the nodal values are represented as arrays. To obtain equations for the nodal degrees of freedom, we take the test function to be the tensor product basis $\varphi = \ell_i(\xi)\ell_j(\eta)$. Then, for example,

$$\int_{E,N} J(W_k)_t \varphi d\xi d\eta = \sum_{n,m=0}^{N} \omega_n \omega_m J^{n,m} (W_k^{n,m})_t \ell_i(\xi_n)\, \ell_j(\eta_m) = \omega_i \omega_j J^{i,j} (W_k^{i,j})_t \quad i,j = 0,1,2,\ldots,N, \tag{3.25}$$

for $k = 1, 2, 3$.

We represent each component (3.25) in terms of the matrix-array notation introduced in (3.13) and (3.14) as

$$\mathbf{MJ} \circ (\mathbf{W}_k)_t\, \mathbf{M}, \tag{3.26}$$

where $\mathbf{M}$ is the diagonal matrix of the quadrature weights (the *mass matrix*),

$$\mathbf{M} := \mathrm{diag}(\omega_0, \ldots, \omega_N), \tag{3.27}$$

and we introduce the notation of a component-wise Hadamard product of two matrices with the same dimension

$$\mathbf{A} \circ \mathbf{B} = \mathbf{C}, \quad \text{with} \quad a_{ij}\, b_{ij} = c_{ij}, \quad i,j = 0,\ldots,N. \tag{3.28}$$

Similarly, the integral of the $k$-th component of the $\xi$ contravariant flux in strong form is

$$\int_{E,N} \left(\tilde{F}_k\right)_\xi \varphi d\xi d\eta = \sum_{n,m=0}^{N} \omega_n \omega_m \left(\sum_{l=0}^{N} \tilde{F}_k^{l,m} D_{nl}\right) \ell_i(\xi_n)\, \ell_j(\eta_m) = \omega_i \omega_j \left(\sum_{l=0}^{N} \tilde{F}_k^{l,j} D_{il}\right), \tag{3.29}$$

so we see that

$$\int_{E,N} (\tilde{F}_k)_\xi \varphi d\xi d\eta \to \mathbf{MD}\tilde{\mathbf{F}}_k\mathbf{M}. \tag{3.30}$$

On the other hand, for the weak formulation,

$$\int_{E,N} \tilde{F}_k \varphi_\xi d\xi d\eta = \sum_{n,m=0}^{N} \omega_n \omega_m \tilde{F}_k^{n,m} \ell_i'(\xi_n)\, \ell_j(\eta_m) = \left(\sum_{n=0}^{N} \omega_n \omega_j \tilde{F}_k^{n,j} D_{in}^T\right), \tag{3.31}$$

so

$$\int_{E,N} \tilde{F}_k \varphi_\xi d\xi d\eta \to \mathbf{D}^T\mathbf{M}\tilde{\mathbf{F}}_k\mathbf{M}, \tag{3.32}$$

with a similar result for the $\eta$ direction flux.

The boundary quadratures for the weak form, (3.20), are

$$\oint_{\partial E,N} \left(\tilde{F}_k^*, \tilde{G}_k^*\right) \cdot \hat{n} d\xi \varphi d\eta = \int_{-1,N}^{1} \tilde{F}_k^*(1,\eta)\varphi d\eta - \int_{-1,N}^{1} \tilde{F}_k^*(-1,\eta)\varphi d\eta + \int_{-1,N}^{1} \tilde{G}_k^*(\xi,1) d\xi - \int_{-1,N}^{1} \tilde{G}_k^*(\xi,-1)\varphi d\xi. \tag{3.33}$$

Each term reduces to pointwise values in a similar way. The first term, for instance, is

$$\int_{-1,N}^{1} \tilde{F}_k^*(1,\eta)\varphi d\eta = \int_{-1,N}^{1} \tilde{F}_k^*(1,\eta)\ell_i(1)\ell_j(\eta) d\eta = \omega_j \left(\tilde{F}_k^*\right)^{N,j}. \tag{3.34}$$

We represent the numerical fluxes $\tilde{\mathbf{F}}_k^*$ and $\tilde{\mathbf{G}}_k^*$ consistent to the 2D array notation (3.13) so that the only non-zero entries correspond to the respective interfaces, i.e.

$$\tilde{\mathbf{F}}_{\mathbf{k}}^{*} := \begin{pmatrix} (\tilde{F}_k^*)^{0,0} & \cdots & (\tilde{F}_k^*)^{0,N} \\ 0 & \cdots & 0 \\ \vdots & & \vdots \\ 0 & \cdots & 0 \\ (\tilde{F}_k^*)^{N,0} & \cdots & (\tilde{F}_k^*)^{N,N} \end{pmatrix}, \quad \tilde{\mathbf{G}}^{*} := \begin{pmatrix} (\tilde{G}_k^*)^{0,0} & 0 & \cdots & 0 & (\tilde{G}_k^*)^{0,N} \\ \vdots & \vdots & & \vdots & \vdots \\ (\tilde{G}_k^*)^{N,0} & 0 & \cdots & 0 & (\tilde{G}_k^*)^{N,N} \end{pmatrix}, \tag{3.35}$$

so that $\tilde{\mathbf{F}}_k^*$ only appears at $\xi = \pm 1$ and $\tilde{\mathbf{G}}_k^*$ appears at $\eta = \pm 1$ on the reference element $E$.

To write the approximations in a compact form, we define the matrix operators

$$\begin{aligned} \hat{\mathbf{D}} &:= -\mathbf{M}^{-1}\mathbf{D}^T\mathbf{M} && \text{(scaled derivative matrix)}, \\ \mathbf{S} &:= \operatorname{diag}\left(\frac{1}{\omega_0}, 0, \ldots, 0, -\frac{1}{\omega_N}\right) && \text{(surface matrix)}, \end{aligned} \tag{3.36}$$

with the derivative matrix $\mathbf{D}$ defined in (3.12). Then we rewrite the equations for the nodal degrees of freedom of the DGSEM approximations (3.20) and (3.21) in the algebraically equivalent forms

$$\mathbf{J} \circ (\mathbf{W}_k)_t + \hat{\mathbf{D}}\tilde{\mathbf{F}}_k + \tilde{\mathbf{G}}_k\hat{\mathbf{D}}^T = \mathbf{S}\tilde{\mathbf{F}}_k^* + \tilde{\mathbf{G}}_k^*\mathbf{S}, \tag{3.37}$$

and

$$\mathbf{J} \circ (\mathbf{W}_k)_t + \mathbf{D}\tilde{\mathbf{F}}_k + \tilde{\mathbf{G}}_k\mathbf{D}^T = \mathbf{S}\left(\tilde{\mathbf{F}}_k^* - \tilde{\mathbf{F}}_k\right) + \left(\tilde{\mathbf{G}}_k^* - \tilde{\mathbf{G}}_k\right)\mathbf{S}, \tag{3.38}$$

for $k = 1, 2, 3$. We note that to obtain the results (3.37) and (3.38) we multiplied by the inverse of $\mathbf{M}$ on the left and right.

### 3.4. An equivalent sub-cell flux differencing form

The most important property the DGSEM operators constructed with the LGL quadrature nodes have is that the derivative matrix $\mathbf{D}$ (3.12) is a summation-by-parts (SBP) operator for all polynomial orders, (3.24). This property can be represented in the form of SBP-SAT finite difference operators [15], and we collect relevant results here in Lemma 1.

**Lemma 1** *(SBP-properties). Let the matrix $\mathbf{Q} := \mathbf{MD}$, which represents the mass weighted derivative, as seen in (3.30). The matrix $\mathbf{Q}$ has the SBP-property*

$$\mathbf{Q} + \mathbf{Q}^T = \mathbf{B} := diag(-1, 0, \ldots, 0, 1).$$

*Furthermore, the SBP-property can be used to obtain alternative expressions for the derivative matrix*

$$\begin{aligned} \mathbf{D} &= \mathbf{M}^{-1}\mathbf{Q} = \mathbf{M}^{-1}(\mathbf{B} - \mathbf{Q}^T) = -\mathbf{S} - \mathbf{M}^{-1}\mathbf{Q}^T, \\ \mathbf{D}^T &= (\mathbf{M}^{-1}\mathbf{Q})^T = -\mathbf{S} - \mathbf{Q}\mathbf{M}^{-1}. \end{aligned} \tag{3.39}$$

*So, the derivative matrix $\hat{\mathbf{D}}$ of the weak DG formulation*

$$\hat{\mathbf{D}} = -\mathbf{M}^{-1}\mathbf{Q}^T, \tag{3.40}$$

*satisfies the relations*

$$\begin{aligned} \mathbf{D} &= -\mathbf{S} + \hat{\mathbf{D}}, \\ \mathbf{D}^T &= -\mathbf{S} + \hat{\mathbf{D}}^T. \end{aligned} \tag{3.41}$$

**Proof.** See, for example, [9,15,16,24,25]. □

**Remark 1.** Although the finite difference and spectral element approximations differ (e.g. the spectral element approximate solution is known everywhere, including in between the nodes), the fact that the nodal equations can be written in the same form allows us to use results proved for SBP finite difference methods as needed.

The LGL-based DGSEM operators listed in Lemma 1 are in the sub-class of SBP operators with diagonal norm matrix $\mathbf{M}$. For this class of diagonal norm SBP operators, Fisher and Carpenter [20] proved an astounding relationship: Such operators can always be re-written into an algebraically equivalent sub-cell finite volume type differencing formulation. As an example we rewrite the contravariant flux in the $x$-direction into a telescoping flux form (the contravariant flux in the $y$-direction has an analogous form):

$$\mathbf{D}\tilde{\mathbf{F}}_k = \mathbf{M}^{-1}\mathbf{Q}\tilde{\mathbf{F}}_k = \mathbf{M}^{-1}\mathbf{\Delta}\bar{\tilde{\mathbf{F}}}_k, \tag{3.42}$$

where $\mathbf{\Delta}$ is the $N \times N+1$ differencing matrix

$$\mathbf{\Delta} = \begin{pmatrix} -1 & 1 & 0 & 0 & 0 & 0 \\ 0 & -1 & 1 & 0 & 0 & 0 \\ 0 & 0 & \ddots & \ddots & 0 & 0 \\ 0 & 0 & 0 & -1 & 1 & 0 \\ 0 & 0 & 0 & 0 & -1 & 1 \end{pmatrix}. \tag{3.43}$$

The new flux functions, denoted with an overbar, can be viewed as sub-cell fluxes on a complementary staggered sub-cell grid [14,20].

We restate a slight extension of a Lemma from [9] that enables us to construct high-order entropy conservative fluxes for the flux-differencing DG formulation on curvilinear meshes.

**Lemma 2** *(High-order flux). A two-point high-order entropy conservative flux can be constructed by*

$$\begin{cases} \bar{\tilde{F}}_k^{0,j} = \tilde{F}_k^{0,j}, \\ \bar{\tilde{F}}_k^{i,j} = \sum_{m=i}^{N} \sum_{\ell=0}^{i-1} 2\, Q_{\ell m} \left( F_k^{vol}(\vec{W}^{\ell,j}, \vec{W}^{m,j}) \left\{\!\left\{ Ja_1^1 \right\}\!\right\}_{(\ell,m),j} + G_k^{vol}(\vec{W}^{\ell,j}, \vec{W}^{m,j}) \left\{\!\left\{ Ja_2^1 \right\}\!\right\}_{(\ell,m),j} \right), \quad i = 1, \dots, N, \\ \bar{\tilde{F}}_k^{N+1,j} = \tilde{F}_k^{N,j}, \end{cases} \tag{3.44}$$

*for $k = 1, 2, 3$, a fixed point $j$ in the $y$-direction and for some two point, symmetric flux functions $F_k^{vol}$ and $G_k^{vol}$, e.g.,*

$$F_k^{vol}(\vec{W}^{\ell,j}, \vec{W}^{m,j}) = F_k^{vol}(\vec{W}^{m,j}, \vec{W}^{\ell,j}), \tag{3.45}$$

*that satisfy the entropy conservation condition*

$$[\![\vec{q}]\!]^T (\vec{F}^{vol} + \vec{G}^{vol}) = [\![\phi]\!] + \{\{\vec{q}\}\}^T \vec{s}. \tag{3.46}$$

*The $\tilde{F}_k^{0,j}$ and $\tilde{F}_k^{N,j}$ are the typical contravariant fluxes and $\vec{s}$ is the source term vector. The metric terms $Ja_1^1$ and $Ja_2^1$ are given in (3.17), and the arithmetic mean is defined as*

$$\{\{\cdot\}\}_{(\ell,m),j} := \frac{1}{2} \left( (\cdot)^{\ell,j} + (\cdot)^{m,j} \right). \tag{3.47}$$

**Proof.** This Lemma from [9] is proven for the Cartesian case in [20], and extended to curvilinear meshes in [19, Section 4.5 and Appendix A.3]. The source term extension to the entropy conservation condition (3.46) can, for instance, be found in [3]. □

For computational efficiency we generalize a previous result of Fisher and Carpenter [20, Eq. (3.13)] and rewrite the flux differencing volume term on curvilinear meshes.

**Proposition 1** *(Flux differencing with metric terms). One can use the structure of the SBP matrix $\mathbf{Q}$ and the fluxes on the complimentary grid to eliminate one of the sums in (3.44) to write the flux difference in the x-direction, $\mathbf{M}^{-1}\mathbf{\Delta}\bar{\tilde{\mathbf{F}}}_k$, in the indicial form*

$$\begin{aligned} \left( \mathbf{M}^{-1}\mathbf{\Delta}\bar{\tilde{\mathbf{F}}}_k \right)^{i,j} &= \frac{\bar{\tilde{F}}_k^{i+1,j} - \bar{\tilde{F}}_k^{i,j}}{\omega_i} \\ &= \frac{1}{\omega_i} \sum_{m=0}^{N} 2\, Q_{im} \left( F_k^{vol}(\vec{W}^{i,j}, \vec{W}^{m,j}) \left\{\!\left\{ Ja_1^1 \right\}\!\right\}_{(i,m),j} + G_k^{vol}(\vec{W}^{i,j}, \vec{W}^{m,j}) \left\{\!\left\{ Ja_2^1 \right\}\!\right\}_{(i,m),j} \right), \end{aligned} \tag{3.48}$$

*for $i = 0, \dots, N$. The flux difference in the $y$-direction, $\bar{\tilde{\mathbf{G}}}_k \mathbf{\Delta}^T \mathbf{M}^{-1}$, can be expressed in a similar indicial form*

$$\begin{aligned} \left( \bar{\tilde{\mathbf{G}}}_k \mathbf{\Delta}^T \mathbf{M}^{-1} \right)^{i,j} &= \frac{\bar{\tilde{G}}_k^{i,j+1} - \bar{\tilde{G}}_k^{i,j}}{\omega_j} \\ &= \frac{1}{\omega_j} \sum_{m=0}^{N} 2\, Q_{mj} \left( F_k^{vol}(\vec{W}^{i,j}, \vec{W}^{i,m}) \left\{\!\left\{ Ja_1^2 \right\}\!\right\}_{i,(j,m)} + G_k^{vol}(\vec{W}^{i,j}, \vec{W}^{i,m}) \left\{\!\left\{ Ja_2^2 \right\}\!\right\}_{i,(j,m)} \right), \end{aligned} \tag{3.49}$$

*for $j = 0, \dots, N$.*

**Proof.** The details to derive (3.48) and (3.49) are straightforward and can be found in Appendix A. □

With the definition of the flux differencing formulation complete, we must select the specific form for the volume fluxes $\vec{F}^{vol}$ and $\vec{G}^{vol}$. Depending on the choice of the volume flux it is possible for the flux differencing scheme to recover discretization of alternative split forms of the PDE. The split form of a PDE, often found by averaging the advective and conservative form of the equations, is known to have stabilization properties for non-linear PDE discretization [26–28]. But, due to their form, it is often unclear if the approximation remains globally conservative in the sense of Lax–Wendroff. We see from the telescoping flux difference formulations (3.48) and (3.49) that it is trivial to show conservation of the scheme while maintaining the flexibility and positive stabilization properties of the split form.

In particular, a split form for the derivative of a product of two quantities is

$$(a\,b)_x = \frac{1}{2}(a\,b)_x + \frac{1}{2}(a_x\,b + a\,b_x)\,, \tag{3.50}$$

see [29] for more information on this splitting applied in finite difference methods. To demonstrate the split form property of the flux differencing form we select the form for the first component of the volume flux to be

$$F_1^{vol}(\vec{W}^{i,j}, \vec{W}^{m,j}) = \frac{1}{2}\left((W_1)^{i,j} + (W_1)^{m,j}\right) = \{\{W_1\}\}_{(i,m),j}\,. \tag{3.51}$$

We substitute (3.51) into the first term on the right of (3.48) and after some manipulation obtain

$$\begin{aligned}\frac{1}{\omega_i}\sum_{m=0}^{N} 2\,Q_{im}\,\{\{W_1\}\}_{(i,m),j}\left\{\left\{Ja_1^1\right\}\right\}_{(i,m),j} = \frac{1}{2\omega_i}\Bigg(&\sum_{m=0}^{N} Q_{im}(W_1)^{m,j}(Ja_1^1)^{m,j} + (W_1)^{i,j}\sum_{m=0}^{N} Q_{im}(Ja_1^1)^{m,j} \\ &+ (Ja_1^1)^{i,j}\sum_{m=0}^{N} Q_{im}(W_1)^{m,j}\Bigg),\end{aligned} \tag{3.52}$$

which is the $i$-th row for the discretization of (3.50)

$$\left(Ja_1^1 W_1\right)_x \approx \frac{1}{2}\left(\mathbf{D}\left(\mathbf{Ja}_1^1 \circ \mathbf{W}_1\right) + \mathbf{Ja}_1^1 \circ \mathbf{DW}_1 + \mathbf{W}_1 \circ \mathbf{DJa}_1^1\right). \tag{3.53}$$

That is, the product of two averages in (3.48) creates a discretization of the standard split form of a quadratic product. In a similar fashion the product of three averages creates a discretization of the standard split form of a triple product proposed by Kennedy and Gruber [28]. This is a remarkable property of the flux differencing form (3.48). Inserting an arithmetic mean or products of arithmetic means into the flux differencing scheme creates a discrete version of a particular split form of the equation. Complete details and proofs of this property of (3.48) can be found in [30].

So, rewriting the volume contributions of the DGSEM into the flux differencing form grants us additional flexibility to construct an approximation that discretizes alternative split forms of the PDE. From such alternative split forms of the shallow water equations it is possible to create an entropy conservative numerical approximation [8]. This gives us the motivation to select the internal volume fluxes in such a way that the total energy of the numerical scheme will be conserved discretely. We note that the only alteration needed to change a standard DGSEM code to an entropy stable one is to change the volume contributions to the flux differencing form and select appropriate volume fluxes, see Appendix D, and select entropy stable numerical fluxes for the surface contributions.

To summarize, we have rewritten the volume contributions of the standard strong form DGSEM (3.38) into an equivalent flux differencing framework

$$\mathbf{J} \circ (\mathbf{W}_k)_t + \mathbf{M}^{-1}\mathbf{\Delta}\overline{\tilde{\mathbf{F}}}_k + \overline{\tilde{\mathbf{G}}}_k\mathbf{\Delta}^T\mathbf{M}^{-1} = \mathbf{S}\left(\tilde{\mathbf{F}}_k^* - \tilde{\mathbf{F}}_k\right) + \left(\tilde{\mathbf{G}}_k^* - \tilde{\mathbf{G}}_k\right)\mathbf{S}, \quad k = 1, 2, 3, \tag{3.54}$$

where the flux differencing is computed in each direction according to the form (3.48) or (3.49). The flux differencing representation guarantees that with a chosen pair of symmetric volume fluxes the approximation (3.54) remains high-order and conservative. Additionally, if the volume fluxes in (3.48) and the surface fluxes in (3.38) are carefully constructed then the approximation is also provably entropy conservative [20]. Note that one can independently select an entropy conservative volume flux that has a different form than an entropy conservative surface flux. We will show in the next section that the additional flexibility to select different fluxes in the volume and at the surface allows the construction of an entropy conservative approximation for the shallow water equations that is also well-balanced.

## 4. Entropy stable DGSEM for the 2D shallow water equations

In this section, we construct the volume and surface fluxes, following the ideas of Tadmor, e.g. [12,13], that discretely conserve the entropy. We denote the entropy conservative approximation as the *ECDGSEM*. Entropy conservation is only valid, however, for smooth solutions and not discontinuous ones (shocks). In Sec. 4.2, we use the entropy conserving scheme as the starting point and add dissipation in a controlled way to guarantee that entropy is always dissipated at shocks, resulting in an entropy stable approximation denoted by *ESDGSEM*.

### 4.1. ECDGSEM on curvilinear meshes

The flux differencing formulation of the strong form DGSEM on curvilinear meshes (3.54) provides a compact notation for the ECDGSEM for which the previous results of Fisher and Carpenter [20] for conservation and entropy conservation apply. To ensure that the approximation remains well-balanced we use the extra flexibility of the flux differencing form that allows us to select different entropy conservative volume and surface fluxes. The discretization of the source term is also divided into volume and surface contributions. The surface parts depend on averages, $\{\{\cdot\}\}$, and jumps, $[\![\cdot]\!]$, across the interface. We denote the jumps for an arbitrary nodal quantity $\mathcal{W}$ consistent to notation (3.13):

$$[\![\mathcal{W}]\!]_\xi := \begin{pmatrix} [\![\mathcal{W}]\!]_\xi^{0,0} & \cdots & [\![\mathcal{W}]\!]_\xi^{0,N} \\ 0 & \cdots & 0 \\ \vdots & & \vdots \\ 0 & \cdots & 0 \\ [\![\mathcal{W}]\!]_\xi^{N,0} & \cdots & [\![\mathcal{W}]\!]_\xi^{N,N} \end{pmatrix}, \qquad [\![\mathcal{W}]\!]_\eta := \begin{pmatrix} [\![\mathcal{W}]\!]_\eta^{0,0} & 0 & \cdots & 0 & [\![\mathcal{W}]\!]_\eta^{0,N} \\ \vdots & \vdots & & \vdots & \vdots \\ [\![\mathcal{W}]\!]_\eta^{N,0} & 0 & \cdots & 0 & [\![\mathcal{W}]\!]_\eta^{N,N} \end{pmatrix}, \tag{4.1}$$

where we distinguish between jumps in $\xi$ direction, $[\![\mathcal{W}]\!]_\xi$, and $\eta$ direction, $[\![\mathcal{W}]\!]_\eta$. The averages of a nodal quantity are defined analogously. Whereas the local average operators are symmetric and hence don't prefer a direction, we define the local jumps according to the $\xi$ and $\eta$ coordinate directions: at the $\xi = -1$ and the $\eta = -1$ interfaces we compute the local jumps as the "inner" value minus the "outer" value, whereas for the $\xi = 1$ and $\eta = 1$ interfaces the local jumps are computed as the "outer" value minus the "inner" value.

**Theorem 1** *(Curvilinear ECDGSEM). The semi-discrete flux difference form of the two dimensional ECDGSEM for the shallow water equations on curvilinear grids*

$$\mathbf{J} \circ (\mathbf{W}_k)_t + \mathbf{M}^{-1} \boldsymbol{\Delta} \overline{\tilde{\mathbf{F}}}_k + \overline{\tilde{\mathbf{G}}}_k \boldsymbol{\Delta}^T \mathbf{M}^{-1} = \mathbf{S} \left( \tilde{\mathbf{F}}_k^{*,ec} - \tilde{\mathbf{F}}_k \right) + \left( \tilde{\mathbf{G}}_k^{*,ec} - \tilde{\mathbf{G}}_k \right) \mathbf{S} + \mathbf{source}_k, \quad k = 1, 2, 3, \tag{4.2}$$

*where for the flux differencing components (3.48) and (3.49), we use the entropy conserving volume fluxes*

$$\vec{F}^{vol}(\vec{W}^{i,j}, \vec{W}^{m,j}) := \begin{pmatrix} \{\{hu\}\}_{(i,m),j} \\ \{\{hu\}\}_{(i,m),j} \{\{u\}\}_{(i,m),j} + g \{\{h\}\}^2_{(i,m),j} - \frac{1}{2} g \left\{\{h^2\}\right\}_{(i,m),j} \\ \{\{hu\}\}_{(i,m),j} \{\{v\}\}_{(i,m),j} \end{pmatrix},$$

$$\vec{G}^{vol}(\vec{W}^{i,j}, \vec{W}^{i,m}) := \begin{pmatrix} \{\{hv\}\}_{i,(j,m)} \\ \{\{hv\}\}_{i,(j,m)} \{\{u\}\}_{i,(j,m)} \\ \{\{hv\}\}_{i,(j,m)} \{\{v\}\}_{i,(j,m)} + g \{\{h\}\}^2_{i,(j,m)} - \frac{1}{2} g \left\{\{h^2\}\right\}_{i,(j,m)} \end{pmatrix}, \tag{4.3}$$

*in combination with the entropy conserving surface numerical fluxes*

$$\vec{F}^{*,ec}(\vec{W}^+, \vec{W}^-) := \begin{pmatrix} \{\{h\}\} \{\{u\}\} \\ \{\{h\}\} \{\{u\}\}^2 + \frac{1}{2} g \left\{\{h^2\}\right\} \\ \{\{h\}\} \{\{u\}\} \{\{v\}\} \end{pmatrix},$$

$$\vec{G}^{*,ec}(\vec{W}^+, \vec{W}^-) := \begin{pmatrix} \{\{h\}\} \{\{v\}\} \\ \{\{h\}\} \{\{u\}\} \{\{v\}\} \\ \{\{h\}\} \{\{v\}\}^2 + \frac{1}{2} g \left\{\{h^2\}\right\} \end{pmatrix}, \tag{4.4}$$

*where in (4.4) the $\{\{\cdot\}\}$ indicates the average of the two neighboring states $\vec{W}^+$ and $\vec{W}^-$ with the source term discretization*

$$\mathbf{source} := \frac{g}{2} \begin{pmatrix} 0 \\ -\mathbf{h} \circ \left[ \mathbf{y}_\eta \circ \mathbf{D}\mathbf{b} + \mathbf{D}(\mathbf{y}_\eta \circ \mathbf{b}) - \mathbf{y}_\xi \circ \mathbf{b}\mathbf{D}^T - (\mathbf{y}_\xi \circ \mathbf{b})\mathbf{D}^T \right] + \mathbf{M}^{-1} \left( \mathbf{y}_\eta \circ \{\{\mathbf{h}\}\}_\xi \circ [\![\mathbf{b}]\!]_\xi \right) - \left( \mathbf{y}_\xi \circ \{\{\mathbf{h}\}\}_\eta \circ [\![\mathbf{b}]\!]_\eta \right) \mathbf{M}^{-1} \\ -\mathbf{h} \circ \left[ -\mathbf{x}_\eta \circ \mathbf{D}\mathbf{b} - \mathbf{D}(\mathbf{x}_\eta \circ \mathbf{b}) + \mathbf{x}_\xi \circ \mathbf{b}\mathbf{D}^T + (\mathbf{x}_\xi \circ \mathbf{b})\mathbf{D}^T \right] - \mathbf{M}^{-1} \left( \mathbf{x}_\eta \circ \{\{\mathbf{h}\}\}_\xi \circ [\![\mathbf{b}]\!]_\xi \right) + \left( \mathbf{x}_\xi \circ \{\{\mathbf{h}\}\}_\eta \circ [\![\mathbf{b}]\!]_\eta \right) \mathbf{M}^{-1} \end{pmatrix}, \tag{4.5}$$

*has the following properties:*

*1.1 Discrete conservation of the mass and discrete conservation of the momentum if the bottom topography is constant.*
*1.2 Discrete conservation of the total energy, which is an entropy function for the shallow water equations. Hence it preserves the entropy of the system.*
*1.3 Discrete well-balanced property for arbitrary bottom topographies.*

**Proof.** We prove the result in three parts.

**Proof of Part 1.1.** The discrete conservation of the numerical scheme follows directly from the telescoping flux differencing form of the approximation [20]. □

**Proof of Part 1.2.** To rigorously show that these scheme is entropy conservative we make the connection to the equivalent split form as introduced in the last section (3.52). We assemble the discrete energy equation in C.1 and provide full details that the resulting discrete approximation is conservative. □

**Proof of Part 1.3.** The complete proof of well-balancedness for the curvilinear ECDGSEM is provided in Appendix C.2. However, it is necessary to describe the construction of the bottom topography discretization. For the two dimensional problem in general coordinates we require discrete approximations for $b_x$ and $b_y$, or more compactly, $\nabla b$. From (3.3) we know the explicit form of the gradient in computational coordinates is

$$J\nabla b = \left[ y_\eta \frac{\partial b}{\partial \xi} - y_\xi \frac{\partial b}{\partial \eta} \, , \; -x_\eta \frac{\partial b}{\partial \xi} + x_\xi \frac{\partial b}{\partial \eta} \right]^T . \tag{4.6}$$

We treat each piece of the source term as a quadratic split form (3.50). For example the first component from (4.6) is

$$b_x = \frac{1}{2}\left( \frac{\partial (y_\eta b)}{\partial \xi} + y_\eta \frac{\partial b}{\partial \xi} + b \frac{\partial y_\eta}{\partial \xi} \right) - \frac{1}{2}\left( \frac{\partial (y_\xi b)}{\partial \eta} + y_\xi \frac{\partial b}{\partial \eta} + b \frac{\partial y_\xi}{\partial \eta} \right). \tag{4.7}$$

We then approximate the bottom contribution from the discrete approximation of the quadratic split form (3.53). So, we have the approximations for the derivative of the bottom topography

$$\begin{aligned} b_x &\approx \frac{1}{2}\left( \mathbf{D}(\mathbf{y}_\eta \circ \mathbf{b}) + \mathbf{y}_\eta \circ \mathbf{D}\mathbf{b} + \mathbf{b} \circ \mathbf{D}\mathbf{y}_\eta - (\mathbf{y}_\xi \circ \mathbf{b})\mathbf{D}^T - \mathbf{y}_\xi \circ \mathbf{b}\mathbf{D}^T - \mathbf{b} \circ \mathbf{y}_\xi \mathbf{D}^T \right), \\ b_y &\approx \frac{1}{2}\left( -\mathbf{D}(\mathbf{x}_\eta \circ \mathbf{b}) - \mathbf{x}_\eta \circ \mathbf{D}\mathbf{b} - \mathbf{b} \circ \mathbf{D}\mathbf{x}_\eta + (\mathbf{x}_\xi \circ \mathbf{b})\mathbf{D}^T + \mathbf{x}_\xi \circ \mathbf{b}\mathbf{D}^T + \mathbf{b} \circ \mathbf{x}_\xi \mathbf{D}^T \right). \end{aligned} \tag{4.8}$$

The bottom topography discretization could immediately be treated in a flux differencing way with the result (3.48). However, we know that the approximation satisfies the metric identities (3.16). So we cancel extraneous terms in (4.8) and obtain a more computationally efficient form of the source term volume contributions in (4.2)

$$\begin{aligned} b_x &\approx \frac{1}{2}\left( \mathbf{D}(\mathbf{y}_\eta \circ \mathbf{b}) + \mathbf{y}_\eta \circ \mathbf{D}\mathbf{b} - (\mathbf{y}_\xi \circ \mathbf{b})\mathbf{D}^T - \mathbf{y}_\xi \circ \mathbf{b}\mathbf{D}^T \right), \\ b_y &\approx \frac{1}{2}\left( -\mathbf{D}(\mathbf{x}_\eta \circ \mathbf{b}) - \mathbf{x}_\eta \circ \mathbf{D}\mathbf{b} + (\mathbf{x}_\xi \circ \mathbf{b})\mathbf{D}^T + \mathbf{x}_\xi \circ \mathbf{b}\mathbf{D}^T \right). \end{aligned} \tag{4.9}$$

The surface contributions follow from a similar logic in that we require the derivative of $b$ at the boundary (in this case the jump). □

**Remark 2** *(Metric identities).* The proof of the entropy conservation Property 1.2 requires that the metric identities (3.16) hold discretely. Specifically this is used in (C.21) to cancel terms.

**Remark 3** *(One-dimensional bottom formulation).* In one space dimension we use the following approximation of the source term for an element $G$

$$g\, h\, b_x \approx g\, \mathbf{h}\, \mathbf{D}\vec{b} + \frac{1}{2} g \left\{\{h\}\right\}_{\xi=-1}^{G} [\![b]\!]_{\xi=-1}^{G} \frac{1}{\omega_0}\vec{e}_1 + \frac{1}{2} g \left\{\{h\}\right\}_{\xi=+1}^{G} [\![b]\!]_{\xi=+1}^{G} \frac{1}{\omega_N}\vec{e}_{N+1}. \tag{4.10}$$

Here $\{\{h\}\}_{\xi=-1}^{G}$ is the average water height at the left interface node of element $G$ and the right interface node of element $G-1$, $\{\{h\}\}_{\xi=+1}^{G}$ is the average water height at the right interface node of element $G$ and the left interface node of element $G+1$:

$$\begin{aligned} \left\{\{h\}\right\}_{\xi=-1}^{G} &= \frac{1}{2}(h_0^G + h_N^{G-1}), \\ \left\{\{h\}\right\}_{\xi=+1}^{G} &= \frac{1}{2}(h_N^G + h_0^{G+1}). \end{aligned} \tag{4.11}$$

In the same fashion the jump in bottom topography is defined as

$$\begin{aligned} [\![b]\!]^G_{\xi=-1} &= b^G_0 - b^{G-1}_N, \\ [\![b]\!]^G_{\xi=+1} &= b^{G+1}_0 - b^G_N. \end{aligned} \tag{4.12}$$

The quadrature weights are denoted by $\omega_0$ and $\omega_N$ and the $N+1$ dimensional unit vectors are denoted by $\vec{e}_1$ and $\vec{e}_{N+1}$.

### 4.2. Entropy stable DGSEM

The ECDGSEM presented so far conserves the entropy in the semi-discrete approximation. However, the solution of the shallow water equations may develop discontinuities (shocks) in finite time even for smooth initial data. We know in the presence of discontinuities that the conservation law for the entropy function (2.6) must be replaced by the entropy inequality (2.8) [13]. Thus, we add numerical dissipation to the ECDGSEM so that the entropy is guaranteed to be dissipated (or conserved for smooth well resolved solutions), thereby ensuring that a discrete version of the entropy inequality holds.

A typical way to add dissipation in a discontinuous Galerkin approximation is via the definition of the numerical surface flux function. Most often, such numerical surface flux functions are (approximate) Riemann solvers that inherently add dissipation near shocks (or where the solution is otherwise underresolved). We follow this basic idea and add dissipation in the spirit of Riemann solvers at the element interfaces to add dissipation to the ECDGSEM.

To derive the dissipative numerical surface flux, we note that the physical fluxes (2.2) have the associated flux Jacobians

$$\mathbf{A}_f = \vec{f}_{\vec{w}} = \begin{pmatrix} 0 & 1 & 0 \\ gh - u^2 & 2u & 0 \\ -uv & v & u \end{pmatrix}, \tag{4.13}$$

and

$$\mathbf{A}_g = \vec{g}_{\vec{w}} = \begin{pmatrix} 0 & 0 & 1 \\ -uv & v & u \\ gh - v^2 & 0 & 2v \end{pmatrix}. \tag{4.14}$$

The eigenvalues of (4.13) are $u+c$, $u$, $u-c$ and for (4.14) $v+c$, $v$, $v-c$ with the wave speed $c = \sqrt{gh}$. The matrices of eigenvectors of (4.13) and (4.14) are

$$\mathbf{R}_f = \begin{pmatrix} 1 & 0 & 1 \\ u+c & 0 & u-c \\ v & 1 & v \end{pmatrix}, \tag{4.15}$$

and

$$\mathbf{R}_g = \begin{pmatrix} 1 & 0 & 1 \\ u & 1 & u \\ v+c & 0 & v-c \end{pmatrix}, \tag{4.16}$$

respectively.

The dissipation term also requires the entropy Jacobian matrix $\mathbf{H} = \vec{q}_{\vec{w}}$. To obtain $\mathbf{H}$, we express the conservative variables $\vec{w} = (h, hu, hv)^T$ in terms of the entropy variables $\vec{q} = (g(h+b) - \frac{1}{2}u^2 - \frac{1}{2}v^2, u, v)^T$:

$$\begin{aligned} w_1 &= \frac{1}{g}q_1 - b + \frac{1}{2g}(q_2^2 + q_3^2), \\ w_2 &= \frac{1}{g}q_1 q_2 - b q_2 + \frac{1}{2g}(q_2^3 + q_2 q_3^2), \\ w_3 &= \frac{1}{g}q_1 q_3 - b q_3 + \frac{1}{2g}(q_2^2 q_3 + q_3^3). \end{aligned} \tag{4.17}$$

Differentiating (4.17) directly leads to the entropy Jacobian matrix

$$\mathbf{H} = \frac{1}{g}\begin{pmatrix} 1 & u & v \\ u & gh + u^2 & uv \\ v & uv & gh + v^2 \end{pmatrix}. \tag{4.18}$$

With an appropriate scaling for the right eigenvectors we obtain the set of entropy scaled eigenvectors [11]

$$\mathbf{H} = (\mathbf{RT})(\mathbf{RT})^T, \tag{4.19}$$

which relates the right eigenvectors to the entropy Jacobian. For the scaling, we consider the matrix

$$\mathbf{T} = \mathrm{diag}(\sqrt{s_1}, \sqrt{s_2}, \sqrt{s_3}), \tag{4.20}$$

with scaling parameters on the diagonal only. We define $\mathbf{Z} = \mathbf{T}^2$ and have the identity in a new form

$$\mathbf{H} = \mathbf{R}\mathbf{Z}\mathbf{R}^T. \tag{4.21}$$

For the eigenvectors of the $f$ flux Jacobian, $\mathbf{R}_f$, we find

$$s_1 = \frac{1}{2g}, \quad s_2 = h, \quad s_3 = \frac{1}{2g}. \tag{4.22}$$

A straightforward calculation shows that the same scaling applies to for the eigenvectors of the flux Jacobian in the $y$-direction.

Now we have all the necessary components to define the entropy stable numerical surface flux functions. We subtract the dissipation term required for dissipation in the $x$-direction

$$\vec{F}^{*,es} = \vec{F}^{*,ec} - \frac{1}{2}\mathbf{R}_f \left|\mathbf{\Lambda}_f\right| \mathbf{Z}\mathbf{R}_f^T [\![ \vec{q} ]\!], \tag{4.23}$$

and the $y$-direction

$$\vec{G}^{*,es} = \vec{G}^{*,ec} - \frac{1}{2}\mathbf{R}_g \left|\mathbf{\Lambda}_g\right| \mathbf{Z}\mathbf{R}_g^T [\![ \vec{q} ]\!], \tag{4.24}$$

where $\mathbf{\Lambda}_f$ and $\mathbf{\Lambda}_g$ are the diagonal matrices containing the eigenvalues previously computed. We use the arithmetic average values at an element interfaces to compute the right eigenvector, scaling, and eigenvalue matrices in (4.23) and (4.24).

It is important that the dissipation terms depend on the jumps of the entropy variables and not on the jump of the conserved quantities as would be common in standard Riemann solver-based numerical surface flux functions. If we compute the discrete entropy equation by multiplying the scheme with the entropy variables, we obtain contributions of the form $-\frac{1}{2}[\![ \vec{q} ]\!]^T \mathbf{R}_f \left|\mathbf{\Lambda}_f\right| \mathbf{Z}\mathbf{R}_f^T [\![ \vec{q} ]\!]$ at each interface that are guaranteed to be negative due to the positivity of the matrix $\mathbf{R}_f \left|\mathbf{\Lambda}_f\right| \mathbf{Z}\mathbf{R}_f^T$. Writing in terms of the jumps in the entropy variables ensures that entropy is dissipated when the jump in entropy variables across interfaces is large (e.g. shocks) and is nearly preserved when the jumps are small for well resolved smooth solutions.

We finally present the main contribution of the present work, an entropy stable DGSEM (ESDGSEM) for the shallow water equations.

**Theorem 2** *(Curvilinear ESDGSEM). The semi-discrete form of the two dimensional ESDGSEM formulation for the shallow water equations on curvilinear grids is given by*

$$\mathbf{J} \circ (\mathbf{W}_k)_t + \mathbf{M}^{-1}\mathbf{\Delta}\overline{\tilde{\mathbf{F}}}_k + \overline{\tilde{\mathbf{G}}}_k \mathbf{\Delta}^T \mathbf{M}^{-1} = \mathbf{S}\left(\tilde{\mathbf{F}}_k^{*,es} - \tilde{\mathbf{F}}_k\right) + \left(\tilde{\mathbf{G}}_k^{*,es} - \tilde{\mathbf{G}}_k\right)\mathbf{S} + \mathbf{source}_k, \quad k = 1, 2, 3, \tag{4.25}$$

*where the flux differencing components use the volume fluxes (4.3) in combination with the entropy stable numerical surface fluxes (4.23) and (4.24) and the source term discretization (4.5). The approximation has the following properties:*

*2.1 Discrete conservation of the mass and discrete conservation of the momentum if the bottom topography is constant.*
*2.2 Discrete entropy stability.*
*2.3 The well-balanced property for arbitrary bottom topographies.*

**Proof.** The ESDGSEM follows directly from the curvilinear ECDGSEM presented in Theorem 1. To guarantee entropy stability we replace the entropy conserving numerical fluxes (4.4) at element interfaces with the entropy stable numerical fluxes (4.23), (4.24). For the "lake at rest" initial conditions the jump in entropy variables is zero, $[\![ \vec{q} ]\!] = 0$, so the additional dissipation term vanishes and does not affect the well-balanced property of the scheme. □

## 5. Numerical results

In this section, we use the entropy conserving (4.2) and entropy stable (4.25) numerical schemes on several test cases to numerically verify the theoretical findings from Theorems 1 and 2. To integrate the systems in time we use the five stage, fourth order Runge–Kutta time integrator of Carpenter and Kennedy [31]. First, to verify the convergence, conservation and well-balancedness of the approximations we use a structured curvilinear mesh depicted in Fig. 1. Elements are numbered by counting from left to right and bottom to top. We also simulate a bore-shear interaction as well as the numerical generation of potential vorticity generated from the passage of a non-uniform bore. After all theoretical findings are verified numerically, we present a simulated partial dam break from a parabolic dam with a discontinuous bottom topography in the downstream region of the flow. The partial dam break problem serves to exercise each component of the ESDGSEM approximation.

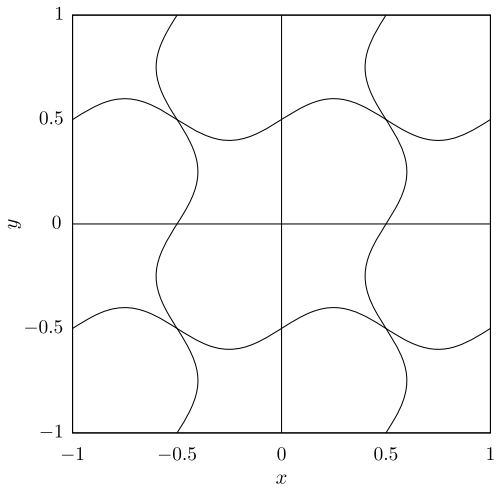



**Fig. 1.** The curvilinear mesh used for verification of convergence, conservation, and well-balancedness.

### 5.1. Convergence

We first test the convergence of the entropy conserving and entropy stable approximations with a smooth solution test problem. We use the method of manufactured solutions to create an analytic solution

$$\begin{aligned} H(x,y,t) &= h(x,y,t) + b_1(x,y) = 8 + \cos(x)\sin(y)\cos(t), \\ u(x,y,t) &= 0.5, \\ v(x,y,t) &= 1.5. \end{aligned} \tag{5.1}$$

The manufactured solution (5.1) introduces additional source terms to the equations of the form

$$\begin{aligned} s_1 &:= H_t + u(H_x - (b_1)_x) + v(H_y - (b_1)_y), \\ s_2 &:= uH_t + u^2(H_x - (b_1)_x) + uv(H_y - (b_1)_y) + H_x(H - b_1), \\ s_3 &:= vH_t + uv(H_x - (b_1)_x) + v^2(H_y - (b_1)_y) + H_y(H - b_1), \end{aligned} \tag{5.2}$$

where derivatives regarding $H$ and $b_1$ are computed analytically. We solve this problem on the domain $[-1,1]^2$ with the smooth bottom topography

$$b_1(x,y) = 2 + 0.5\sin(2\pi x) + 0.5\cos(2\pi y). \tag{5.3}$$

The gravitational constant is set to $g = 1$.

We vary the polynomial degree on the mesh given in Fig. 1 and observe exponential convergence up to $N = 16$ ($N = 15$ for ESDGSEM) for $\Delta t = 1/2000$ and $N = 17$ ($N = 16$ for ESDGSEM) for $\Delta t = 1/4000$, when the errors introduced by the time integrator become dominant. We present semi-log plots in Fig. 2 for the entropy conserving scheme and Fig. 3 for the entropy stable scheme. As previously observed, e.g. [8,14–16], we find a suboptimal order of convergence for odd polynomial degree $N$ for the purely entropy conserving scheme. However, both the ECDGSEM and ESDGSEM are spectrally accurate for smooth problems.

### 5.2. Conservation of mass and momentum

We next numerically verify that mass and momentum are conserved, Property 1.1 of Theorem 1, using a constant bottom topography. Additionally, with the specific numerical volume fluxes (4.3) and surface fluxes (4.4) the approximation will conserve the total energy (modulo dissipative effects of the time integrator). Also, for a non-constant bottom topography the momentum equations become balance laws, and we show that mass and entropy are still conserved discretely, even for discontinuous bottom topographies.

The problem that we choose to model is a dam break on the domain $\Omega = [-1,1]^2$. The dam break is initialized along the vertical line $x = 0$ on the curvilinear mesh shown in Fig. 1 with periodic boundary conditions and a polynomial degree of $N = 5$. The gravitational constant is again set to $g = 1$. The dam break problem uses the initial conditions

$$h(x,y,0) = \begin{cases} 5 - b(x,y) & \text{if } x < 0 \\ 4 - b(x,y) & \text{if } x > 0 \end{cases}, \quad u(x,y,0) = v(x,y,0) = 0. \tag{5.4}$$

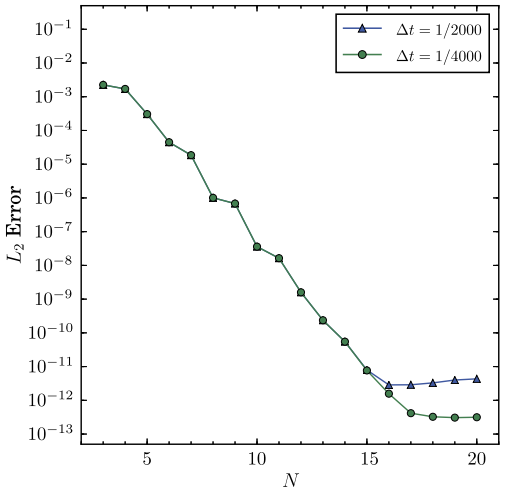



**Fig. 2.** Semi-log plot shows the spectral convergence in space and fourth order accuracy in time for of the ECDGSEM scheme applied to a smooth solution in Sec. 5.1.

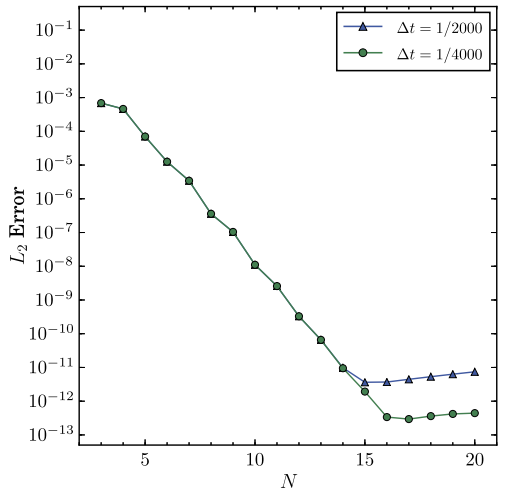



**Fig. 3.** Semi-log plot shows the spectral convergence in space and fourth order accuracy in time for the ESDGSEM scheme applied to a smooth solution in Sec. 5.1.

**Table 1**
Errors in the conserved quantities, mass, momentum, and total energy, at $T = 1$ over a constant bottom topography. In the energy conservation results we observe the temporal accuracy of the time integrator.

| $\Delta t$ | $\Delta$Mass | $\Delta$Momentum X | $\Delta$Momentum Y | $\Delta$Energy | Temporal order |
|---|---|---|---|---|---|
| 1/1000 | 3.55E−14 | 2.66E−13 | 4.32E−17 | 4.79E−08 | – |
| 1/2000 | 2.49E−14 | 2.66E−13 | 9.95E−16 | 3.01E−09 | 3.99 |
| 1/4000 | 3.20E−14 | 2.66E−13 | 1.71E−15 | 1.89E−10 | 3.99 |
| 1/8000 | 3.20E−14 | 2.66E−13 | 1.46E−15 | 1.18E−11 | 4.00 |

### *5.2.1. Dam break over a flat bottom*

We demonstrate the entropy conservative properties of the ECDGSEM scheme, Property 1.2 of Theorem 1. We consider a flat bottom topography, $b \equiv 0$, and solve the dam break on the curvilinear mesh Fig. 1. The differences in mass, momentum, and total energy are listed in Table 1. The error in the discrete energy reflects the dissipative influence of the time integrator. Otherwise, we see that the conservation in mass and momentum is on the order of machine precision for each time step value considered. By shrinking the time step we see that we can drive the error in the discrete total energy to machine precision, converging at the fourth order accuracy of the time integrator.

**Table 2**
Errors in the mass and total energy at $T = 1$ for the discontinuous bottom topography (5.5). In the energy conservation results we observe the temporal accuracy of the time integrator.

| $\Delta t$ | $\Delta$Mass | $\Delta$Energy | Temporal order |
|---|---|---|---|
| 1/1000 | 5.33E−14 | 2.16E−08 | – |
| 1/2000 | 1.78E−14 | 1.35E−09 | 4.00 |
| 1/4000 | 2.84E−14 | 8.48E−11 | 3.99 |
| 1/8000 | 3.55E−15 | 5.32E−12 | 3.99 |

**Table 3**
$L_2$-error of the approximate total water height, $H = h + b$, to the "lake at rest" problem on the curvilinear mesh shown in Fig. 1 at $T = 1$.

| $N$ | $L_2$-error ECDGSEM | $L_2$-error ESDGSEM |
|---|---|---|
| 3 | 8.84E−15 | 5.37E−15 |
| 4 | 8.75E−15 | 5.02E−15 |
| 5 | 1.85E−14 | 1.55E−14 |

#### 5.2.2. Dam break over a discontinuous bump

Next we examine the conservative properties of the numerical scheme for a discontinuous bottom topography. Momentum will no longer be conserved, but the mass is conserved and the error in the total energy reduces as the time step is refined. These properties are demonstrated in the numerical test presented in Table 2. For the discontinuous bottom topography we consider

$$b_2(x, y) = \begin{cases} 2 + 0.5 \sin(2\pi x) + 0.5 \cos(2\pi y), & \text{for element } 2 \times 2 \\ 0, & \text{otherwise} \end{cases}, \tag{5.5}$$

which is the bottom topography (5.3) restricted to a single element. If we use the entropy conserving scheme without added stabilization and periodic boundaries, we expect the entropy (total energy) to be conserved in the scheme. Table 2 shows that the error in the total energy shrinks with the fourth order accuracy of the time integrator as the time step is refined. Also, we see that mass is conserved to machine precision for all time steps.

### 5.3. Well-balancedness over a discontinuous bottom

Next we show that the curvilinear entropy conserving numerical scheme (4.2) is well-balanced, numerically demonstrating Property 1.3 of Theorem 1. We focus, particularly, on a discontinuous bottom topography. So, we configure a "lake at rest" test problem as in (2.9)

$$\begin{aligned} &h + b_2(x, y) = 5, \\ &u = v = 0, \end{aligned} \tag{5.6}$$

with the discontinuous bottom topography (5.5). The boundary conditions are set to be periodic. We use the curvilinear mesh in Fig. 1 on the domain $\Omega = [-1, 1]^2$ and vary the polynomial degree $N$. The time step is fixed at $\Delta t = 1/1000$. Table 3 shows that the $L_2$-error of the approximate total water height, $H = h + b_2$, is of the magnitude of round-off errors for both the ECDGSEM and the ESDGSEM.

### 5.4. Dam break over a discontinuous bump

Next we compute the solution of a dam break problem using both the ECDGSEM and the ESDGSEM. This numerical example demonstrates that the entropy stable approximation removes spurious oscillations in the post-shock regions of the flow introduced by the entropy conservative approximation. For the numerical test we set inflow/outflow Dirichlet boundaries along the vertical lines $x = 0$ and $x = 10$ and periodic boundaries along the horizontal lines $y = 0$ and $y = 10$ on the domain $\Omega = [0, 10]^2$. We use a rectangular mesh with sizes varying from $20 \times 20$, $40 \times 40$, $80 \times 80$ to $160 \times 160$ elements and polynomial degree of $N = 4$. The gravitational constant is again set to $g = 1$. The initial conditions are

$$h(x, y, 0) = \begin{cases} 3.5 - b_3(x, y) & \text{if } x < 5 \\ 2.5 - b_3(x, y) & \text{if } x > 5 \end{cases}, \quad u(x, y, 0) = v(x, y, 0) = 0, \tag{5.7}$$

so we initialize the problem with a height discontinuity on the element interfaces at $x = 5.0$. As a bottom topography we use

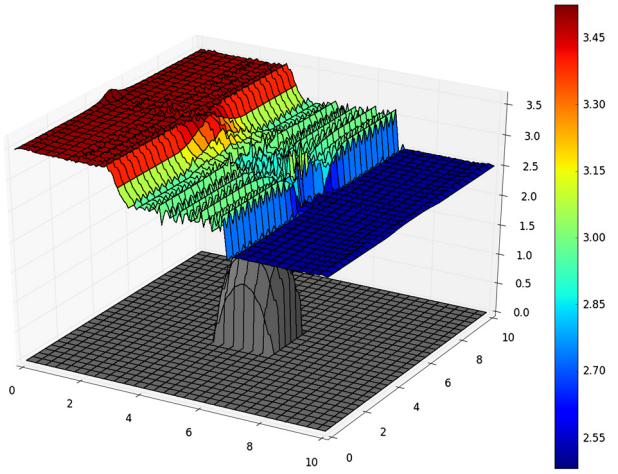



**Fig. 4.** ECDGSEM, dam break over a discontinuous bump on $40 \times 40$ elements at $T = 1$ and $CFL = 0.1$.

$$b_3(x, y) = \begin{cases} 2.0 - (x-5)^2 - (y-5)^2, & \text{if } |x-5| < 1 \text{ and } |y-5| < 1 \\ 0, & \text{otherwise} \end{cases}, \tag{5.8}$$

which is a box with a smooth top that has its center at $(5.0, 5.0)$, side lengths of 2, and is initialized discontinuously along the edges of the box, which align with cell interfaces.

The results shown in Fig. 4 for the purely conserving scheme show that the ECDGSEM produces severe ringing in the post-shock region of the approximation. The entropy stable approximation removes these spurious oscillations except near the discontinuity at the shock front. We show the computed entropy stable solution in Fig. 5, where we present a grid refinement study for the entropy stable approximation. It is clear that the additional dissipation smoothes the spurious oscillations and the ESDGSEM provides a more physical solution to the dam break problem over the discontinuous bump. Nevertheless, we note that, although entropy stable, the ESDGSEM is not completely oscillation-free [3].

### 5.5. Non-linear breaking shallow waters waves

This test problem simulates the interaction of a hydraulic bore in a shear flow. We also observe how the numerical scheme generates potential vorticity through the passage of a non-uniform bore [32,33]. For smooth flows the potential vorticity

$$\Pi = \frac{\Lambda}{h}, \quad \Lambda = \frac{\partial v}{\partial x} - \frac{\partial u}{\partial y}, \tag{5.9}$$

is a conserved quantity [33,34]. Hydraulic bores are discontinuities in the flow where energy is dissipated but mass and momentum are conserved. By design the dissipation in the ESDGSEM is generated proportional to the magnitude of the jump in the entropy variables which are large near discontinuities but spectrally small in smooth regions of the flow. Since the dissipation is only applied near bores, potential vorticity can be generated through non-uniform shallow water wave breaking.

To see how the ESDGSEM generates potential vorticity we begin with an initial flow that has zero vorticity. We consider a flow where the bottom topography is zero, $b \equiv 0$, with the initial "linear" gravity wave

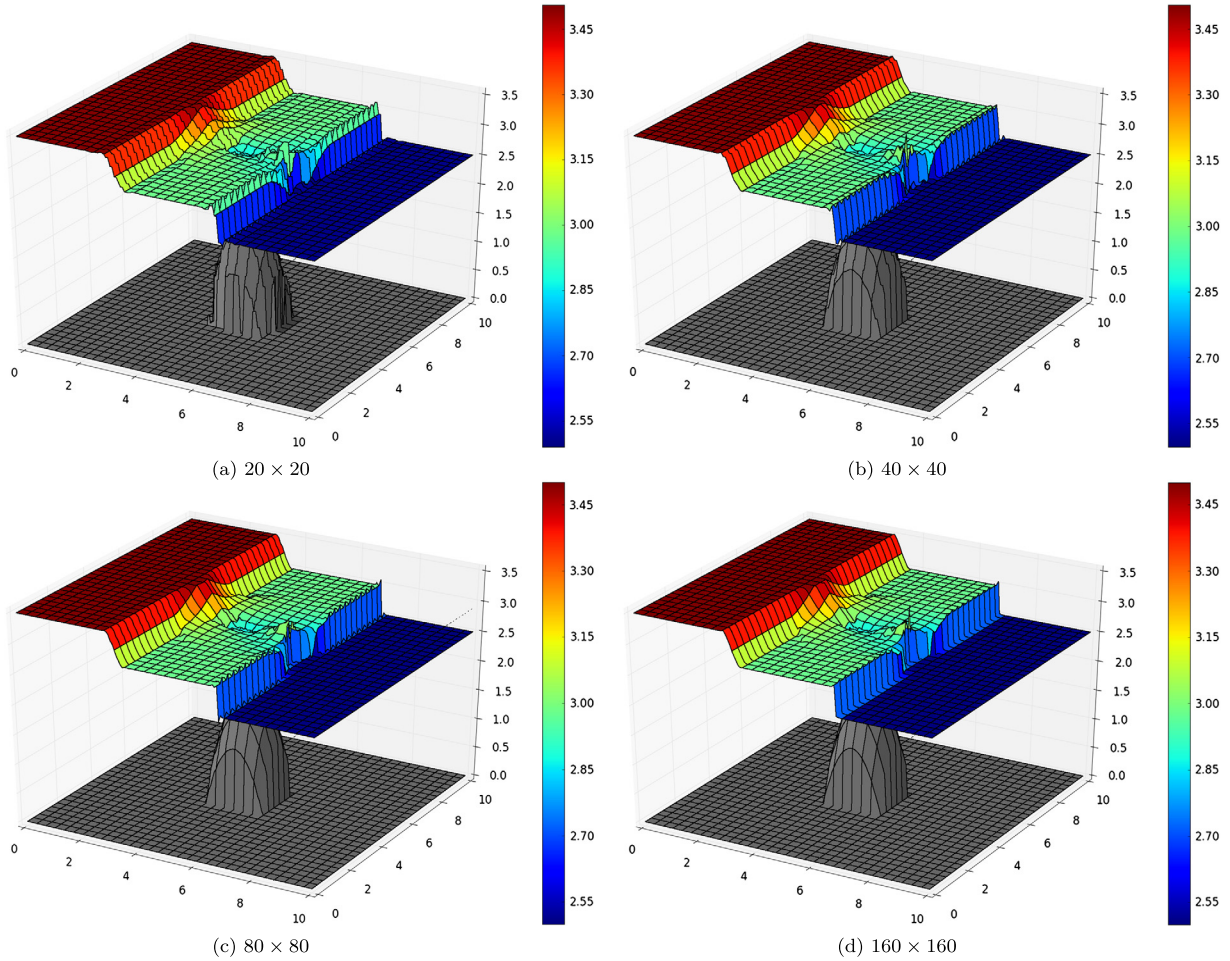
$$\begin{aligned} h(x, y) &= 1 + A \sin(ly) \sin(kx) \\ u(x, y) &= -\frac{kAg}{\omega} \sin(ly) \sin(kx) \\ v(x, y) &= \frac{lAg}{\omega} \cos(ly) \cos(kx) \end{aligned} \tag{5.10}$$

in the rectangular domain $\Omega = [-0.5, 0.5]^2$. We set solid wall boundary conditions at $y = \pm 0.5$ and periodic boundary conditions in the $x$-direction. The quantities in the initial conditions (5.10) are

$$k = 2\pi m, \quad l = (2n+1)\pi, \quad \omega^2 = g(k^2 + l^2), \quad A = 0.1, \quad g = 1, \quad m = 2, \quad n = 0. \tag{5.11}$$

We run two simulations for the initial conditions (5.10) each with 40,000 degrees of freedom:

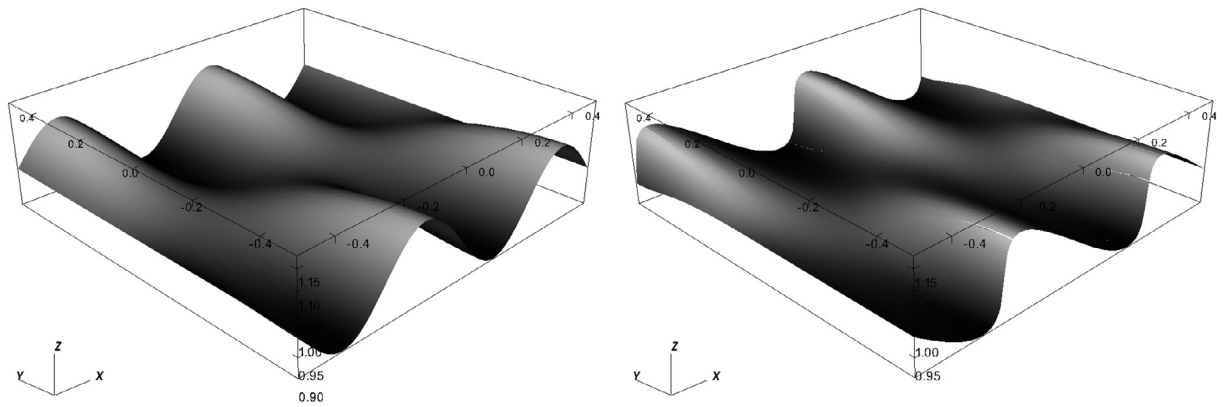
1. $N = 1$ with a uniform $100 \times 100$ Cartesian mesh,
2. $N = 3$ with a uniform $50 \times 50$ Cartesian mesh.




(a) $20 \times 20$ (b) $40 \times 40$

(c) $80 \times 80$ (d) $160 \times 160$

**Fig. 5.** Grid refinement study for the dam break problem modeled by the ESDGSEM at four grid resolutions with $CFL = 0.1$ and $N = 4$.

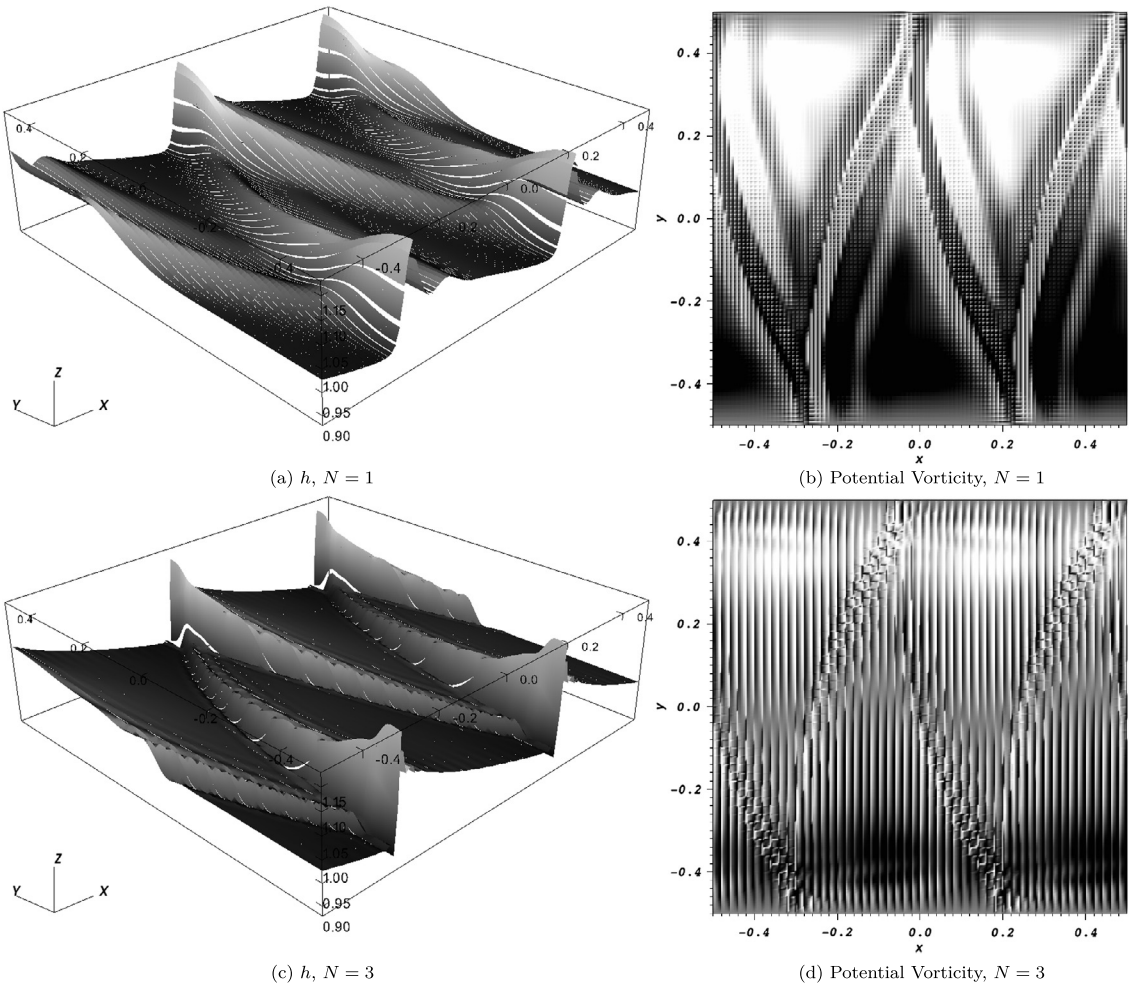



(a) $T = 0.0$ (b) $T = 0.5$

**Fig. 6.** Three dimensional visualization of the initial water height and the water height just before wave breaking occurs at $t \approx 0.5$.

The first configuration makes the ESDGSEM a second order spatial approximation which can be directly compared to previous results, namely Fig. 21 in [32] or Fig. 4 in [33]. The other configuration yields a higher order spatial approximation to be used for comparison with the low-order computation.

Due to the non-linearity in the shallow water equations, the higher amplitudes in the "linear" gravity waves begin to break at $t \approx 0.5$. The breaking waves create peaks at the crests and troughs of the free surface near to the walls, as shown in Fig. 6. The breaking extends to the interior, and bores moving in the negative $x$-direction are formed. The bores are aligned




(a) $h$, $N = 1$ (b) Potential Vorticity, $N = 1$

(c) $h$, $N = 3$ (d) Potential Vorticity, $N = 3$

**Fig. 7.** At left is a three dimensional visualization of the water height, $h$, at $T = 2$ where wave breaking has occurred and bores are generated. On the right is the approximate potential vorticity (5.5) where the color ranges between $-0.02$ (black) to 0.02 (white). Numerical artifacts near element boundaries are visible due to the local derivative computation, without post-processing, of (5.5).

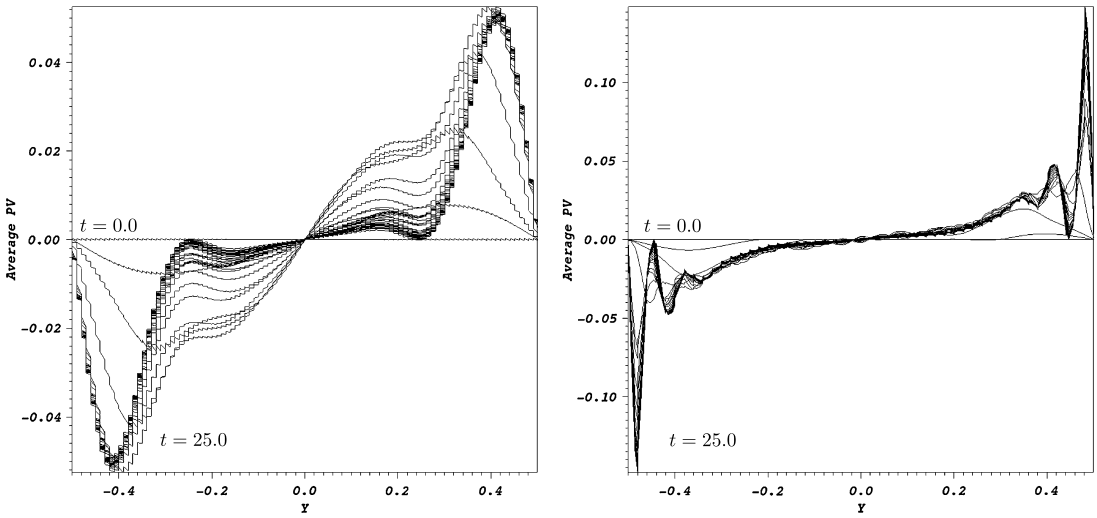
in the $y$-direction with some curvature shown at $T = 2$ for $N = 1$ and $N = 3$ in the left part of Fig. 7. We also present, in the right part of Fig. 7, the point-wise potential vorticity at $T = 2$ computed using the local derivative to approximate the vorticity $\Lambda$. The computed water height and potential vorticity for $N = 1$ compares well with the results of Tassi et al. [33]. For the $N = 3$ computation we see there are some oscillations in the vicinity of the discontinuities and higher resolution in the smooth parts of the flow. The generated potential vorticity follows the shape of the discontinuities in the solution.

We again note that ESDGSEM adds dissipation to ensure entropy stability but is not guaranteed to be overshoot free. Hence, the solution is oscillatory at the sharp fronts and these oscillations are even stronger for the raw gradients. We use raw gradients without any post-processing of the numerical solution to calculate the potential vorticity. This explains the noise at the element boundaries in the potential vorticity plots, especially for the high-order $N = 3$ case.

We also plot the $x$-averaged potential vorticity generation over time in Fig. 8. This serves to demonstrate how the flow starts with potential vorticity close to zero and develops potential vorticity close to the solid wall boundaries. Near the final time of $T = 25$ the potential vorticity remains almost constant. Again we see the impact of the higher order method where oscillations occur near the shocks. The magnitude of the $x$-averaged potential vorticity is higher in the $N = 3$ case.

### 5.6. Parabolic dam break

In Secs. 5.1–5.4 we have verified the theoretical properties of the EC and ESDGSEM. For the next example we combine each aspect of the numerical scheme and model the fluid flow from the partial break of a parabolic dam. First, we will demonstrate the well-balancedness of the ESDGSEM approximation on curvilinear grids, i.e. numerical verification of Property 2.3 of Theorem 2. To do so we consider the solution before the failure of the dam, which amounts to two “lake at rest” problems on the left and right sides of the dam. On the right side of the dam we also place a discontinuous bottom topography. Then, we allow the dam to fail and examine the flow.




(a) $N = 1$ (b) $N = 3$

**Fig. 8.** $x$-Averaged potential vorticity over time.

**Table 4**
$L_2$-error of the approximation of the total water height, $H = h + b$, to the "lake at rest" problem for the parabolic dam at $T = 5$ for various values of $N$. The second column shows the error to the left of the curved dam where there is no bottom topography. The third column gives the error to the right of the curved dam where there is a discontinuous bottom given by (5.13).

| $N$ | $L_2$-error ESDGSEM (left) | $L_2$-error ESDGSEM (right) |
|---|---|---|
| 3 | 5.52E−14 | 4.21E−14 |
| 4 | 7.04E−14 | 6.22E−13 |
| 5 | 1.82E−13 | 1.05E−13 |

For both numerical tests in this section we use a domain $\Omega = [-5, 5]^2$, which is divided into 1600 quadrilateral elements. We model a parabolic dam placed near the center of the domain $\Omega$ with the curve

$$x = \frac{1}{25}y^2 - \frac{1}{4}. \tag{5.12}$$

Finally, for each configuration, we place a discontinuous bottom topography on the downstream side of the dam of the form

$$b_4(x, y) = \begin{cases} 2.0 + \ln(x - 1.25) & \text{if } x \geq 2.25, \\ 0 & \text{if } x < 2.25, \end{cases} \tag{5.13}$$

*5.6.1. ESDGSEM well-balancedness*

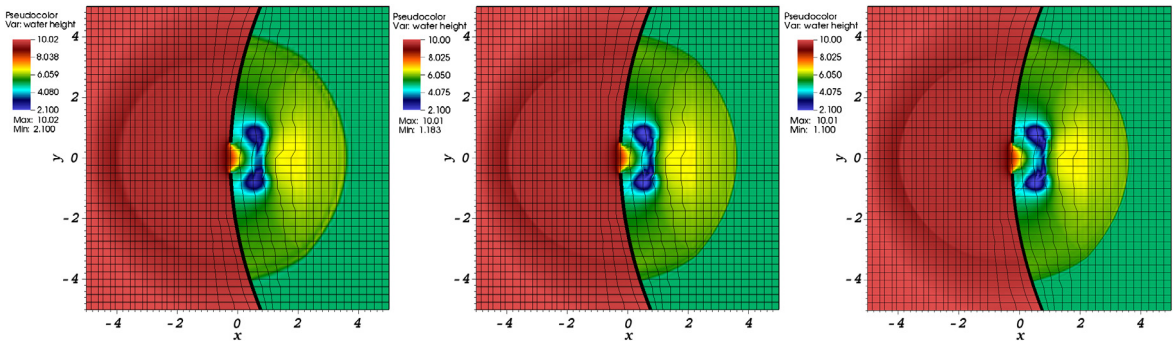
We first solve the "lake at rest" problem on either side of the dam before it fails. We consider the water height to the left of the dam to be higher than the water on the right of the dam. The initial conditions are

$$h(x, y, 0) = \begin{cases} 10 - b_4(x) & \text{if } x < \dfrac{1}{25}y^2 - \dfrac{1}{4}, \\ 5 - b_4(x) & \text{if } x > \dfrac{1}{25}y^2 - \dfrac{1}{4}, \end{cases} \quad , \quad u(x, y, 0) = v(x, y, 0) = 0. \tag{5.14}$$

We set periodic boundary conditions for each lake individually. This test serves to demonstrate the well-balancedness of the ESDGSEM on a curvilinear mesh, including a discontinuous source term (5.13), Property 2.3 of Theorem 2. For the test problem we take the time step to be $\Delta t = 1/5000$ and integrate to a final time of $T = 5$. We present the $L_2$ error in the approximation of the constant total water height, $H = h + b$, in Table 4. We find that on either side of the parabolic dam the error in the computed water height is on the order of machine precision.

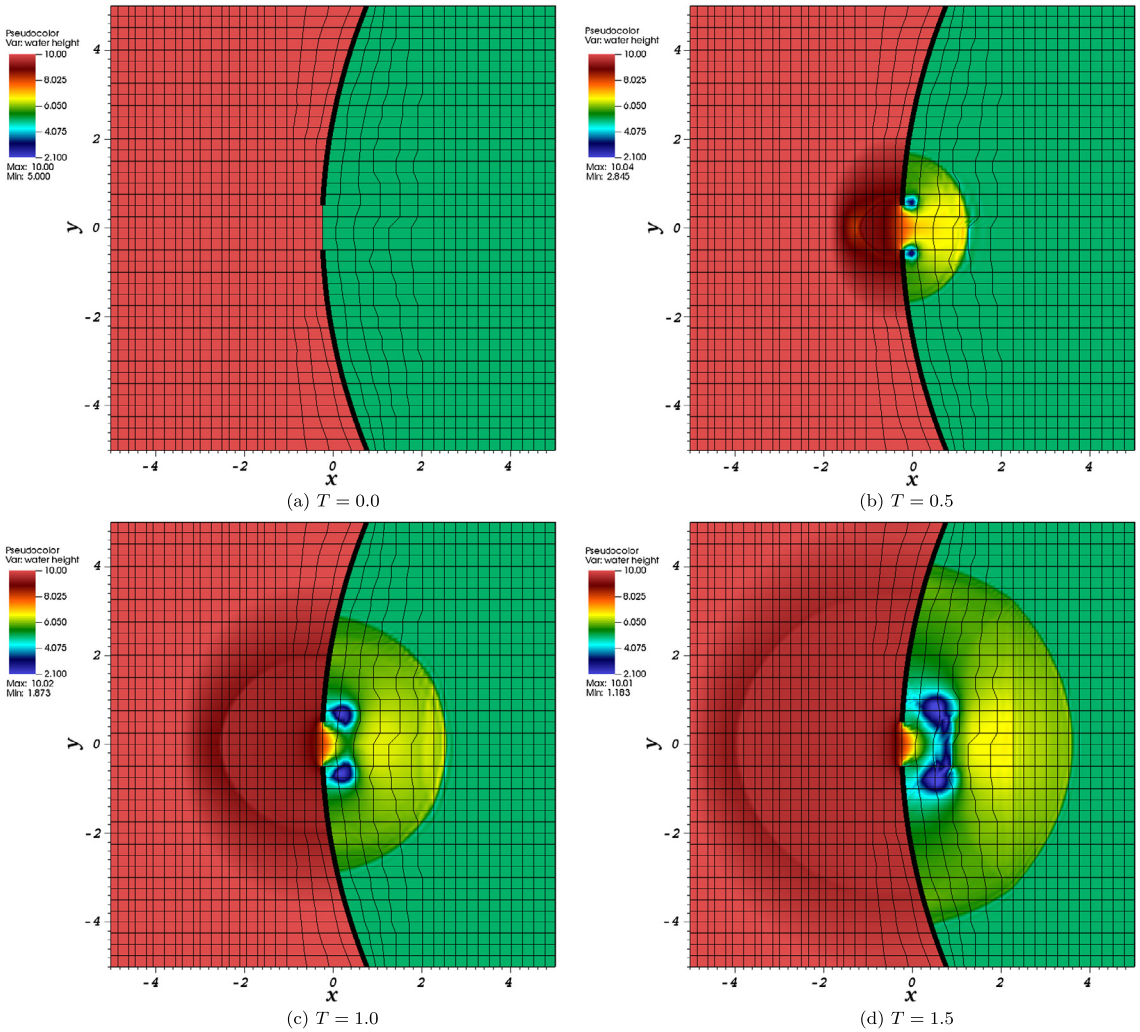
*5.6.2. Partial dam break with discontinuous bottom topography*

The final demonstration considers the partial failure of a parabolic dam. The initial conditions are given by (5.14). The boundary conditions are periodic along the lines $y = 5$ and $y = -5$, Dirichlet along the lines $x = 5$ and $x = -5$, and reflecting




(a) $N = 3$ (b) $N = 5$ (c) $N = 7$

**Fig. 9.** Grid convergence study for the ESDGSEM approximation of the parabolic partial dam break configuration with $\Delta t = 1/1500$ at $T = 1.5$. The overlay of quadrilaterals represents the mesh and the thick black line represents the unbroken portion of the parabolic dam.



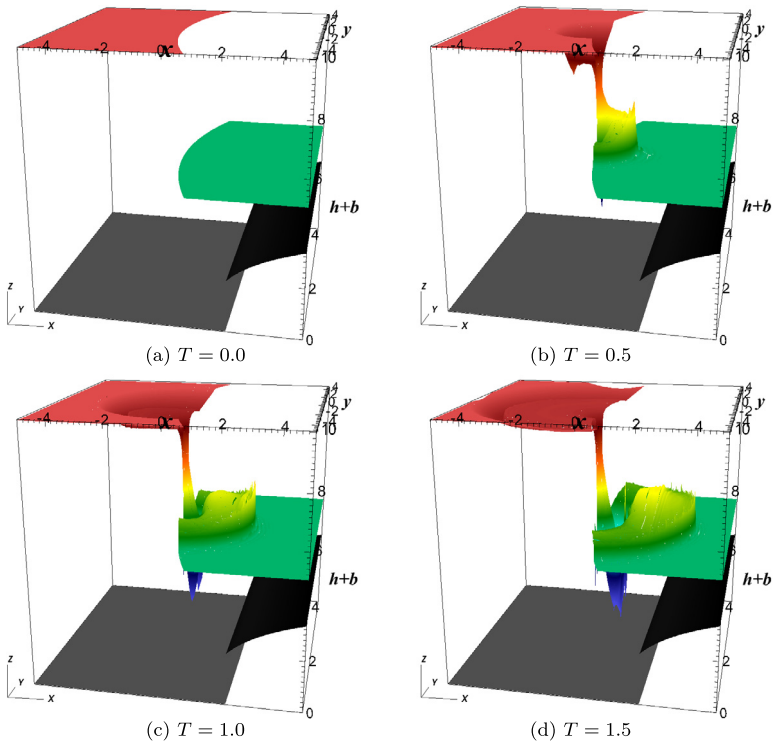

(a) $T = 0.0$ (b) $T = 0.5$

(c) $T = 1.0$ (d) $T = 1.5$

**Fig. 10.** ESDGSEM approximation for the parabolic partial dam break at four times with $N = 5$ and $\Delta t = 1/1500$. The overlay of quadrilaterals represents the mesh and the thick black line represents the unbroken portion of the parabolic dam.

wall boundary states along the unbroken parts of the parabolic dam. We assume an instantaneous failure of the portion of the dam in the region $y \in [-0.5, 0.5]$. It is only in this region that the two states interact.

First, we provide a visual grid convergence study for this complex test problem that has no analytical solution. In Fig. 9 we provide the computed solution of the water height for three polynomial orders $N = 3$, $N = 5$, and $N = 7$, with $\Delta t =$




(a) $T = 0.0$ (b) $T = 0.5$

(c) $T = 1.0$ (d) $T = 1.5$

**Fig. 11.** Three dimensional visualization of the ESDGSEM approximation for the parabolic partial dam break at various times with $N = 5$ and $\Delta t = 1/1500$. Here the interaction of the flow with the discontinuous bottom topography is clear.

$1/1500$, integrated to a final time of $T = 1.5$. The overlay of quadrilaterals represents the spectral element mesh. We see from the numerical $N$-refinement study that the waves in the approximation are well-resolved for $N = 5$ and $N = 7$.

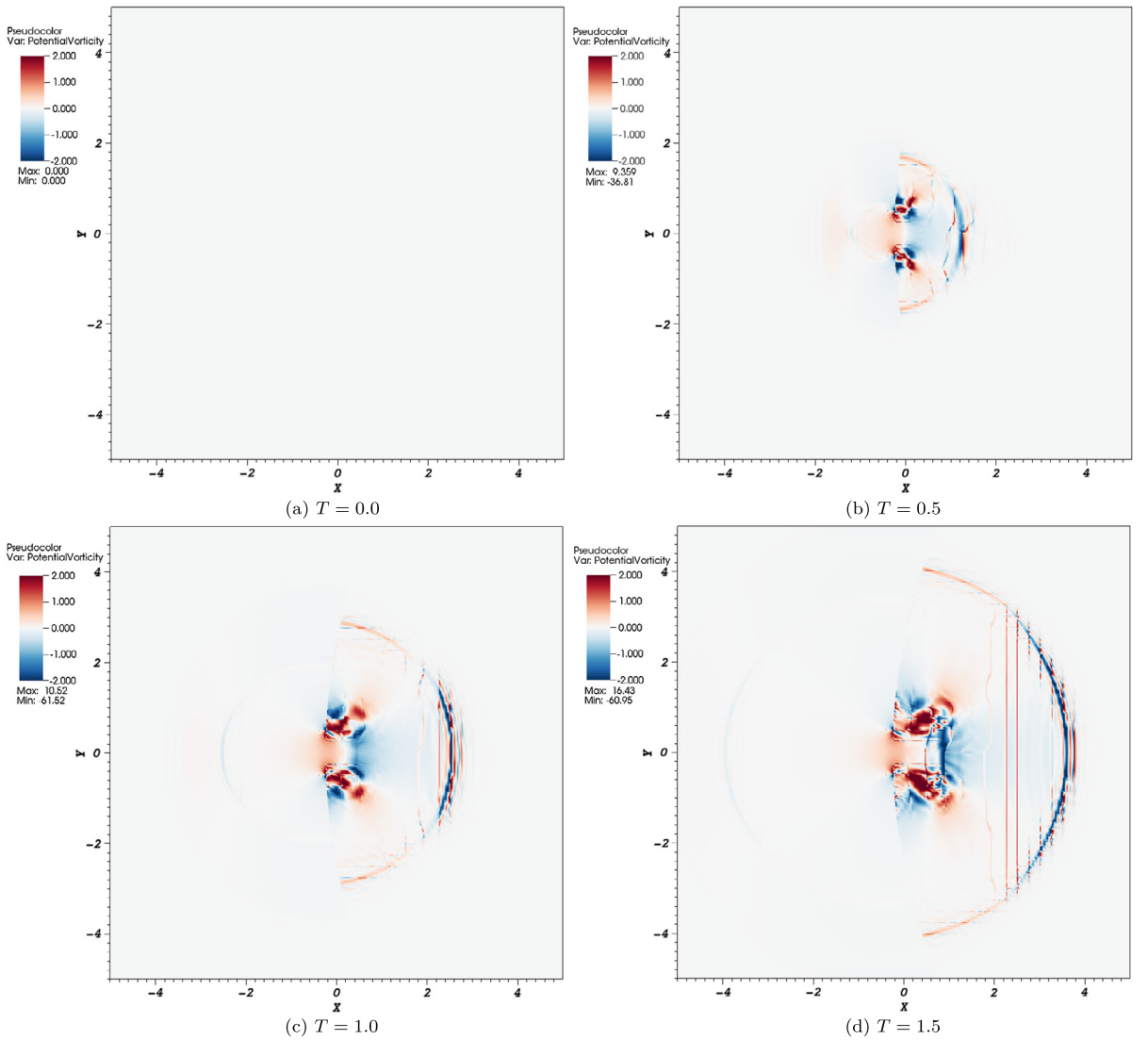
From the grid convergence study we know that the computation is sufficiently well-resolved with polynomial order $N = 5$ in each element. So with $N = 5$, we show the evolution of the water height of the partial dam break problem at times $T = 0.0$, $T = 0.5$, $T = 1.0$, and $T = 1.5$ in Fig. 10. Again for this computation, we chose a time step of $\Delta t = 1/1500$. This numerical test combines each aspect of the ESDGSEM approximation, i.e., a discontinuous solution, curvilinear mesh and discontinuous bottom topography. The pseudocolor plots in Fig. 10 show the propagation of eddies near the dam break. We provide in Fig. 11 a three dimensional visualization of the partial dam break where we can see on the downstream side of the dam the interaction of the flow with the discontinuous bottom topography (5.13). Lastly, Fig. 12 visualizes the evolution of the potential vorticity (5.9) for the partial dam break problem.

The numerical solution of the parabolic dam break problem demonstrates that the entropy stable numerical approximation can capture shock and rarefaction waves. However, the dissipation added to guarantee entropy stability is *not* designed to make the method overshoot free. Additional shock capturing techniques for DG type methods are necessary to remove the remaining spurious oscillations, e.g., [35].

Lastly, we note that a standard DGSEM scheme is unstable when solving the partial dam break problem on a parabolic dam, even for very small time steps, as the water height becomes negative.

## 6. Conclusion

In this work we developed high-order entropy conserving and entropy stable DGSEM discretization for the two dimensional shallow water equations on general curvilinear meshes. To highlight the conservative property of the approximation on curvilinear meshes we reformulated the approximation into an equivalent flux differencing form. With this reformulation it is straightforward to demonstrate local conservation. Applying results of Fisher and Carpenter [20], a careful choice of the numerical volume and surface fluxes leads to an entropy conservative scheme. The flux differencing form also provided additional flexibility to guarantee that the approximation remains well-balanced. For non-constant bottom topographies we found that the recovery of special steady states of the shallow water equations depends on a special discretization of the non-linear source term. By considering a particular source term discretization we maintained well-balancedness for discontinuous bottom topographies in general curvilinear coordinates. Finally, it is known that energy must be dissipated at shocks, but the entropy conserving scheme is dissipation free modulo any dissipative effects of the time integrator. The numerical solution can therefore capture shocks and rarefactions accurately but at the cost of significant post-shock oscillations. Thus, we provided entropy stable numerical surface fluxes to add dissipation to the scheme and control overshoots. Note that the dissipation added is merely the amount necessary to guarantee entropy stability and is *not* designed to make the method




(a) $T = 0.0$ (b) $T = 0.5$

(c) $T = 1.0$ (d) $T = 1.5$

**Fig. 12.** Potential vorticity generated by the ESDGSEM approximation for the parabolic partial dam break at four times with $N = 5$ and $\Delta t = 1/1500$.

overshoot free. Slope limiting or other shock capturing techniques that are compatible with the entropy stable scheme is a subject of ongoing research. It is important to note that the results presented herein have no shock capturing procedures.

We provided six numerical examples to demonstrate and underline the theoretical findings. The simulation of the flow from a parabolic shaped partial dam break exercised each component of the novel ESDGSEM approximation.

## Appendix A. Proof of Proposition 1

**Proof.** We show the flux difference formula (3.48) in $i$-direction and fix $j$. We recall the high-order flux extension on curvilinear grids (3.44)

$$\begin{cases} \tilde{\tilde{F}}_k^{0,j} = \tilde{F}_k^{0,j}, \\ \tilde{\tilde{F}}_k^{i,j} = \sum_{m=i}^{N} \sum_{\ell=0}^{i-1} 2\, Q_{\ell m} \left( F_k^{vol}(\vec{W}^{\ell,j}, \vec{W}^{m,j}) \left\{\!\left\{ Ja_1^1 \right\}\!\right\}_{(\ell,m),j} + G_k^{vol}(\vec{W}^{\ell,j}, \vec{W}^{m,j}) \left\{\!\left\{ Ja_2^1 \right\}\!\right\}_{(\ell,m),j} \right), \quad i = 1, \dots, N, \\ \tilde{\tilde{F}}_k^{N+1,j} = \tilde{F}_k^{N,j}, \end{cases} \tag{A.1}$$

and consider the special cases $i = 0$ and $i = N$ first. For $i = 0$ we have

$$\begin{aligned}\bar{\tilde{F}}_k^{1,j} - \bar{\tilde{F}}_k^{0,j} &= \sum_{m=1}^{N} 2Q_{0m}\left(F_k^{vol}(\vec{W}^{0,j},\vec{W}^{m,j})\left\{\left\{Ja_1^1\right\}\right\}_{(0,m),j} + G_k^{vol}(\vec{W}^{0,j},\vec{W}^{m,j})\left\{\left\{Ja_2^1\right\}\right\}_{(0,m),j}\right) - \tilde{F}_k^{0,j},\\ &= \sum_{m=0}^{N} 2Q_{0m}\left(F_k^{vol}(\vec{W}^{0,j},\vec{W}^{m,j})\left\{\left\{Ja_1^1\right\}\right\}_{(0,m),j} + G_k^{vol}(\vec{W}^{0,j},\vec{W}^{m,j})\left\{\left\{Ja_2^1\right\}\right\}_{(0,m),j}\right),\end{aligned} \tag{A.2}$$

where we use the fact that $Q_{00} = -\frac{1}{2}$. For $i = N$ we have

$$\begin{aligned}\bar{\tilde{F}}_k^{N+1,j} - \bar{\tilde{F}}_k^{N,j} &= \tilde{F}_k^{N,j} - \sum_{m=0}^{N-1} 2Q_{mN}\left(F_k^{vol}(\vec{W}^{m,j},\vec{W}^{N,j})\left\{\left\{Ja_1^1\right\}\right\}_{(m,N),j} + G_k^{vol}(\vec{W}^{m,j},\vec{W}^{N,j})\left\{\left\{Ja_2^1\right\}\right\}_{(m,N),j}\right),\\ &= \tilde{F}_k^{N,j} + \sum_{m=0}^{N-1} 2Q_{Nm}\left(F_k^{vol}(\vec{W}^{m,j},\vec{W}^{N,j})\left\{\left\{Ja_1^1\right\}\right\}_{(m,N),j} + G_k^{vol}(\vec{W}^{m,j},\vec{W}^{N,j})\left\{\left\{Ja_2^1\right\}\right\}_{(m,N),j}\right),\\ &= \sum_{m=0}^{N} 2Q_{Nm}\left(F_k^{vol}(\vec{W}^{m,j},\vec{W}^{N,j})\left\{\left\{Ja_1^1\right\}\right\}_{(m,N),j} + G_k^{vol}(\vec{W}^{m,j},\vec{W}^{N,j})\left\{\left\{Ja_2^1\right\}\right\}_{(m,N),j}\right),\end{aligned} \tag{A.3}$$

where we use the fact that $Q_{NN} = \frac{1}{2}$. For $i = 1,\dots,N-1$ we examine $\bar{\tilde{F}}_k^{i+1,j}$ to get

$$\begin{aligned}\bar{\tilde{F}}_k^{i+1,j} &= \sum_{m=i+1}^{N-1}\sum_{\ell=1}^{i} 2Q_{\ell m}\left(F_k^{vol}(\vec{W}^{\ell,j},\vec{W}^{m,j})\left\{\left\{Ja_1^1\right\}\right\}_{(\ell,m),j} + G_k^{vol}(\vec{W}^{\ell,j},\vec{W}^{m,j})\left\{\left\{Ja_2^1\right\}\right\}_{(\ell,m),j}\right),\\ &= \sum_{m=i}^{N-1}\sum_{\ell=1}^{i} 2Q_{\ell m}\left(F_k^{vol}(\vec{W}^{\ell,j},\vec{W}^{m,j})\left\{\left\{Ja_1^1\right\}\right\}_{(\ell,m),j} + G_k^{vol}(\vec{W}^{\ell,j},\vec{W}^{m,j})\left\{\left\{Ja_2^1\right\}\right\}_{(\ell,m),j}\right)\\ &\quad - \sum_{\ell=1}^{i} 2Q_{\ell i}\left(F_k^{vol}(\vec{W}^{\ell,j},\vec{W}^{i,j})\left\{\left\{Ja_1^1\right\}\right\}_{(\ell,i),j} + G_k^{vol}(\vec{W}^{\ell,j},\vec{W}^{i,j})\left\{\left\{Ja_2^1\right\}\right\}_{(\ell,i),j}\right),\\ &= \sum_{m=i}^{N-1}\sum_{\ell=1}^{i-1} 2Q_{\ell m}\left(F_k^{vol}(\vec{W}^{\ell,j},\vec{W}^{m,j})\left\{\left\{Ja_1^1\right\}\right\}_{(\ell,m),j} + G_k^{vol}(\vec{W}^{\ell,j},\vec{W}^{m,j})\left\{\left\{Ja_2^1\right\}\right\}_{(\ell,m),j}\right)\\ &\quad + \sum_{m=i}^{N-1} 2Q_{im}\left(F_k^{vol}(\vec{W}^{i,j},\vec{W}^{m,j})\left\{\left\{Ja_1^1\right\}\right\}_{(i,m),j} + G_k^{vol}(\vec{W}^{i,j},\vec{W}^{m,j})\left\{\left\{Ja_2^1\right\}\right\}_{(i,m),j}\right)\\ &\quad - \sum_{\ell=1}^{i} 2Q_{\ell i}\left(F_k^{vol}(\vec{W}^{\ell,j},\vec{W}^{i,j})\left\{\left\{Ja_1^1\right\}\right\}_{(\ell,i),j} + G_k^{vol}(\vec{W}^{\ell,j},\vec{W}^{i,j})\left\{\left\{Ja_2^1\right\}\right\}_{(\ell,i),j}\right),\\ &= \bar{\tilde{F}}_k^{i,j} + \sum_{m=1}^{N-1} 2Q_{im}\left(F_k^{vol}(\vec{W}^{i,j},\vec{W}^{m,j})\left\{\left\{Ja_1^1\right\}\right\}_{(i,m),j} + G_k^{vol}(\vec{W}^{i,j},\vec{W}^{m,j})\left\{\left\{Ja_2^1\right\}\right\}_{(i,m),j}\right),\end{aligned} \tag{A.4}$$

where we used that $Q_{ij} = -Q_{ij}$ for $i \neq j$ and $Q_{ii} = 0$ for $i = 1,\dots,N-1$ in the last step. For the general difference we obtain

$$\bar{\tilde{F}}_k^{i+1,j} - \bar{\tilde{F}}_k^{i,j} = \sum_{m=1}^{N-1} 2Q_{im}\left(F_k^{vol}(\vec{W}^{i,j},\vec{W}^{m,j})\left\{\left\{Ja_1^1\right\}\right\}_{(i,m),j} + G_k^{vol}(\vec{W}^{i,j},\vec{W}^{m,j})\left\{\left\{Ja_2^1\right\}\right\}_{(i,m),j}\right). \tag{A.5}$$

Thus, we are able to generalize the calculation of the flux difference for $i = 0,\dots N$

$$\bar{\tilde{F}}_k^{i+1,j} - \bar{\tilde{F}}_k^{i,j} = \sum_{m=0}^{N} 2Q_{im}\left(F_k^{vol}(\vec{W}^{i,j},\vec{W}^{m,j})\left\{\left\{Ja_1^1\right\}\right\}_{(i,m),j} + G_k^{vol}(\vec{W}^{i,j},\vec{W}^{m,j})\left\{\left\{Ja_2^1\right\}\right\}_{(i,m),j}\right). \tag{A.6}$$

We then premultiply by the inverse of $\mathbf{M}$ to obtain the desired flux differencing result (3.48) for $\mathbf{M}^{-1}\boldsymbol{\Delta}\bar{\tilde{\mathbf{F}}}$

$$\frac{\bar{\tilde{F}}_k^{i+1,j} - \bar{\tilde{F}}_k^{i,j}}{\omega_i} = \frac{1}{\omega_i}\sum_{m=0}^{N} 2Q_{im}\left(F_k^{vol}(\vec{W}^{i,j},\vec{W}^{m,j})\left\{\left\{Ja_1^1\right\}\right\}_{(i,m),j} + G_k^{vol}(\vec{W}^{i,j},\vec{W}^{m,j})\left\{\left\{Ja_2^1\right\}\right\}_{(i,m),j}\right). \tag{A.7}$$

An identical strategy can be used in the $j$ index direction to rewrite the flux difference in the $y$-direction, $\overline{\widetilde{\mathbf{G}}}_k \boldsymbol{\Delta}^T \mathbf{M}^{-1}$, in the similar indicial form (3.49). □

## Appendix B. Non-linear correction terms

**Lemma 3** *(Non-linear correction terms). The discrete derivative* **Df** *can be recast into a consistent sub-cell flux-difference formulation for which the Lax–Wendroff theorem holds. Furthermore the term*

$$\boldsymbol{\alpha} \circ \mathbf{D}\boldsymbol{\beta} + \boldsymbol{\beta} \circ \mathbf{D}\boldsymbol{\alpha}, \tag{B.1}$$

*where* $\boldsymbol{\alpha}$ *and* $\boldsymbol{\beta}$ *are the point-wise nodal representations of functions* $\alpha$ *and* $\beta$*, is a consistent and conservative approximation of the derivative of the corresponding flux* $(\alpha\,\beta)_x$*. Similarly, we have for the derivative in* $y$*-direction*

$$\boldsymbol{\alpha} \circ (\boldsymbol{\beta}\,\mathbf{D}^T) + \boldsymbol{\beta} \circ (\boldsymbol{\alpha}\,\mathbf{D}^T), \tag{B.2}$$

*which is a consistent and conservative approximation of the derivative of the corresponding flux* $(\alpha\,\beta)_y$*. If we subtract the discretization of* $(\alpha\,\beta)_x$ *from (B.1) and* $(\alpha\,\beta)_y$ *from (B.2), we obtain the errors in the associated discrete product rules*

$$\begin{aligned} \mathbf{s}_{\alpha\beta} &:= -\mathbf{D}(\boldsymbol{\alpha} \circ \boldsymbol{\beta}) + \boldsymbol{\alpha} \circ \mathbf{D}\boldsymbol{\beta} + \boldsymbol{\beta} \circ \mathbf{D}\boldsymbol{\alpha}, \\ \mathbf{s}^T_{\alpha\beta} &:= -(\boldsymbol{\alpha} \circ \boldsymbol{\beta})\mathbf{D}^T + \boldsymbol{\alpha} \circ \boldsymbol{\beta}\mathbf{D}^T + \boldsymbol{\beta} \circ \boldsymbol{\alpha}\mathbf{D}^T. \end{aligned} \tag{B.3}$$

*The discrete mean value of the terms (B.3) are zero*

$$\begin{aligned} \mathbf{1}^T \mathbf{M}\, \mathbf{s}_{\alpha\beta}\, \mathbf{M}\mathbf{1} &= \mathbf{0}, \\ \mathbf{1}^T \mathbf{M}\, \mathbf{s}^T_{\alpha\beta}\, \mathbf{M}\mathbf{1} &= \mathbf{0}, \end{aligned} \tag{B.4}$$

*for all matrices* $\boldsymbol{\alpha}, \boldsymbol{\beta} \in \mathbb{R}^{(N+1)\times(N+1)}$.

**Proof.** In Fisher et al. [14] the authors proved the first part of the lemma regarding equation (B.1) for any diagonal norm SBP operator, such as the DGSEM-LGL operator. In [16], the author showed that the discrete mean value of terms with a structure as in (B.3) is exactly zero in the one-dimensional case. We demonstrate that the 1D result extends to 2D. Without loss of generality, we examine $\mathbf{s}_{\alpha\beta}$. The discrete mean value is given by

$$\begin{aligned} \mathbf{1}^T \mathbf{M}\, \mathbf{s}_{\alpha\beta}\, \mathbf{M}\mathbf{1} &= -\mathbf{1}^T \left( (\mathbf{MD})(\boldsymbol{\alpha} \circ \boldsymbol{\beta}) + \boldsymbol{\alpha} \circ (\mathbf{MD})\boldsymbol{\beta} + \boldsymbol{\beta} \circ (\mathbf{MD})\boldsymbol{\alpha} \right) \mathbf{M}\mathbf{1}, \\ &= \mathbf{1}^T \left( -(\mathbf{B} - \mathbf{D}^T\mathbf{M})(\boldsymbol{\alpha} \circ \boldsymbol{\beta}) + \boldsymbol{\alpha} \circ (\mathbf{B} - \mathbf{D}^T\mathbf{M})\boldsymbol{\beta} + \boldsymbol{\beta} \circ (\mathbf{MD})\boldsymbol{\alpha} \right) \mathbf{M}\mathbf{1}, \\ &= \mathbf{1}^T \left( \mathbf{D}^T\mathbf{M}(\boldsymbol{\alpha} \circ \boldsymbol{\beta}) - \boldsymbol{\alpha} \circ (\mathbf{D}^T\mathbf{M})\boldsymbol{\beta} + \boldsymbol{\beta} \circ (\mathbf{MD})\boldsymbol{\alpha} \right) \mathbf{M}\mathbf{1}, \\ &= (\mathbf{D}\mathbf{1})\mathbf{M}(\boldsymbol{\alpha} \circ \boldsymbol{\beta}) + \mathbf{1}^T \left( -\boldsymbol{\alpha} \circ (\mathbf{D}^T\mathbf{M})\boldsymbol{\beta} + \boldsymbol{\beta} \circ (\mathbf{MD})\boldsymbol{\alpha} \right) \mathbf{M}\mathbf{1}, \\ &= \mathbf{1}^T \left( -\boldsymbol{\alpha} \circ (\mathbf{D}^T\mathbf{M})\boldsymbol{\beta} + \boldsymbol{\beta} \circ (\mathbf{MD})\boldsymbol{\alpha} \right) \mathbf{M}\mathbf{1}, \end{aligned} \tag{B.5}$$

where we used in the calculation (B.5) that the diagonal matrices $\mathbf{M}$ and $\mathbf{B}$ commute with the Hadamard product. We introduce additional notation to split matrices column by column

$$\boldsymbol{\beta}_i := \begin{pmatrix} 0 & & \beta_{0i} & 0 & \\ & \ddots & \vdots & & \ddots \\ & 0 & \beta_{Ni} & & 0 \end{pmatrix}, \quad \boldsymbol{\alpha}_i := \begin{pmatrix} 0 & & \alpha_{0i} & 0 & \\ & \ddots & \vdots & & \ddots \\ & 0 & \alpha_{Ni} & & 0 \end{pmatrix}, \tag{B.6}$$

With this notation, we have

$$\boldsymbol{\beta} = \sum_{i=0}^{N} \boldsymbol{\beta}_i, \quad \boldsymbol{\alpha} = \sum_{i=0}^{N} \boldsymbol{\alpha}_i, \tag{B.7}$$

and thus simplify (B.5) further to find

$$\begin{aligned} \mathbf{1}^T \mathbf{M}\, \mathbf{s}_{\alpha\beta}\, \mathbf{M}\mathbf{1} &= \mathbf{1}^T \left( -\boldsymbol{\alpha} \circ (\mathbf{D}^T\mathbf{M}) \left( \sum_{i=0}^{N} \boldsymbol{\beta}_i \right) + \boldsymbol{\beta} \circ (\mathbf{MD}) \left( \sum_{i=0}^{N} \boldsymbol{\alpha}_i \right) \right) \mathbf{M}\mathbf{1}, \\ &= \mathbf{1}^T \left( -\left( \sum_{i=0}^{N} \boldsymbol{\alpha} \circ (\mathbf{D}^T\mathbf{M})\boldsymbol{\beta}_i \right) + \left( \sum_{i=0}^{N} \boldsymbol{\beta} \circ (\mathbf{MD})\boldsymbol{\alpha}_i \right) \right) \mathbf{M}\mathbf{1}. \end{aligned} \tag{B.8}$$

We denote the $i$-th column of $\boldsymbol{\alpha}$ by $\vec{\alpha}_i$ and the $i$-th column of $\boldsymbol{\beta}$ by $\vec{\beta}_i$. With this column-wise notation we find

$$\begin{aligned}\boldsymbol{\alpha} \circ (\mathbf{D}^T\mathbf{M})\boldsymbol{\beta}_i &= \operatorname{diag}(\vec{\alpha}_i)(\mathbf{D}^T\mathbf{M})\boldsymbol{\beta}_i,\\ \boldsymbol{\beta} \circ (\mathbf{MD})\boldsymbol{\alpha}_i &= \operatorname{diag}(\vec{\beta}_i)(\mathbf{MD})\boldsymbol{\alpha}_i.\end{aligned} \tag{B.9}$$

Substituting (B.9) into (B.8) we find

$$\begin{aligned}\mathbf{1}^T\mathbf{M}\,\mathbf{s}_{\alpha\beta}\,\mathbf{M}\mathbf{1} &= \mathbf{1}^T\left(-\left(\sum_{i=0}^{N}\operatorname{diag}(\vec{\alpha}_i)(\mathbf{D}^T\mathbf{M})\boldsymbol{\beta}_i\right)+\left(\sum_{i=0}^{N}\operatorname{diag}(\vec{\beta}_i)(\mathbf{MD})\boldsymbol{\alpha}_i\right)\right)\mathbf{M}\mathbf{1},\\ &= \left(\sum_{i=0}^{N}\left(-\mathbf{1}^T\operatorname{diag}(\vec{\alpha}_i)(\mathbf{D}^T\mathbf{M})\boldsymbol{\beta}_i+\mathbf{1}^T\operatorname{diag}(\vec{\beta}_i)(\mathbf{MD})\boldsymbol{\alpha}_i\right)\right)\mathbf{M}\mathbf{1},\\ &= \left(\sum_{i=0}^{N}\left(-\vec{\alpha}_i^T(\mathbf{D}^T\mathbf{M})\boldsymbol{\beta}_i+\vec{\beta}_i^T(\mathbf{MD})\boldsymbol{\alpha}_i\right)\right)\mathbf{M}\mathbf{1}.\end{aligned} \tag{B.10}$$

We examine the interior terms of (B.10) individually. Note that the quantity $-\vec{\alpha}_i^T(\mathbf{D}^T\mathbf{M})\boldsymbol{\beta}_i+\vec{\beta}_i^T(\mathbf{MD})\boldsymbol{\alpha}_i$ is only non-zero in the $i$-th column. The $i$-th column entries are

$$-\vec{\alpha}_i^T(\mathbf{D}^T\mathbf{M})\vec{\beta}_i+\vec{\beta}_i^T(\mathbf{MD})\vec{\alpha}_i = -\vec{\alpha}_i^T(\mathbf{D}^T\mathbf{M})\vec{\beta}_i+\vec{\alpha}_i^T(\mathbf{D}^T\mathbf{M})\vec{\beta}_i = \vec{0}. \tag{B.11}$$

Thus, each entry of the terms in the sum (B.10) vanish. So it follows that the discrete mean value $\mathbf{1}^T\mathbf{M}\,\mathbf{s}_{\alpha\beta}\,\mathbf{M}\mathbf{1}=0$. The proof for $\mathbf{s}_{\alpha\beta}^T$ is done similarly. □

## Appendix C. Proof of Theorem 1

### C.1. Proof of Property 1.2

**Proof.** To thoroughly show that the DGSEM scheme is entropy conserving we connect to the split-form DG scheme that is implicitly solved by the flux differencing formulation. We obtain a discrete equation for the entropy by adding the discrete equations scaled by the entropy variables $\vec{q}=(g(h+b)-\frac{1}{2}u^2-\frac{1}{2}v^2,u,v)$. We examine the full split forms individually. To obtain the extended split forms, we use Lemma 1 from [30], which, extended to two dimensions with omitted $j$-index, states

$$\begin{aligned}\sum_{m=0}^{N}2\mathbf{D}_{im}\{\{a\}\}_{im} &= (\mathbf{Da})_i,\\ \sum_{m=0}^{N}2\mathbf{D}_{im}\{\{a\}\}_{im}\{\{b\}\}_{im} &= \frac{1}{2}(\mathbf{D}(\mathbf{a}\circ\mathbf{b})+\mathbf{a}\circ\mathbf{Db}+\mathbf{b}\circ\mathbf{Da})_i,\\ \sum_{m=0}^{N}2\mathbf{D}_{im}\{\{a\}\}_{im}\{\{b\}\}_{im}\{\{c\}\}_{im} &= \frac{1}{4}(\mathbf{D}(\mathbf{a}\circ\mathbf{b}\circ\mathbf{c})+\mathbf{a}\circ\mathbf{D}(\mathbf{b}\circ\mathbf{c})+\mathbf{b}\circ\mathbf{D}(\mathbf{a}\circ\mathbf{c})+\mathbf{c}\circ\mathbf{D}(\mathbf{a}\circ\mathbf{b})\\ &\quad+\mathbf{b}\circ\mathbf{c}\circ\mathbf{Da}+\mathbf{a}\circ\mathbf{c}\circ\mathbf{Db}+\mathbf{a}\circ\mathbf{b}\circ\mathbf{Dc})_i.\end{aligned} \tag{C.1}$$

Note that these terms can be recast into an equivalent forms where the $\mathbf{D}$ matrix is applied to the full product. For the single average this is already the case. For the second equation we see

$$\frac{1}{2}(\mathbf{D}(\mathbf{a}\circ\mathbf{b})+\mathbf{a}\circ\mathbf{Db}+\mathbf{b}\circ\mathbf{Da})_i = \mathbf{D}(\mathbf{a}\circ\mathbf{b})+\frac{1}{2}(-\mathbf{D}(\mathbf{a}\circ\mathbf{b})+\mathbf{a}\circ\mathbf{Db}+\mathbf{b}\circ\mathbf{Da}), \tag{C.2}$$

where the right hand side term is the desired term plus a discrete product rule error term. For the triple averages we find that

$$\begin{aligned}&\frac{1}{4}(\mathbf{D}(\mathbf{a}\circ\mathbf{b}\circ\mathbf{c})+\mathbf{a}\circ\mathbf{D}(\mathbf{b}\circ\mathbf{c})+\mathbf{b}\circ\mathbf{D}(\mathbf{a}\circ\mathbf{c})+\mathbf{c}\circ\mathbf{D}(\mathbf{a}\circ\mathbf{b})+\mathbf{b}\circ\mathbf{c}\circ\mathbf{Da}+\mathbf{a}\circ\mathbf{c}\circ\mathbf{Db}+\mathbf{a}\circ\mathbf{b}\circ\mathbf{Dc})_i,\\ &\quad=\mathbf{D}(\mathbf{a}\circ\mathbf{b}\circ\mathbf{c})_i+\frac{1}{4}(-\mathbf{D}(\mathbf{a}\circ\mathbf{b}\circ\mathbf{c})+\mathbf{a}\circ\mathbf{D}(\mathbf{b}\circ\mathbf{c})+\mathbf{b}\circ\mathbf{c}\circ\mathbf{Da})_i\\ &\qquad+\frac{1}{4}(-\mathbf{D}(\mathbf{a}\circ\mathbf{b}\circ\mathbf{c})+\mathbf{b}\circ\mathbf{D}(\mathbf{a}\circ\mathbf{c})+\mathbf{a}\circ\mathbf{c}\circ\mathbf{Db})_i\\ &\qquad+\frac{1}{4}(-\mathbf{D}(\mathbf{a}\circ\mathbf{b}\circ\mathbf{c})+\mathbf{c}\circ\mathbf{D}(\mathbf{a}\circ\mathbf{b})+\mathbf{a}\circ\mathbf{b}\circ\mathbf{Dc})_i,\end{aligned} \tag{C.3}$$

where, once again, we have the **D** matrix applied to the full product and three discrete product rule error terms. We know from Lemma 3 that these discrete product rule error terms do not affect the conservation property. For the first term we will later use the SBP Properties Lemma 1 to have a conservative approximation to the derivative plus a surface term

$$\mathbf{D}(\mathbf{a}\circ\mathbf{b}\circ\mathbf{c}) = -\mathbf{S}(\mathbf{a}\circ\mathbf{b}\circ\mathbf{c}) + \hat{\mathbf{D}}(\mathbf{a}\circ\mathbf{b}\circ\mathbf{c}). \tag{C.4}$$

This surface term will be taken into consideration to show that the total surface contributions are zero.

We proceed by extending the flux differencing formulation into full split forms for all three equations. The first equation in flux differencing form is

$$\begin{aligned}
&\mathbf{J}\circ(\mathbf{h})_t + \sum_{m=0}^{N} 2\,\mathbf{D}_{im}\left(\{\{hu\}\}_{(i,m),j}\left\{\left\{y_\eta\right\}\right\}_{(i,m),j} + \{\{hv\}\}_{(i,m),j}\left\{\left\{-x_\eta\right\}\right\}_{(i,m),j}\right)\\
&\quad + \sum_{m=0}^{N} 2\,\mathbf{D}_{mj}\left(\{\{hu\}\}_{i,(j,m)}\left\{\left\{-y_\xi\right\}\right\}_{i,(j,m)} + \{\{hv\}\}_{i,(j,m)}\left\{\left\{x_\xi\right\}\right\}_{i,(j,m)}\right)\\
&\quad = \mathbf{S}\left(\tilde{\mathbf{F}}_1^* - \tilde{\mathbf{F}}_1\right) + \left(\tilde{\mathbf{G}}_1^* - \tilde{\mathbf{G}}_1\right)\mathbf{S},
\end{aligned} \tag{C.5}$$

and, extended to full split form using (C.1), becomes

$$\begin{aligned}
&\mathbf{J}\circ(\mathbf{h})_t + \frac{1}{2}\left(\mathbf{D}(\mathbf{h}\circ\mathbf{u}\circ\mathbf{y}_\eta) + \mathbf{y}_\eta\circ\mathbf{D}(\mathbf{h}\circ\mathbf{u}) + \mathbf{h}\circ\mathbf{u}\circ\mathbf{D}(\mathbf{y}_\eta)\right) - \frac{1}{2}\left(\mathbf{D}(\mathbf{h}\circ\mathbf{v}\circ\mathbf{x}_\eta) + \mathbf{x}_\eta\circ\mathbf{D}(\mathbf{h}\circ\mathbf{v}) + \mathbf{h}\circ\mathbf{v}\circ\mathbf{D}\mathbf{x}_\eta\right)\\
&\quad - \frac{1}{2}\left((\mathbf{h}\circ\mathbf{u}\circ\mathbf{y}_\xi)\mathbf{D}^T + \mathbf{y}_\xi\circ(\mathbf{h}\circ\mathbf{u})\mathbf{D}^T + \mathbf{h}\circ\mathbf{u}\circ(\mathbf{y}_\xi)\mathbf{D}^T\right)\\
&\quad + \frac{1}{2}\left((\mathbf{h}\circ\mathbf{v}\circ\mathbf{x}_\xi)\mathbf{D}^T + \mathbf{x}_\xi\circ(\mathbf{h}\circ\mathbf{v})\mathbf{D}^T + \mathbf{h}\circ\mathbf{v}\circ\mathbf{x}_\xi\mathbf{D}^T\right)\\
&\quad = \mathbf{S}\left(\tilde{\mathbf{F}}_1^* - \tilde{\mathbf{F}}_1\right) + \left(\tilde{\mathbf{G}}_1^* - \tilde{\mathbf{G}}_1\right)\mathbf{S}.
\end{aligned} \tag{C.6}$$

For the $hu$ equation

$$\begin{aligned}
&\mathbf{J}\circ(\mathbf{hu})_t + \sum_{m=0}^{N} 2\,\mathbf{D}_{im}\left(\{\{hu\}\}_{(i,m),j}\left\{\left\{y_\eta\right\}\right\}_{(i,m),j}\{\{u\}\}_{(i,m),j} + g\,\{\{h\}\}^2_{(i,m),j}\left\{\left\{y_\eta\right\}\right\}_{(i,m),j}\right.\\
&\quad \left. - \frac{1}{2}g\left\{\left\{h^2\right\}\right\}_{(i,m),j}\left\{\left\{y_\eta\right\}\right\}_{(i,m),j} - \{\{hv\}\}_{(i,m),j}\left\{\left\{x_\eta\right\}\right\}_{(i,m),j}\{\{u\}\}_{(i,m),j}\right)\\
&\quad + \sum_{m=0}^{N} 2\,\mathbf{D}_{jm}\left(-\{\{hu\}\}_{i,(j,m)}\left\{\left\{y_\xi\right\}\right\}_{i,(j,m)}\{\{u\}\}_{i,(j,m)} - g\,\{\{h\}\}^2_{i,(j,m)}\left\{\left\{y_\xi\right\}\right\}_{i,(j,m)}\right.\\
&\quad \left. + \frac{1}{2}g\left\{\left\{h^2\right\}\right\}_{i,(j,m)}\left\{\left\{y_\xi\right\}\right\}_{i,(j,m)} + \{\{hv\}\}_{i,(j,m)}\left\{\left\{x_\xi\right\}\right\}_{i,(j,m)}\{\{u\}\}_{i,(j,m)}\right)\\
&\quad = \mathbf{S}\left(\tilde{\mathbf{F}}_2^* - \tilde{\mathbf{F}}_2\right) + \left(\tilde{\mathbf{G}}_2^* - \tilde{\mathbf{G}}_2\right)\mathbf{S} + \mathbf{source}_2,
\end{aligned} \tag{C.7}$$

we substitute the source term discretization (4.5) and use the average extensions (C.1) to find

$$\begin{aligned}
&\mathbf{J}\circ(\mathbf{hu})_t + \frac{1}{4}\left(\mathbf{D}\left(\mathbf{hu}\circ\mathbf{u}\circ\mathbf{y}_\eta\right) + \mathbf{hu}\circ\mathbf{D}\left(\mathbf{y}_\eta\circ\mathbf{u}\right) + \mathbf{y}_\eta\circ\mathbf{D}\left(\mathbf{hu}\circ\mathbf{u}\right) + \mathbf{u}\circ\mathbf{D}\left(\mathbf{y}_\eta\circ\mathbf{hu}\right) + \mathbf{hu}\circ\mathbf{u}\circ\mathbf{D}\left(\mathbf{y}_\eta\right)\right.\\
&\quad \left. + \mathbf{y}_\eta\circ\mathbf{hu}\circ\mathbf{Du} + \mathbf{u}\circ\mathbf{y}_\eta\circ\mathbf{D}\left(\mathbf{hu}\right)\right) - \frac{1}{4}\left(\mathbf{D}\left(\mathbf{hv}\circ\mathbf{u}\circ\mathbf{x}_\eta\right) + \mathbf{hv}\circ\mathbf{D}\left(\mathbf{x}_\eta\circ\mathbf{u}\right)\right.\\
&\quad \left. + \mathbf{x}_\eta\circ\mathbf{D}\left(\mathbf{hv}\circ\mathbf{u}\right) + \mathbf{u}\circ\mathbf{D}\left(\mathbf{x}_\eta\circ\mathbf{hv}\right) + \mathbf{hv}\circ\mathbf{u}\circ\mathbf{D}\left(\mathbf{x}_\eta\right) + \mathbf{x}_\eta\circ\mathbf{hv}\circ\mathbf{Du} + \mathbf{x}_\eta\circ\mathbf{u}\circ\mathbf{D}\left(\mathbf{hv}\right)\right)\\
&\quad + \frac{1}{2}g\left(\mathbf{h}\circ\mathbf{D}\left(\mathbf{y}_\eta\circ(\mathbf{h}+\mathbf{b})\right) + \mathbf{y}_\eta\circ\mathbf{h}\circ\mathbf{D}\left(\mathbf{h}+\mathbf{b}\right)\right) - \frac{1}{4}\left(\left(\mathbf{hu}\circ\mathbf{u}\circ\mathbf{y}_\xi\right)\mathbf{D}^T + \mathbf{hu}\circ\left(\mathbf{y}_\xi\circ\mathbf{u}\right)\mathbf{D}^T\right.\\
&\quad \left. + \mathbf{y}_\xi\circ(\mathbf{hu}\circ\mathbf{u})\,\mathbf{D}^T + \mathbf{u}\circ\left(\mathbf{y}_\xi\circ\mathbf{hu}\right)\mathbf{D}^T + \mathbf{hu}\circ\mathbf{u}\circ\left(\mathbf{y}_\xi\right)\mathbf{D}^T + \mathbf{y}_\xi\circ\mathbf{hu}\circ\mathbf{u}\mathbf{D}^T + \mathbf{y}_\xi\circ\mathbf{u}\circ(\mathbf{hu})\,\mathbf{D}^T\right)\\
&\quad + \frac{1}{4}\left(\left(\mathbf{hv}\circ\mathbf{u}\circ\mathbf{x}_\xi\right)\mathbf{D}^T + \mathbf{hv}\circ\left(\mathbf{x}_\xi\circ\mathbf{u}\right)\mathbf{D}^T + \mathbf{x}_\xi\circ(\mathbf{hv}\circ\mathbf{u})\,\mathbf{D}^T + \mathbf{u}\circ\left(\mathbf{x}_\xi\circ\mathbf{hv}\right)\mathbf{D}^T + \mathbf{hv}\circ\mathbf{u}\circ\left(\mathbf{x}_\xi\right)\mathbf{D}^T\right.\\
&\quad \left. + \mathbf{x}_\xi\circ\mathbf{hv}\circ\mathbf{u}\mathbf{D}^T + \mathbf{x}_\xi\circ\mathbf{u}\circ(\mathbf{hv})\,\mathbf{D}^T\right) - \frac{1}{2}g\left(\mathbf{h}\circ\left(\mathbf{y}_\xi\circ(\mathbf{h}+\mathbf{b})\right)\mathbf{D}^T + \mathbf{y}_\xi\circ\mathbf{h}\circ(\mathbf{h}+\mathbf{b})\,\mathbf{D}^T\right)\\
&\quad = \mathbf{S}\left(\tilde{\mathbf{F}}_2^* - \tilde{\mathbf{F}}_2\right) + \left(\tilde{\mathbf{G}}_2^* - \tilde{\mathbf{G}}_2\right)\mathbf{S} - \frac{g}{2}\mathbf{M}^{-1}\left(\mathbf{y}_\eta\circ\{\{\mathbf{h}\}\}_\xi\circ[\![\mathbf{b}]\!]_\xi\right) - \frac{g}{2}\left(-\mathbf{y}_\xi\circ\{\{\mathbf{h}\}\}_\eta\circ[\![\mathbf{b}]\!]_\eta\right)\mathbf{M}^{-1}.
\end{aligned} \tag{C.8}$$

Analogously, we obtain the full split form extension of the $hv$ equation

$$
\begin{aligned}
&\mathbf{J}\circ(\mathbf{hv})_t + \frac{1}{4}\left(\mathbf{D}\left(\mathbf{hu}\circ\mathbf{v}\circ\mathbf{y}_\eta\right) + \mathbf{hu}\circ\mathbf{D}\left(\mathbf{y}_\eta\circ\mathbf{v}\right) + \mathbf{y}_\eta\circ\mathbf{D}\left(\mathbf{hu}\circ\mathbf{v}\right) + \mathbf{v}\circ\mathbf{D}\left(\mathbf{y}_\eta\circ\mathbf{hu}\right)\right.\\
&\quad\left. + \mathbf{hu}\circ\mathbf{v}\circ\mathbf{D}\left(\mathbf{y}_\eta\right) + \mathbf{y}_\eta\circ\mathbf{hu}\circ\mathbf{Dv} + \mathbf{v}\circ\mathbf{y}_\eta\circ\mathbf{D}\left(\mathbf{hu}\right)\right)\\
&\quad - \frac{1}{4}\left(\mathbf{D}\left(\mathbf{hv}\circ\mathbf{v}\circ\mathbf{x}_\eta\right) + \mathbf{hv}\circ\mathbf{D}\left(\mathbf{x}_\eta\circ\mathbf{v}\right) + \mathbf{x}_\eta\circ\mathbf{D}\left(\mathbf{hv}\circ\mathbf{v}\right) + \mathbf{v}\circ\mathbf{D}\left(\mathbf{x}_\eta\circ\mathbf{hv}\right) + \mathbf{hv}\circ\mathbf{v}\circ\mathbf{D}\left(\mathbf{x}_\eta\right)\right.\\
&\quad\left. + \mathbf{x}_\eta\circ\mathbf{hv}\circ\mathbf{Dv} + \mathbf{x}_\eta\circ\mathbf{v}\circ\mathbf{D}\left(\mathbf{hv}\right)\right) - \frac{1}{2}g\left(\mathbf{h}\circ\mathbf{D}\left(\mathbf{x}_\eta\circ(\mathbf{h}+\mathbf{b})\right) + \mathbf{x}_\eta\circ\mathbf{h}\circ\mathbf{D}\left(\mathbf{h}+\mathbf{b}\right)\right)\\
&\quad - \frac{1}{4}\left(\left(\mathbf{hu}\circ\mathbf{v}\circ\mathbf{y}_\xi\right)\mathbf{D}^T + \mathbf{hu}\circ\left(\mathbf{y}_\xi\circ\mathbf{v}\right)\mathbf{D}^T + \mathbf{y}_\xi\circ\left(\mathbf{hu}\circ\mathbf{v}\right)\mathbf{D}^T + \mathbf{v}\circ\left(\mathbf{y}_\xi\circ\mathbf{hu}\right)\mathbf{D}^T + \mathbf{hu}\circ\mathbf{v}\circ\left(\mathbf{y}_\xi\right)\mathbf{D}^T\right.\\
&\qquad\left. + \mathbf{y}_\xi\circ\mathbf{hu}\circ\mathbf{v}\mathbf{D}^T + \mathbf{y}_\xi\circ\circ\mathbf{v}\circ\left(\mathbf{hu}\right)\mathbf{D}^T\right)\\
&\quad + \frac{1}{4}\left(\left(\mathbf{hv}\circ\mathbf{v}\circ\mathbf{x}_\xi\right)\mathbf{D}^T + \mathbf{hv}\circ\left(\mathbf{x}_\xi\circ\mathbf{v}\right)\mathbf{D}^T + \mathbf{x}_\xi\circ\left(\mathbf{hv}\circ\mathbf{v}\right)\mathbf{D}^T + \mathbf{v}\circ\left(\mathbf{x}_\xi\circ\mathbf{hv}\right)\mathbf{D}^T + \mathbf{hv}\circ\mathbf{v}\circ\left(\mathbf{x}_\xi\right)\mathbf{D}^T\right.\\
&\quad\left. + \mathbf{x}_\xi\circ\mathbf{hv}\circ\mathbf{v}\mathbf{D}^T + \mathbf{x}_\xi\circ\mathbf{v}\circ\left(\mathbf{hv}\right)\mathbf{D}^T\right) - \frac{1}{2}g\left(\mathbf{h}\circ\left(\mathbf{x}_\xi\circ(\mathbf{h}+\mathbf{b})\right)\mathbf{D}^T + \mathbf{x}_\xi\circ\mathbf{h}\circ(\mathbf{h}+\mathbf{b})\,\mathbf{D}^T\right)\\
&\quad = \mathbf{S}\left(\tilde{\mathbf{F}}_3^* - \tilde{\mathbf{F}}_3\right) + \left(\tilde{\mathbf{G}}_3^* - \tilde{\mathbf{G}}_3\right)\mathbf{S} - \frac{g}{2}\mathbf{M}^{-1}\left(-\mathbf{x}_\eta\circ\{\{\mathbf{h}\}\}_\xi\circ[\![\mathbf{b}]\!]_\xi\right) - \frac{g}{2}\left(\mathbf{x}_\xi\circ\{\{\mathbf{h}\}\}_\eta\circ[\![\mathbf{b}]\!]_\eta\right)\mathbf{M}^{-1}.
\end{aligned}
\tag{C.9}
$$

We add the three equations (C.6), (C.8) and (C.9), scaled by the entropy variables $\vec{q} = \left(g(h+b) - \frac{1}{2}u^2 - \frac{1}{2}v^2, u, v\right)$, to show that the scheme fulfills a discrete entropy conservation law. For simplicity we sort each piece by their metric terms in this step. The scaled $h$-equation is

$$
\begin{aligned}
&\left(g(\mathbf{h}+\mathbf{b}) - \frac{1}{2}\mathbf{u}^2 - \frac{1}{2}\mathbf{v}^2\right)\circ\mathbf{J}\circ(\mathbf{h})_t\\
&+ \frac{1}{2}g\left[\mathbf{h}\circ\mathbf{D}(\mathbf{h}\circ\mathbf{u}\circ\mathbf{y}_\eta) + \mathbf{h}\circ\mathbf{y}_\eta\circ\mathbf{D}(\mathbf{h}\circ\mathbf{u}) + \mathbf{h}^2\circ\mathbf{u}\circ\mathbf{D}(\mathbf{y}_\eta) + \mathbf{b}\circ\mathbf{D}(\mathbf{h}\circ\mathbf{u}\circ\mathbf{y}_\eta)\right.\\
&\left.+ \mathbf{b}\circ\mathbf{y}_\eta\circ\mathbf{D}(\mathbf{h}\circ\mathbf{u}) + \mathbf{b}\circ\mathbf{h}\circ\mathbf{u}\circ\mathbf{D}(\mathbf{y}_\eta)\right]\\
&- \frac{1}{4}\left[\mathbf{u}^2\circ\mathbf{D}(\mathbf{h}\circ\mathbf{u}\circ\mathbf{y}_\eta) + \mathbf{y}_\eta\circ\mathbf{u}^2\circ\mathbf{D}(\mathbf{h}\circ\mathbf{u}) + \mathbf{h}\circ\mathbf{u}^3\circ\mathbf{D}(\mathbf{y}_\eta) + \mathbf{v}^2\circ\mathbf{D}(\mathbf{h}\circ\mathbf{u}\circ\mathbf{y}_\eta)\right.\\
&\left.+ \mathbf{y}_\eta\circ\mathbf{v}^2\circ\mathbf{D}(\mathbf{h}\circ\mathbf{u}) + \mathbf{h}\circ\mathbf{u}\circ\mathbf{v}^2\circ\mathbf{D}(\mathbf{y}_\eta)\right]\\
&- \frac{1}{2}g\left[\mathbf{h}\circ(\mathbf{h}\circ\mathbf{u}\circ\mathbf{y}_\xi)\mathbf{D}^T + \mathbf{y}_\xi\circ\mathbf{h}\circ(\mathbf{h}\circ\mathbf{u})\mathbf{D}^T + \mathbf{h}^2\circ\mathbf{u}\circ(\mathbf{y}_\xi)\mathbf{D}^T + \mathbf{b}\circ(\mathbf{h}\circ\mathbf{u}\circ\mathbf{y}_\xi)\mathbf{D}^T\right.\\
&\left.+ \mathbf{y}_\xi\circ\mathbf{b}\circ(\mathbf{h}\circ\mathbf{u})\mathbf{D}^T + \mathbf{h}\circ\mathbf{b}\circ\mathbf{u}\circ(\mathbf{y}_\xi)\mathbf{D}^T\right]\\
&+ \frac{1}{4}\left[\mathbf{u}^2\circ(\mathbf{h}\circ\mathbf{u}\circ\mathbf{y}_\xi)\mathbf{D}^T + \mathbf{y}_\xi\circ\mathbf{u}^2\circ(\mathbf{h}\circ\mathbf{u})\mathbf{D}^T + \mathbf{h}\circ\mathbf{u}^3\circ(\mathbf{y}_\xi)\mathbf{D}^T + \mathbf{v}^2\circ(\mathbf{h}\circ\mathbf{u}\circ\mathbf{y}_\xi)\mathbf{D}^T\right.\\
&\left.+ \mathbf{y}_\xi\circ\mathbf{v}^2\circ(\mathbf{h}\circ\mathbf{u})\mathbf{D}^T + \mathbf{h}\circ\mathbf{u}\circ\mathbf{v}^2\circ(\mathbf{y}_\xi)\mathbf{D}^T\right]\\
&- \frac{1}{2}g\left[\mathbf{h}\circ\mathbf{D}(\mathbf{h}\circ\mathbf{v}\circ\mathbf{x}_\eta) + \mathbf{x}_\eta\circ\mathbf{h}\circ\mathbf{D}(\mathbf{h}\circ\mathbf{v}) + \mathbf{h}^2\circ\mathbf{v}\circ\mathbf{D}(\mathbf{x}_\eta) + \mathbf{b}\circ\mathbf{D}(\mathbf{h}\circ\mathbf{v}\circ\mathbf{x}_\eta)\right.\\
&\left.+ \mathbf{x}_\eta\circ\mathbf{b}\circ\mathbf{D}(\mathbf{h}\circ\mathbf{v}) + \mathbf{h}\circ\mathbf{v}\circ\mathbf{b}\circ\mathbf{D}(\mathbf{x}_\eta)\right]\\
&+ \frac{1}{4}\left[\mathbf{u}^2\circ\mathbf{D}(\mathbf{h}\circ\mathbf{v}\circ\mathbf{x}_\eta) + \mathbf{x}_\eta\circ\mathbf{u}^2\circ\mathbf{D}(\mathbf{h}\circ\mathbf{v}) + \mathbf{h}\circ\mathbf{u}^2\circ\mathbf{v}\circ\mathbf{D}(\mathbf{x}_\eta) + \mathbf{v}^2\circ\mathbf{D}(\mathbf{h}\circ\mathbf{v}\circ\mathbf{x}_\eta)\right.\\
&\left.+ \mathbf{x}_\eta\circ\mathbf{v}^2\circ\mathbf{D}(\mathbf{h}\circ\mathbf{v}) + \mathbf{h}\circ\mathbf{v}^3\circ\mathbf{D}(\mathbf{x}_\eta)\right]\\
&+ \frac{1}{2}g\left[\mathbf{h}\circ(\mathbf{h}\circ\mathbf{v}\circ\mathbf{x}_\xi)\mathbf{D}^T + \mathbf{x}_\xi\circ\mathbf{h}\circ(\mathbf{h}\circ\mathbf{v})\mathbf{D}^T + \mathbf{h}^2\circ\mathbf{v}\circ(\mathbf{x}_\xi)\mathbf{D}^T + \mathbf{b}\circ(\mathbf{h}\circ\mathbf{v}\circ\mathbf{x}_\xi)\mathbf{D}^T\right.\\
&\left.+ \mathbf{x}_\xi\circ\mathbf{b}\circ(\mathbf{h}\circ\mathbf{v})\mathbf{D}^T + \mathbf{h}\circ\mathbf{v}\circ\mathbf{b}\circ(\mathbf{x}_\xi)\mathbf{D}^T\right]\\
&- \frac{1}{4}\left[\mathbf{u}^2\circ(\mathbf{h}\circ\mathbf{v}\circ\mathbf{x}_\xi)\mathbf{D}^T + \mathbf{x}_\xi\circ\mathbf{u}^2\circ(\mathbf{h}\circ\mathbf{v})\mathbf{D}^T + \mathbf{h}\circ\mathbf{v}\circ\mathbf{u}^2\circ(\mathbf{x}_\xi)\mathbf{D}^T + \mathbf{v}^2\circ(\mathbf{h}\circ\mathbf{v}\circ\mathbf{x}_\xi)\mathbf{D}^T\right.\\
&\left.+ \mathbf{x}_\xi\circ\mathbf{v}^2\circ(\mathbf{h}\circ\mathbf{v})\mathbf{D}^T + \mathbf{h}\circ\mathbf{v}^3\circ(\mathbf{x}_\xi)\mathbf{D}^T\right]\\
&= \left(g(\mathbf{h}+\mathbf{b}) - \frac{1}{2}\mathbf{u}^2 - \frac{1}{2}\mathbf{v}^2\right)\circ\mathbf{S}\left(\tilde{\mathbf{F}}_1^* - \tilde{\mathbf{F}}_1\right) + \left(g(\mathbf{h}+\mathbf{b}) - \frac{1}{2}\mathbf{u}^2 - \frac{1}{2}\mathbf{v}^2\right)\circ\left(\tilde{\mathbf{G}}_1^* - \tilde{\mathbf{G}}_1\right)\mathbf{S}.
\end{aligned}
\tag{C.10}
$$

For the scaled $hu$-equation we have

$$
\begin{aligned}
&\mathbf{u}\circ\mathbf{J}\circ(\mathbf{hu})_t\\
&+\frac{1}{4}\Big[\mathbf{u}\circ\mathbf{D}\left(\mathbf{hu}\circ\mathbf{u}\circ\mathbf{y}_\eta\right)+\mathbf{hu}\circ\mathbf{u}\circ\mathbf{D}\left(\mathbf{y}_\eta\circ\mathbf{u}\right)+\mathbf{u}^2\circ\mathbf{D}\left(\mathbf{y}_\eta\circ\mathbf{hu}\right)+\mathbf{y}_\eta\circ\mathbf{u}\circ\mathbf{D}\left(\mathbf{hu}\circ\mathbf{u}\right)+\mathbf{hu}\circ\mathbf{u}^2\circ\mathbf{D}\left(\mathbf{y}_\eta\right)\\
&+\mathbf{y}_\eta\circ\mathbf{hu}\circ\mathbf{u}\circ\mathbf{Du}+\mathbf{y}_\eta\circ\mathbf{u}^2\circ\mathbf{D}\left(\mathbf{hu}\right)\Big]\\
&+\frac{1}{2}g\left[\mathbf{h}\circ\mathbf{u}\circ\mathbf{D}\left(\mathbf{y}_\eta\circ\mathbf{h}\right)+\mathbf{y}_\eta\circ\mathbf{h}\circ\mathbf{u}\circ\mathbf{D}\left(\mathbf{h}\right)+\mathbf{h}\circ\mathbf{u}\circ\mathbf{D}\left(\mathbf{y}_\eta\circ\mathbf{b}\right)+\mathbf{y}_\eta\circ\mathbf{h}\circ\mathbf{u}\circ\mathbf{D}\left(\mathbf{b}\right)\right]\\
&-\frac{1}{4}\Big[\mathbf{u}\circ\left(\mathbf{hu}\circ\mathbf{u}\circ\mathbf{y}_\xi\right)\mathbf{D}^T+\mathbf{hu}\circ\mathbf{u}\circ\left(\mathbf{y}_\xi\circ\mathbf{u}\right)\mathbf{D}^T+\mathbf{y}_\xi\circ\mathbf{u}\circ\left(\mathbf{hu}\circ\mathbf{u}\right)\mathbf{D}^T+\mathbf{u}^2\circ\left(\mathbf{y}_\xi\circ\mathbf{hu}\right)\mathbf{D}^T+\mathbf{hu}\circ\mathbf{u}^2\circ\left(\mathbf{y}_\xi\right)\mathbf{D}^T\\
&+\mathbf{y}_\xi\circ\mathbf{hu}\circ\mathbf{u}\circ(\mathbf{u})\mathbf{D}^T+\mathbf{y}_\xi\circ\mathbf{u}^2\circ(\mathbf{hu})\,\mathbf{D}^T\Big]\\
&-\frac{1}{2}g\left[\mathbf{h}\circ\mathbf{u}\circ\left(\mathbf{y}_\xi\circ\mathbf{h}\right)\mathbf{D}^T+\mathbf{y}_\xi\circ\mathbf{h}\circ\mathbf{u}\circ(\mathbf{h})\,\mathbf{D}^T+\mathbf{h}\circ\mathbf{u}\circ\left(\mathbf{y}_\xi\circ\mathbf{b}\right)\mathbf{D}^T+\mathbf{y}_\xi\circ\mathbf{h}\circ\mathbf{u}\circ(\mathbf{b})\,\mathbf{D}^T\right]\\
&-\frac{1}{4}\Big[\mathbf{u}\circ\mathbf{D}\left(\mathbf{hv}\circ\mathbf{u}\circ\mathbf{x}_\eta\right)+\mathbf{hv}\circ\mathbf{u}\circ\mathbf{D}\left(\mathbf{x}_\eta\circ\mathbf{u}\right)+\mathbf{x}_\eta\circ\mathbf{u}\circ\mathbf{D}\left(\mathbf{hv}\circ\mathbf{u}\right)+\mathbf{u}^2\circ\mathbf{D}\left(\mathbf{x}_\eta\circ\mathbf{hv}\right)+\mathbf{hv}\circ\mathbf{u}^2\circ\mathbf{D}\left(\mathbf{x}_\eta\right)\\
&+\mathbf{x}_\eta\circ\mathbf{hv}\circ\mathbf{u}\circ\mathbf{Du}+\mathbf{x}_\eta\circ\mathbf{u}^2\circ\mathbf{D}\left(\mathbf{hv}\right)\Big]\\
&+\frac{1}{4}\Big[\mathbf{u}\circ\left(\mathbf{hv}\circ\mathbf{u}\circ\mathbf{x}_\xi\right)\mathbf{D}^T+\mathbf{hv}\circ\mathbf{u}\circ\left(\mathbf{x}_\xi\circ\mathbf{u}\right)\mathbf{D}^T+\mathbf{x}_\xi\circ\mathbf{u}\circ\left(\mathbf{hv}\circ\mathbf{u}\right)\mathbf{D}^T+\mathbf{u}^2\circ\left(\mathbf{x}_\xi\circ\mathbf{hv}\right)\mathbf{D}^T+\mathbf{hv}\circ\mathbf{u}^2\circ\left(\mathbf{x}_\xi\right)\mathbf{D}^T\\
&+\mathbf{x}_\xi\circ\mathbf{hv}\circ\mathbf{u}\circ(\mathbf{u})\mathbf{D}^T+\mathbf{x}_\xi\circ\mathbf{u}^2\circ(\mathbf{hv})\,\mathbf{D}^T\Big]\\
&=\mathbf{u}\circ\mathbf{S}\left(\tilde{\mathbf{F}}_2^*-\tilde{\mathbf{F}}_2\right)+\mathbf{u}\circ\left(\tilde{\mathbf{G}}_2^*-\tilde{\mathbf{G}}_2\right)\mathbf{S}-\frac{g}{2}\mathbf{u}\circ\mathbf{M}^{-1}\left(\mathbf{y}_\eta\circ\{\{\mathbf{h}\}\}_\xi\circ[\![\mathbf{b}]\!]_\xi\right)-\frac{g}{2}\mathbf{u}\circ\left(-\mathbf{y}_\xi\circ\{\{\mathbf{h}\}\}_\eta\circ[\![\mathbf{b}]\!]_\eta\right)\mathbf{M}^{-1},
\end{aligned}
\tag{C.11}
$$

and finally the scaled $hv$-equation is

$$
\begin{aligned}
&\mathbf{v}\circ\mathbf{J}\circ(\mathbf{hv})_t\\
&+\frac{1}{4}\Big[\mathbf{v}\circ\mathbf{D}\left(\mathbf{hu}\circ\mathbf{v}\circ\mathbf{y}_\eta\right)+\mathbf{hu}\circ\mathbf{v}\circ\mathbf{D}\left(\mathbf{y}_\eta\circ\mathbf{v}\right)+\mathbf{y}_\eta\circ\mathbf{v}\circ\mathbf{D}\left(\mathbf{hu}\circ\mathbf{v}\right)+\mathbf{v}^2\circ\mathbf{D}\left(\mathbf{y}_\eta\circ\mathbf{hu}\right)+\mathbf{hu}\circ\mathbf{v}^2\circ\mathbf{D}\left(\mathbf{y}_\eta\right)\\
&+\mathbf{y}_\eta\circ\mathbf{hu}\circ\mathbf{v}\circ\mathbf{D}(\mathbf{v})+\mathbf{v}^2\circ\mathbf{y}_\eta\circ\mathbf{D}\left(\mathbf{hu}\right)\Big]\\
&-\frac{1}{4}\Big[\mathbf{v}\circ\left(\mathbf{hu}\circ\mathbf{v}\circ\mathbf{y}_\xi\right)\mathbf{D}^T+\mathbf{hu}\circ\mathbf{v}\circ\left(\mathbf{y}_\xi\circ\mathbf{v}\right)\mathbf{D}^T+\mathbf{y}_\xi\circ\mathbf{v}\circ\left(\mathbf{hu}\circ\mathbf{v}\right)\mathbf{D}^T+\mathbf{v}^2\circ\left(\mathbf{y}_\xi\circ\mathbf{hu}\right)\mathbf{D}^T+\mathbf{hu}\circ\mathbf{v}^2\circ\left(\mathbf{y}_\xi\right)\mathbf{D}^T\\
&+\mathbf{y}_\xi\circ\mathbf{hu}\circ\mathbf{v}\circ(\mathbf{v})\mathbf{D}^T+\mathbf{y}_\xi\circ\mathbf{v}^2\circ(\mathbf{hu})\,\mathbf{D}^T\Big]\\
&-\frac{1}{4}\Big[\mathbf{v}\circ\mathbf{D}\left(\mathbf{hv}\circ\mathbf{v}\circ\mathbf{x}_\eta\right)+\mathbf{hv}\circ\mathbf{v}\circ\mathbf{D}\left(\mathbf{x}_\eta\circ\mathbf{v}\right)+\mathbf{x}_\eta\circ\mathbf{v}\circ\mathbf{D}\left(\mathbf{hv}\circ\mathbf{v}\right)+\mathbf{v}^2\circ\mathbf{D}\left(\mathbf{x}_\eta\circ\mathbf{hv}\right)+\mathbf{hv}\circ\mathbf{v}^2\circ\mathbf{D}\left(\mathbf{x}_\eta\right)\\
&+\mathbf{x}_\eta\circ\mathbf{hv}\circ\mathbf{v}\circ\mathbf{D}(\mathbf{v})+\mathbf{x}_\eta\circ\mathbf{v}^2\circ\mathbf{D}\left(\mathbf{hv}\right)\Big]\\
&-\frac{1}{2}g\left[\mathbf{h}\circ\mathbf{v}\circ\mathbf{D}\left(\mathbf{x}_\eta\circ\mathbf{h}\right)+\mathbf{x}_\eta\circ\mathbf{h}\circ\mathbf{v}\circ\mathbf{D}\left(\mathbf{h}\right)+\mathbf{h}\circ\mathbf{v}\circ\mathbf{D}\left(\mathbf{x}_\eta\circ\mathbf{b}\right)+\mathbf{x}_\eta\circ\mathbf{h}\circ\mathbf{v}\circ\mathbf{D}\left(\mathbf{b}\right)\right]\\
&+\frac{1}{4}\Big[\mathbf{v}\circ\left(\mathbf{hv}\circ\mathbf{v}\circ\mathbf{x}_\xi\right)\mathbf{D}^T+\mathbf{hv}\circ\mathbf{v}\circ\left(\mathbf{x}_\xi\circ\mathbf{v}\right)\mathbf{D}^T+\mathbf{x}_\xi\circ\mathbf{v}\circ\left(\mathbf{hv}\circ\mathbf{v}\right)\mathbf{D}^T+\mathbf{v}^2\circ\left(\mathbf{x}_\xi\circ\mathbf{hv}\right)\mathbf{D}^T+\mathbf{hv}\circ\mathbf{v}^2\circ\left(\mathbf{x}_\xi\right)\mathbf{D}^T\\
&+\mathbf{x}_\xi\circ\mathbf{hv}\circ\mathbf{v}\circ(\mathbf{v})\mathbf{D}^T+\mathbf{x}_\xi\circ\mathbf{v}^2\circ(\mathbf{hv})\,\mathbf{D}^T\Big]\\
&+\frac{1}{2}g\left[\mathbf{h}\circ\mathbf{v}\circ\left(\mathbf{x}_\xi\circ\mathbf{h}\right)\mathbf{D}^T+\mathbf{x}_\xi\circ\mathbf{h}\circ\mathbf{v}\circ(\mathbf{h})\,\mathbf{D}^T+\mathbf{h}\circ\mathbf{v}\circ\left(\mathbf{x}_\xi\circ(\mathbf{b})\right)\mathbf{D}^T+\mathbf{x}_\xi\circ\mathbf{h}\circ\mathbf{v}\circ(\mathbf{b})\,\mathbf{D}^T\right]\\
&=\mathbf{v}\circ\mathbf{S}\left(\tilde{\mathbf{F}}_3^*-\tilde{\mathbf{F}}_3\right)+\mathbf{v}\circ\left(\tilde{\mathbf{G}}_3^*-\tilde{\mathbf{G}}_3\right)\mathbf{S}-\frac{g}{2}\mathbf{v}\circ\mathbf{M}^{-1}\left(\mathbf{x}_\eta\circ\{\{\mathbf{h}\}\}_\xi\circ[\![\mathbf{b}]\!]_\xi\right)-\frac{g}{2}\mathbf{v}\circ\left(-\mathbf{x}_\xi\circ\{\{\mathbf{h}\}\}_\eta\circ[\![\mathbf{b}]\!]_\eta\right)\mathbf{M}^{-1}.
\end{aligned}
\tag{C.12}
$$

The goal is to obtain an equation for the total energy of the form

$$
\begin{aligned}
&\mathbf{J}\circ\left(\frac{1}{2}g\mathbf{h}^2+g\mathbf{h}\circ\mathbf{b}+\frac{1}{2}\mathbf{h}(\mathbf{u}^2+\mathbf{v}^2)\right)_t\\
&\quad+\hat{\mathbf{D}}\left(\frac{1}{2}\mathbf{y}_\eta\circ\mathbf{h}\circ\mathbf{u}^3+\frac{1}{2}\mathbf{y}_\eta\circ\mathbf{h}\circ\mathbf{u}\circ\mathbf{v}^2+g\mathbf{y}_\eta\circ\mathbf{h}^2\circ\mathbf{u}+\mathbf{y}_\eta\circ g\mathbf{h}\circ\mathbf{u}\circ\mathbf{b}\right)\\
&\quad-\hat{\mathbf{D}}\left(\frac{1}{2}\mathbf{x}_\eta\circ\mathbf{h}\circ\mathbf{v}^3+\frac{1}{2}\mathbf{x}_\eta\circ\mathbf{h}\circ\mathbf{u}^2\circ\mathbf{v}+g\mathbf{x}_\eta\circ\mathbf{h}^2\circ\mathbf{v}+g\mathbf{x}_\eta\circ\mathbf{h}\circ\mathbf{v}\circ\mathbf{b}\right)\\
&\quad-\left(\frac{1}{2}\mathbf{y}_\xi\circ\mathbf{h}\circ\mathbf{u}^3+\frac{1}{2}\mathbf{y}_\xi\circ\mathbf{h}\circ\mathbf{u}\circ\mathbf{v}^2+g\mathbf{y}_\xi\circ\mathbf{h}^2\circ\mathbf{u}+g\mathbf{y}_\xi\circ\mathbf{h}\circ\mathbf{u}\circ\mathbf{b}\right)\hat{\mathbf{D}}^T\\
&\quad+\left(\frac{1}{2}\mathbf{x}_\xi\circ\mathbf{h}\circ\mathbf{v}^3+\frac{1}{2}\mathbf{x}_\xi\circ\mathbf{h}\circ\mathbf{u}^2\circ\mathbf{v}+g\mathbf{x}_\xi\circ\mathbf{h}^2\circ\mathbf{v}+g\mathbf{x}_\xi\circ\mathbf{h}\circ\mathbf{v}\circ\mathbf{b}\right)\hat{\mathbf{D}}^T\\
&=\text{consistent, conservative RHS.}
\end{aligned}
\tag{C.13}
$$

To do so we assemble the above terms from (C.10)–(C.12) one by one to show that any additional terms are discrete product rule error terms and thus do not affect conservation.

We begin with the time derivative terms. From the added scaled equations (C.10), (C.11) and (C.12) we see that

$$
\begin{aligned}
&\left(g(\mathbf{h}+\mathbf{b})-\frac{1}{2}\mathbf{u}^2-\frac{1}{2}\mathbf{v}^2\right)\circ\mathbf{J}\circ(\mathbf{h})_t+\mathbf{u}\circ\mathbf{J}\circ(\mathbf{hu})_t+\mathbf{v}\circ\mathbf{J}\circ(\mathbf{hv})_t\\
&=g\mathbf{J}\circ\left(\frac{1}{2}\mathbf{h}^2+\mathbf{b}\circ\mathbf{h}\right)_t+\mathbf{J}\circ\left(-\frac{1}{2}\mathbf{u}^2\circ\mathbf{h}_t+\mathbf{u}\circ(\mathbf{hu})_t\right)+\mathbf{J}\circ\left(-\frac{1}{2}\mathbf{v}^2\circ\mathbf{h}_t+\mathbf{v}\circ(\mathbf{hv})_t\right),\\
&=g\mathbf{J}\circ\left(\frac{1}{2}\mathbf{h}^2+\mathbf{b}\circ\mathbf{h}\right)_t+\mathbf{J}\circ\left(-\frac{1}{2}\mathbf{u}^2\circ\mathbf{h}_t+\mathbf{u}^2\circ(\mathbf{h})_t+\mathbf{u}\circ\mathbf{h}\circ(\mathbf{u})_t\right)\\
&\quad+\mathbf{J}\circ\left(-\frac{1}{2}\mathbf{v}^2\circ\mathbf{h}_t+\mathbf{v}^2\circ(\mathbf{h})_t+\mathbf{v}\circ\mathbf{h}\circ(\mathbf{v})_t\right),\\
&=g\mathbf{J}\circ\left(\frac{1}{2}\mathbf{h}^2+\mathbf{b}\circ\mathbf{h}\right)_t+\mathbf{J}\circ\left(\frac{1}{2}\mathbf{u}^2\circ\mathbf{h}_t+\mathbf{u}\circ\mathbf{h}\circ(\mathbf{u})_t\right)+\mathbf{J}\circ\left(\frac{1}{2}\mathbf{v}^2\circ\mathbf{h}_t+\mathbf{v}\circ\mathbf{h}\circ(\mathbf{v})_t\right),\\
&=g\mathbf{J}\circ\left(\frac{1}{2}\mathbf{h}^2+\mathbf{b}\circ\mathbf{h}\right)_t+\mathbf{J}\circ\left(\frac{1}{2}\mathbf{u}^2\circ\mathbf{h}_t+\frac{1}{2}\mathbf{h}\circ(\mathbf{u}^2)_t\right)+\mathbf{J}\circ\left(\frac{1}{2}\mathbf{v}^2\circ\mathbf{h}_t+\frac{1}{2}\mathbf{h}\circ(\mathbf{v}^2)_t\right),\\
&=g\mathbf{J}\circ\left(\frac{1}{2}\mathbf{h}^2+\mathbf{b}\circ\mathbf{h}\right)_t+\frac{1}{2}\mathbf{J}\circ\left(\mathbf{u}^2\circ\mathbf{h}\right)_t+\frac{1}{2}\mathbf{J}\circ\left(\mathbf{v}^2\circ\mathbf{h}\right)_t,\\
&=\mathbf{J}\circ\left(\frac{1}{2}g\mathbf{h}^2+g\mathbf{b}\circ\mathbf{h}+\frac{1}{2}\mathbf{u}^2\circ\mathbf{h}+\frac{1}{2}\mathbf{v}^2\circ\mathbf{h}\right)_t,
\end{aligned}
\tag{C.14}
$$

where we assume continuity in time, such that we are able to apply the continuous product rule.

We treat the four different metric terms of the curvilinear approximation $y_\eta$, $y_\xi$, $x_\eta$ and $x_\xi$ separately and start with $y_\eta$. The corresponding terms collected from the added entropy-scaled equations (C.10)–(C.12) are

$$
\begin{aligned}
&\frac{1}{2}g\left[\mathbf{h}\circ\mathbf{D}(\mathbf{h}\circ\mathbf{u}\circ\mathbf{y}_\eta)+\mathbf{h}\circ\mathbf{y}_\eta\circ\mathbf{D}(\mathbf{h}\circ\mathbf{u})+\mathbf{h}^2\circ\mathbf{u}\circ\mathbf{D}(\mathbf{y}_\eta)+\mathbf{b}\circ\mathbf{D}(\mathbf{h}\circ\mathbf{u}\circ\mathbf{y}_\eta)\right.\\
&\left.+\mathbf{b}\circ\mathbf{y}_\eta\circ\mathbf{D}(\mathbf{h}\circ\mathbf{u})+\mathbf{b}\circ\mathbf{h}\circ\mathbf{u}\circ\mathbf{D}(\mathbf{y}_\eta)\right]\\
&-\frac{1}{4}\left[\mathbf{u}^2\circ\mathbf{D}(\mathbf{h}\circ\mathbf{u}\circ\mathbf{y}_\eta)+\mathbf{y}_\eta\circ\mathbf{u}^2\circ\mathbf{D}(\mathbf{h}\circ\mathbf{u})+\mathbf{h}\circ\mathbf{u}^3\circ\mathbf{D}(\mathbf{y}_\eta)+\mathbf{v}^2\circ\mathbf{D}(\mathbf{h}\circ\mathbf{u}\circ\mathbf{y}_\eta)\right.\\
&\left.+\mathbf{y}_\eta\circ\mathbf{v}^2\circ\mathbf{D}(\mathbf{h}\circ\mathbf{u})+\mathbf{h}\circ\mathbf{u}\circ\mathbf{v}^2\circ\mathbf{D}(\mathbf{y}_\eta)\right]\\
&+\frac{1}{4}\left[\mathbf{u}\circ\mathbf{D}\left(\mathbf{hu}\circ\mathbf{u}\circ\mathbf{y}_\eta\right)+\mathbf{hu}\circ\mathbf{u}\circ\mathbf{D}\left(\mathbf{y}_\eta\circ\mathbf{u}\right)+\mathbf{u}^2\circ\mathbf{D}\left(\mathbf{y}_\eta\circ\mathbf{hu}\right)+\mathbf{y}_\eta\circ\mathbf{u}\circ\mathbf{D}\left(\mathbf{hu}\circ\mathbf{u}\right)\right.\\
&\left.+\mathbf{hu}\circ\mathbf{u}^2\circ\mathbf{D}\left(\mathbf{y}_\eta\right)+\mathbf{y}_\eta\circ\mathbf{hu}\circ\mathbf{u}\circ\mathbf{Du}+\mathbf{y}_\eta\circ\mathbf{u}^2\circ\mathbf{D}\left(\mathbf{hu}\right)\right]\\
&+\frac{1}{2}g\left[\mathbf{h}\circ\mathbf{u}\circ\mathbf{D}\left(\mathbf{y}_\eta\circ\mathbf{h}\right)+\mathbf{y}_\eta\circ\mathbf{h}\circ\mathbf{u}\circ\mathbf{D}\left(\mathbf{h}\right)+\mathbf{h}\circ\mathbf{u}\circ\mathbf{D}\left(\mathbf{y}_\eta\circ\mathbf{b}\right)+\mathbf{y}_\eta\circ\mathbf{h}\circ\mathbf{u}\circ\mathbf{D}\left(\mathbf{b}\right)\right]\\
&+\frac{1}{4}\left[\mathbf{v}\circ\mathbf{D}\left(\mathbf{hu}\circ\mathbf{v}\circ\mathbf{y}_\eta\right)+\mathbf{hu}\circ\mathbf{v}\circ\mathbf{D}\left(\mathbf{y}_\eta\circ\mathbf{v}\right)+\mathbf{y}_\eta\circ\mathbf{v}\circ\mathbf{D}\left(\mathbf{hu}\circ\mathbf{v}\right)+\mathbf{v}^2\circ\mathbf{D}\left(\mathbf{y}_\eta\circ\mathbf{hu}\right)+\mathbf{hu}\circ\mathbf{v}^2\circ\mathbf{D}\left(\mathbf{y}_\eta\right)\right.\\
&\left.+\mathbf{y}_\eta\circ\mathbf{hu}\circ\mathbf{v}\circ\mathbf{D}(\mathbf{v})+\mathbf{v}^2\circ\mathbf{y}_\eta\circ\mathbf{D}\left(\mathbf{hu}\right)\right].
\end{aligned}
\tag{C.15}
$$

After canceling terms (C.15) can be manipulated by adding zero and carefully grouping terms to obtain the four terms from the discrete energy equation (C.13). This results in several discrete product rule error terms and two terms that contain discrete derivatives of the metric terms

$$
\begin{aligned}
&\frac{1}{2}\mathbf{D}\left(\mathbf{h}\circ\mathbf{u}^3\circ\mathbf{y}_\eta\right)+\frac{1}{4}\left(-\mathbf{D}\left(\mathbf{h}\circ\mathbf{u}^3\circ\mathbf{y}_\eta\right)+\mathbf{u}\circ\mathbf{D}\left(\mathbf{h}\circ\mathbf{u}^2\circ\mathbf{y}_\eta\right)+\mathbf{y}_\eta\circ\mathbf{h}\circ\mathbf{u}^2\circ\mathbf{D}\mathbf{u}\right)\\
&+\frac{1}{4}\left(-\mathbf{D}\left(\mathbf{h}\circ\mathbf{u}^3\circ\mathbf{y}_\eta\right)+\mathbf{h}\circ\mathbf{u}^2\circ\mathbf{D}\left(\mathbf{y}_\eta\circ\mathbf{u}\right)+\mathbf{u}\circ\mathbf{y}_\eta\circ\mathbf{D}\left(\mathbf{h}\circ\mathbf{u}^2\right)\right)\\
&+\frac{1}{2}\mathbf{D}\left(\mathbf{y}_\eta\circ\mathbf{h}\circ\mathbf{u}\circ\mathbf{v}^2\right)+\frac{1}{4}\left(-\mathbf{D}\left(\mathbf{y}_\eta\circ\mathbf{h}\circ\mathbf{u}\circ\mathbf{v}^2\right)+\mathbf{v}\circ\mathbf{D}\left(\mathbf{h}\mathbf{u}\circ\mathbf{v}\circ\mathbf{y}_\eta\right)+\mathbf{y}_\eta\circ\mathbf{v}\circ\mathbf{h}\mathbf{u}\circ\mathbf{D}\mathbf{v}\right)\\
&+\frac{1}{4}\left(-\mathbf{D}\left(\mathbf{y}_\eta\circ\mathbf{h}\circ\mathbf{u}\circ\mathbf{v}^2\right)+\mathbf{h}\circ\mathbf{u}\circ\mathbf{v}\circ\mathbf{D}\left(\mathbf{y}_\eta\circ\mathbf{v}\right)+\mathbf{y}_\eta\circ\mathbf{v}\circ\mathbf{D}\left(\mathbf{h}\mathbf{u}\circ\mathbf{v}\right)\right)+g\mathbf{D}\left(\mathbf{y}_\eta\circ\mathbf{h}^2\circ\mathbf{u}\right)\\
&+\frac{1}{2}g\left(-\mathbf{D}\left(\mathbf{y}_\eta\circ\mathbf{h}^2\circ\mathbf{u}\right)+\mathbf{h}\circ\left(\mathbf{D}(\mathbf{h}\circ\mathbf{u}\circ\mathbf{y}_\eta)\right)+\mathbf{y}_\eta\circ\mathbf{h}\circ\mathbf{u}\circ\mathbf{D}\left(\mathbf{h}\right)\right)\\
&+\frac{1}{2}g\left(-\mathbf{D}\left(\mathbf{y}_\eta\circ\mathbf{h}^2\circ\mathbf{u}\right)+\mathbf{h}\circ\mathbf{u}\mathbf{D}\left(\mathbf{y}_\eta\circ\mathbf{h}\right)+\mathbf{y}_\eta\circ\mathbf{h}\circ\mathbf{D}(\mathbf{h}\circ\mathbf{u})\right)\\
&+g\mathbf{D}\left(\mathbf{y}_\eta\circ\mathbf{h}\circ\mathbf{u}\circ\mathbf{b}\right)+\frac{1}{2}g\left(-\mathbf{D}\left(\mathbf{y}_\eta\circ g\mathbf{h}\circ\mathbf{u}\circ\mathbf{b}\right)+\mathbf{b}\circ\mathbf{h}\circ\mathbf{u}\circ\mathbf{D}(\mathbf{y}_\eta)+\mathbf{h}\circ\mathbf{u}\circ\mathbf{D}\left(\mathbf{y}_\eta\circ\mathbf{b}\right)\right)\\
&+\frac{1}{2}g\left(-\mathbf{D}\left(\mathbf{y}_\eta\circ g\mathbf{h}\circ\mathbf{u}\circ\mathbf{b}\right)+\mathbf{b}\circ\mathbf{D}(\mathbf{h}\circ\mathbf{u}\circ\mathbf{y}_\eta)+\mathbf{y}_\eta\circ\mathbf{h}\circ\mathbf{u}\circ\mathbf{D}\left(\mathbf{b}\right)\right)\\
&+\frac{1}{2}g\left[\mathbf{b}\circ\mathbf{h}\circ\mathbf{u}\circ\mathbf{D}(\mathbf{y}_\eta)+\mathbf{h}^2\circ\mathbf{u}\circ\mathbf{D}(\mathbf{y}_\eta)\right].
\end{aligned}
\tag{C.16}
$$

The remaining terms in the last row cancel with corresponding terms of other metric terms due to the metric identities (3.18).

Next we collect all the $y_\xi$ terms from the scaled added equations (C.10)–(C.12):

$$
\begin{aligned}
&-\frac{1}{2}g\left[\mathbf{h}\circ(\mathbf{h}\circ\mathbf{u}\circ\mathbf{y}_\xi)\mathbf{D}^T+\mathbf{y}_\xi\circ\mathbf{h}\circ(\mathbf{h}\circ\mathbf{u})\mathbf{D}^T+\mathbf{h}^2\circ\mathbf{u}\circ(\mathbf{y}_\xi)\mathbf{D}^T+\mathbf{b}\circ(\mathbf{h}\circ\mathbf{u}\circ\mathbf{y}_\xi)\mathbf{D}^T\right.\\
&\left.+\mathbf{y}_\xi\circ\mathbf{b}\circ(\mathbf{h}\circ\mathbf{u})\mathbf{D}^T+\mathbf{h}\circ\mathbf{b}\circ\mathbf{u}\circ(\mathbf{y}_\xi)\mathbf{D}^T\right]\\
&+\frac{1}{4}\left[\mathbf{u}^2\circ(\mathbf{h}\circ\mathbf{u}\circ\mathbf{y}_\xi)\mathbf{D}^T+\mathbf{y}_\xi\circ\mathbf{u}^2\circ(\mathbf{h}\circ\mathbf{u})\mathbf{D}^T+\mathbf{h}\circ\mathbf{u}^3\circ(\mathbf{y}_\xi)\mathbf{D}^T+\mathbf{v}^2\circ(\mathbf{h}\circ\mathbf{u}\circ\mathbf{y}_\xi)\mathbf{D}^T\right.\\
&\left.+\mathbf{y}_\xi\circ\mathbf{v}^2\circ(\mathbf{h}\circ\mathbf{u})\mathbf{D}^T+\mathbf{h}\circ\mathbf{u}\circ\mathbf{v}^2\circ(\mathbf{y}_\xi)\mathbf{D}^T\right]\\
&-\frac{1}{4}\left[\mathbf{u}\circ\left(\mathbf{h}\mathbf{u}\circ\mathbf{u}\circ\mathbf{y}_\xi\right)\mathbf{D}^T+\mathbf{h}\mathbf{u}\circ\mathbf{u}\circ\left(\mathbf{y}_\xi\circ\mathbf{u}\right)\mathbf{D}^T+\mathbf{y}_\xi\circ\mathbf{u}\circ(\mathbf{h}\mathbf{u}\circ\mathbf{u})\mathbf{D}^T+\mathbf{u}^2\circ\left(\mathbf{y}_\xi\circ\mathbf{h}\mathbf{u}\right)\mathbf{D}^T\right.\\
&\left.+\mathbf{h}\mathbf{u}\circ\mathbf{u}^2\circ\left(\mathbf{y}_\xi\right)\mathbf{D}^T+\mathbf{y}_\xi\circ\mathbf{h}\mathbf{u}\circ\mathbf{u}\circ(\mathbf{u})\mathbf{D}^T+\mathbf{y}_\xi\circ\mathbf{u}^2\circ(\mathbf{h}\mathbf{u})\,\mathbf{D}^T\right]\\
&-\frac{1}{2}g\left[\mathbf{h}\circ\mathbf{u}\circ\left(\mathbf{y}_\xi\circ\mathbf{h}\right)\mathbf{D}^T+\mathbf{y}_\xi\circ\mathbf{h}\circ\mathbf{u}\circ(\mathbf{h})\,\mathbf{D}^T+\mathbf{h}\circ\mathbf{u}\circ\left(\mathbf{y}_\xi\circ\mathbf{b}\right)\mathbf{D}^T+\mathbf{y}_\xi\circ\mathbf{h}\circ\mathbf{u}\circ(\mathbf{b})\,\mathbf{D}^T\right]\\
&-\frac{1}{4}\left[\mathbf{v}\circ\left(\mathbf{h}\mathbf{u}\circ\mathbf{v}\circ\mathbf{y}_\xi\right)\mathbf{D}^T+\mathbf{h}\mathbf{u}\circ\mathbf{v}\circ\left(\mathbf{y}_\xi\circ\mathbf{v}\right)\mathbf{D}^T+\mathbf{y}_\xi\circ\mathbf{v}\circ(\mathbf{h}\mathbf{u}\circ\mathbf{v})\,\mathbf{D}^T+\mathbf{v}^2\circ\left(\mathbf{y}_\xi\circ\mathbf{h}\mathbf{u}\right)\mathbf{D}^T\right.\\
&\left.+\mathbf{h}\mathbf{u}\circ\mathbf{v}^2\circ\left(\mathbf{y}_\xi\right)\mathbf{D}^T+\mathbf{y}_\xi\circ\mathbf{h}\mathbf{u}\circ\mathbf{v}\circ(\mathbf{v})\mathbf{D}^T+\mathbf{y}_\xi\circ\mathbf{v}^2\circ(\mathbf{h}\mathbf{u})\,\mathbf{D}^T\right]\\
&-\frac{1}{2}g\left[\mathbf{h}\circ(\mathbf{h}\circ\mathbf{u}\circ\mathbf{y}_\xi)\mathbf{D}^T+\mathbf{y}_\xi\circ\mathbf{h}\circ(\mathbf{h}\circ\mathbf{u})\mathbf{D}^T+\mathbf{h}^2\circ\mathbf{u}\circ(\mathbf{y}_\xi)\mathbf{D}^T+\mathbf{b}\circ(\mathbf{h}\circ\mathbf{u}\circ\mathbf{y}_\xi)\mathbf{D}^T\right.\\
&\left.+\mathbf{y}_\xi\circ\mathbf{b}\circ(\mathbf{h}\circ\mathbf{u})\mathbf{D}^T+\mathbf{h}\circ\mathbf{b}\circ\mathbf{u}\circ(\mathbf{y}_\xi)\mathbf{D}^T\right]\\
&-\frac{1}{4}\left[\mathbf{u}\circ\left(\mathbf{h}\mathbf{u}\circ\mathbf{u}\circ\mathbf{y}_\xi\right)\mathbf{D}^T+\mathbf{h}\mathbf{u}\circ\mathbf{u}\circ\left(\mathbf{y}_\xi\circ\mathbf{u}\right)\mathbf{D}^T+\mathbf{y}_\xi\circ\mathbf{u}\circ(\mathbf{h}\mathbf{u}\circ\mathbf{u})\,\mathbf{D}^T+\mathbf{y}_\xi\circ\mathbf{h}\mathbf{u}\circ\mathbf{u}\circ(\mathbf{u})\mathbf{D}^T\right]\\
&-\frac{1}{2}g\left[\mathbf{h}\circ\mathbf{u}\circ\left(\mathbf{y}_\xi\circ\mathbf{h}\right)\mathbf{D}^T+\mathbf{y}_\xi\circ\mathbf{h}\circ\mathbf{u}\circ(\mathbf{h})\,\mathbf{D}^T+\mathbf{h}\circ\mathbf{u}\circ\left(\mathbf{y}_\xi\circ\mathbf{b}\right)\mathbf{D}^T+\mathbf{y}_\xi\circ\mathbf{h}\circ\mathbf{u}\circ(\mathbf{b})\,\mathbf{D}^T\right]\\
&-\frac{1}{4}\left[\mathbf{v}\circ\left(\mathbf{h}\mathbf{u}\circ\mathbf{v}\circ\mathbf{y}_\xi\right)\mathbf{D}^T+\mathbf{h}\mathbf{u}\circ\mathbf{v}\circ\left(\mathbf{y}_\xi\circ\mathbf{v}\right)\mathbf{D}^T+\mathbf{y}_\xi\circ\mathbf{v}\circ(\mathbf{h}\mathbf{u}\circ\mathbf{v})\,\mathbf{D}^T+\mathbf{y}_\xi\circ\mathbf{h}\mathbf{u}\circ\mathbf{v}\circ(\mathbf{v})\mathbf{D}^T\right],
\end{aligned}
\tag{C.17}
$$

and apply the same methods to find a similar result as (C.16)

$$
\begin{aligned}
&-\frac{1}{2}\left(\mathbf{y}_\xi\circ\mathbf{h}\circ\mathbf{u}^3\right)\mathbf{D}^T-\frac{1}{4}\left(-\left(\mathbf{y}_\xi\circ\mathbf{h}\circ\mathbf{u}^3\right)\mathbf{D}^T+\mathbf{u}\circ\left(\mathbf{h}\circ\mathbf{u}^2\circ\mathbf{y}_\xi\right)\mathbf{D}^T+\mathbf{y}_\xi\circ\mathbf{h}\circ\mathbf{u}^2\circ(\mathbf{u})\mathbf{D}^T\right)\\
&-\frac{1}{4}\left(-\left(\mathbf{y}_\xi\circ\mathbf{h}\circ\mathbf{u}^3\right)\mathbf{D}^T+\mathbf{h}\circ\mathbf{u}^2\circ\left(\mathbf{y}_\xi\circ\mathbf{u}\right)\mathbf{D}^T+\mathbf{y}_\xi\circ\mathbf{u}\circ\left(\mathbf{h}\circ\mathbf{u}^2\right)\mathbf{D}^T\right)\\
&-\frac{1}{2}\left(\mathbf{y}_\xi\circ\mathbf{h}\circ\mathbf{u}\circ\mathbf{v}^2\right)\mathbf{D}^T-\frac{1}{4}\left(-\left(\mathbf{y}_\xi\circ\mathbf{h}\circ\mathbf{u}\circ\mathbf{v}^2\right)\mathbf{D}^T+\mathbf{v}\circ\left(\mathbf{hu}\circ\mathbf{v}\circ\mathbf{y}_\xi\right)\mathbf{D}^T+\mathbf{y}_\xi\circ\mathbf{hu}\circ\mathbf{v}\circ(\mathbf{v})\mathbf{D}^T\right)\\
&-\frac{1}{4}\left(-\left(\mathbf{y}_\xi\circ\mathbf{h}\circ\mathbf{u}\circ\mathbf{v}^2\right)\mathbf{D}^T+\mathbf{hu}\circ\mathbf{v}\circ\left(\mathbf{y}_\xi\circ\mathbf{v}\right)\mathbf{D}^T+\mathbf{y}_\xi\circ\mathbf{v}\circ(\mathbf{hu}\circ\mathbf{v})\,\mathbf{D}^T\right)\\
&-g\left(\mathbf{y}_\xi\circ\mathbf{h}^2\circ\mathbf{u}\right)\mathbf{D}^T-\frac{1}{2}g\left(-\left(\mathbf{y}_\xi\circ\mathbf{h}^2\circ\mathbf{u}\right)\mathbf{D}^T+\mathbf{h}\circ(\mathbf{h}\circ\mathbf{u}\circ\mathbf{y}_\xi)\mathbf{D}^T+\mathbf{y}_\xi\circ\mathbf{h}\circ\mathbf{u}\circ(\mathbf{h})\,\mathbf{D}^T\right)\\
&-\frac{1}{2}g\left(-\left(\mathbf{y}_\xi\circ\mathbf{h}^2\circ\mathbf{u}\right)\mathbf{D}^T+\mathbf{h}\circ\mathbf{u}\circ\left(\mathbf{y}_\xi\circ\mathbf{h}\right)\mathbf{D}^T+\mathbf{y}_\xi\circ\mathbf{h}\circ(\mathbf{h}\circ\mathbf{u})\mathbf{D}^T\right)\\
&-g\left(\mathbf{y}_\xi\circ\mathbf{h}\circ\mathbf{u}\circ\mathbf{b}\right)\mathbf{D}^T-\frac{1}{2}g\left(-\left(\mathbf{y}_\xi\circ\mathbf{h}\circ\mathbf{u}\circ\mathbf{b}\right)\mathbf{D}^T+\mathbf{y}_\xi\circ\mathbf{b}\circ(\mathbf{h}\circ\mathbf{u})\mathbf{D}^T+\mathbf{h}\circ\mathbf{u}\circ\left(\mathbf{y}_\xi\circ\mathbf{b}\right)\mathbf{D}^T\right)\\
&-\frac{1}{2}g\left(-\left(\mathbf{y}_\xi\circ\mathbf{h}\circ\mathbf{u}\circ\mathbf{b}\right)\mathbf{D}^T+\mathbf{b}\circ(\mathbf{h}\circ\mathbf{u}\circ\mathbf{y}_\xi)\mathbf{D}^T+\mathbf{y}_\xi\circ\mathbf{h}\circ\mathbf{u}\circ(\mathbf{b})\,\mathbf{D}^T\right)\\
&-\frac{1}{2}g\left[\mathbf{h}\circ\mathbf{b}\circ\mathbf{u}\circ(\mathbf{y}_\xi)\mathbf{D}^T+\mathbf{h}^2\circ\mathbf{u}\circ(\mathbf{y}_\xi)\mathbf{D}^T\right].
\end{aligned}
\tag{C.18}
$$

The procedure is nearly identical for the $x_\eta$ terms

$$
\begin{aligned}
&-\frac{1}{4}\left[\mathbf{u}\circ\mathbf{D}\left(\mathbf{hv}\circ\mathbf{u}\circ\mathbf{x}_\eta\right)+\mathbf{hv}\circ\mathbf{u}\circ\mathbf{D}\left(\mathbf{x}_\eta\circ\mathbf{u}\right)+\mathbf{x}_\eta\circ\mathbf{u}\circ\mathbf{D}\left(\mathbf{hv}\circ\mathbf{u}\right)+\mathbf{x}_\eta\circ\mathbf{hv}\circ\mathbf{u}\circ\mathbf{Du}\right]\\
&-\frac{1}{4}\left[\mathbf{v}\circ\mathbf{D}\left(\mathbf{hv}\circ\mathbf{v}\circ\mathbf{x}_\eta\right)+\mathbf{hv}\circ\mathbf{v}\circ\mathbf{D}\left(\mathbf{x}_\eta\circ\mathbf{v}\right)+\mathbf{x}_\eta\circ\mathbf{v}\circ\mathbf{D}\left(\mathbf{hv}\circ\mathbf{v}\right)+\mathbf{x}_\eta\circ\mathbf{hv}\circ\mathbf{v}\circ\mathbf{D}(\mathbf{v})\right]\\
&-\frac{1}{2}g\left[\mathbf{h}\circ\mathbf{v}\circ\mathbf{D}\left(\mathbf{x}_\eta\circ\mathbf{h}\right)+\mathbf{x}_\eta\circ\mathbf{h}\circ\mathbf{v}\circ\mathbf{D}\left(\mathbf{h}\right)+\mathbf{h}\circ\mathbf{v}\circ\mathbf{D}\left(\mathbf{x}_\eta\circ\mathbf{b}\right)+\mathbf{x}_\eta\circ\mathbf{h}\circ\mathbf{v}\circ\mathbf{D}\left(\mathbf{b}\right)\right]\\
&-\frac{1}{2}g\Big[\mathbf{h}\circ\mathbf{D}(\mathbf{h}\circ\mathbf{v}\circ\mathbf{x}_\eta)+\mathbf{x}_\eta\circ\mathbf{h}\circ\mathbf{D}(\mathbf{h}\circ\mathbf{v})+\mathbf{h}^2\circ\mathbf{v}\circ\mathbf{D}(\mathbf{x}_\eta)+\mathbf{b}\circ\mathbf{D}(\mathbf{h}\circ\mathbf{v}\circ\mathbf{x}_\eta)\\
&+\mathbf{x}_\eta\circ\mathbf{b}\circ\mathbf{D}(\mathbf{h}\circ\mathbf{v})+\mathbf{h}\circ\mathbf{v}\circ\mathbf{b}\circ\mathbf{D}(\mathbf{x}_\eta)\Big]\\
&=\\
&-\frac{1}{2}\mathbf{D}\left(\mathbf{x}_\eta\circ\mathbf{h}\circ\mathbf{v}^3\right)-\frac{1}{4}\left(-\mathbf{D}\left(\mathbf{x}_\eta\circ\mathbf{h}\circ\mathbf{v}^3\right)+\mathbf{v}\circ\mathbf{D}\left(\mathbf{hv}\circ\mathbf{v}\circ\mathbf{x}_\eta\right)+\mathbf{x}_\eta\circ\mathbf{hv}\circ\mathbf{v}\circ\mathbf{D}(\mathbf{v})\right)\\
&-\frac{1}{4}\left(-\mathbf{D}\left(\mathbf{x}_\eta\circ\mathbf{h}\circ\mathbf{v}^3\right)+\mathbf{hv}\circ\mathbf{v}\circ\mathbf{D}\left(\mathbf{x}_\eta\circ\mathbf{v}\right)+\mathbf{x}_\eta\circ\mathbf{v}\circ\mathbf{D}\left(\mathbf{hv}\circ\mathbf{v}\right)\right)\\
&-\frac{1}{2}\mathbf{D}\left(\mathbf{x}_\eta\circ\mathbf{h}\circ\mathbf{u}^2\circ\mathbf{v}\right)-\frac{1}{4}\left(-\mathbf{D}\left(\mathbf{x}_\eta\circ\mathbf{h}\circ\mathbf{u}^2\circ\mathbf{v}\right)+\mathbf{u}\circ\mathbf{D}\left(\mathbf{hv}\circ\mathbf{u}\circ\mathbf{x}_\eta\right)+\mathbf{x}_\eta\circ\mathbf{hv}\circ\mathbf{u}\circ\mathbf{Du}\right)\\
&-\frac{1}{4}\left(-\mathbf{D}\left(\mathbf{x}_\eta\circ\mathbf{h}\circ\mathbf{u}^2\circ\mathbf{v}\right)+\mathbf{hv}\circ\mathbf{u}\circ\mathbf{D}\left(\mathbf{x}_\eta\circ\mathbf{u}\right)+\mathbf{x}_\eta\circ\mathbf{u}\circ\mathbf{D}\left(\mathbf{hv}\circ\mathbf{u}\right)\right)\\
&-g\mathbf{D}\left(\mathbf{x}_\eta\circ\mathbf{h}^2\circ\mathbf{v}\right)-\frac{1}{2}g\left(-\mathbf{D}\left(\mathbf{x}_\eta\circ\mathbf{h}^2\circ\mathbf{v}\right)+\mathbf{h}\circ\mathbf{v}\circ\mathbf{D}\left(\mathbf{x}_\eta\circ\mathbf{h}\right)+\mathbf{x}_\eta\circ\mathbf{h}\circ\mathbf{D}(\mathbf{h}\circ\mathbf{v})\right)\\
&-\frac{1}{2}g\left(-\mathbf{D}\left(\mathbf{x}_\eta\circ\mathbf{h}^2\circ\mathbf{v}\right)+\mathbf{x}_\eta\circ\mathbf{h}\circ\mathbf{v}\circ\mathbf{D}\left(\mathbf{h}\right)+\mathbf{h}\circ\mathbf{D}(\mathbf{h}\circ\mathbf{v}\circ\mathbf{x}_\eta)\right)\\
&-g\mathbf{D}\left(\mathbf{x}_\eta\circ\mathbf{h}\circ\mathbf{v}\circ\mathbf{b}\right)-\frac{1}{2}g\left(-\mathbf{D}\left(\mathbf{x}_\eta\circ\mathbf{h}\circ\mathbf{v}\circ\mathbf{b}\right)+\mathbf{h}\circ\mathbf{v}\circ\mathbf{D}\left(\mathbf{x}_\eta\circ\mathbf{b}\right)+\mathbf{x}_\eta\circ\mathbf{b}\circ\mathbf{D}(\mathbf{h}\circ\mathbf{v})\right)\\
&-\frac{1}{2}g\left(-\mathbf{D}\left(\mathbf{x}_\eta\circ\mathbf{h}\circ\mathbf{v}\circ\mathbf{b}\right)+\mathbf{x}_\eta\circ\mathbf{h}\circ\mathbf{v}\circ\mathbf{D}\left(\mathbf{b}\right)+\mathbf{b}\circ\mathbf{D}(\mathbf{h}\circ\mathbf{v}\circ\mathbf{x}_\eta)\right)\\
&-\frac{1}{2}g\left[\mathbf{h}^2\circ\mathbf{v}\circ\mathbf{D}(\mathbf{x}_\eta)+\mathbf{h}\circ\mathbf{v}\circ\mathbf{b}\circ\mathbf{D}(\mathbf{x}_\eta)\right],
\end{aligned}
\tag{C.19}
$$

and $x_\xi$ terms

$$
\begin{aligned}
&+\frac{1}{4}\left[\mathbf{u}\circ\left(\mathbf{hv}\circ\mathbf{u}\circ\mathbf{x}_\xi\right)\mathbf{D}^T+\mathbf{hv}\circ\mathbf{u}\circ\left(\mathbf{x}_\xi\circ\mathbf{u}\right)\mathbf{D}^T+\mathbf{x}_\xi\circ\mathbf{u}\circ(\mathbf{hv}\circ\mathbf{u})\,\mathbf{D}^T+\mathbf{x}_\xi\circ\mathbf{hv}\circ\mathbf{u}\circ(\mathbf{u})\mathbf{D}^T\right]\\
&+\frac{1}{4}\left[\mathbf{v}\circ\left(\mathbf{hv}\circ\mathbf{v}\circ\mathbf{x}_\xi\right)\mathbf{D}^T+\mathbf{hv}\circ\mathbf{v}\circ\left(\mathbf{x}_\xi\circ\mathbf{v}\right)\mathbf{D}^T+\mathbf{x}_\xi\circ\mathbf{v}\circ(\mathbf{hv}\circ\mathbf{v})\,\mathbf{D}^T+\mathbf{x}_\xi\circ\mathbf{hv}\circ\mathbf{v}\circ(\mathbf{v})\mathbf{D}^T\right]
\end{aligned}
$$

$$
\begin{aligned}
&+\frac{1}{2}g\left[\mathbf{h}\circ(\mathbf{h}\circ\mathbf{v}\circ\mathbf{x}_\xi)\mathbf{D}^T+\mathbf{x}_\xi\circ\mathbf{h}\circ(\mathbf{h}\circ\mathbf{v})\mathbf{D}^T+\mathbf{h}^2\circ\mathbf{v}\circ(\mathbf{x}_\xi)\mathbf{D}^T+\mathbf{b}\circ(\mathbf{h}\circ\mathbf{v}\circ\mathbf{x}_\xi)\mathbf{D}^T\right.\\
&\left.+\mathbf{x}_\xi\circ\mathbf{b}\circ(\mathbf{h}\circ\mathbf{v})\mathbf{D}^T+\mathbf{h}\circ\mathbf{v}\circ\mathbf{b}\circ(\mathbf{x}_\xi)\mathbf{D}^T\right]\\
&+\frac{1}{2}g\left[\mathbf{h}\circ\mathbf{v}\circ\left(\mathbf{x}_\xi\circ\mathbf{h}\right)\mathbf{D}^T+\mathbf{x}_\xi\circ\mathbf{h}\circ\mathbf{v}\circ(\mathbf{h})\,\mathbf{D}^T+\mathbf{h}\circ\mathbf{v}\circ\left(\mathbf{x}_\xi\circ(\mathbf{b})\right)\mathbf{D}^T+\mathbf{x}_\xi\circ\mathbf{h}\circ\mathbf{v}\circ(\mathbf{b})\,\mathbf{D}^T\right]\\
&=\\
&+\frac{1}{2}\left(\mathbf{x}_\xi\circ\mathbf{h}\circ\mathbf{v}^3\right)\mathbf{D}^T+\frac{1}{4}\left(-\left(\mathbf{x}_\xi\circ\mathbf{h}\circ\mathbf{v}^3\right)\mathbf{D}^T+\mathbf{v}\circ\left(\mathbf{h}\mathbf{v}\circ\mathbf{v}\circ\mathbf{x}_\xi\right)\mathbf{D}^T+\mathbf{x}_\xi\circ\mathbf{h}\mathbf{v}\circ\mathbf{v}\circ(\mathbf{v})\mathbf{D}^T\right)\\
&+\frac{1}{4}\left(-\left(\mathbf{x}_\xi\circ\mathbf{h}\circ\mathbf{v}^3\right)\mathbf{D}^T+\mathbf{h}\mathbf{v}\circ\mathbf{u}\circ\left(\mathbf{x}_\xi\circ\mathbf{u}\right)\mathbf{D}^T+\mathbf{x}_\xi\circ\mathbf{u}\circ(\mathbf{h}\mathbf{v}\circ\mathbf{u})\,\mathbf{D}^T\right)\\
&+\frac{1}{2}\left(\mathbf{x}_\xi\circ\mathbf{h}\circ\mathbf{u}^2\circ\mathbf{v}\right)\mathbf{D}^T+\frac{1}{4}\left(-\left(\mathbf{x}_\xi\circ\mathbf{h}\circ\mathbf{u}^2\circ\mathbf{v}\right)\mathbf{D}^T+\mathbf{u}\circ\left(\mathbf{h}\mathbf{v}\circ\mathbf{u}\circ\mathbf{x}_\xi\right)\mathbf{D}^T+\mathbf{x}_\xi\circ\mathbf{h}\mathbf{v}\circ\mathbf{u}\circ(\mathbf{u})\mathbf{D}^T\right)\\
&+\frac{1}{4}\left(-\left(\mathbf{x}_\xi\circ\mathbf{h}\circ\mathbf{u}^2\circ\mathbf{v}\right)\mathbf{D}^T+\mathbf{h}\mathbf{v}\circ\mathbf{u}\circ\left(\mathbf{x}_\xi\circ\mathbf{u}\right)\mathbf{D}^T+\mathbf{x}_\xi\circ\mathbf{u}\circ(\mathbf{h}\mathbf{v}\circ\mathbf{u})\,\mathbf{D}^T\right)\\
&+g\left(\mathbf{x}_\xi\circ\mathbf{h}^2\circ\mathbf{v}\right)\mathbf{D}^T+\frac{1}{2}g\left(-\left(\mathbf{x}_\xi\circ\mathbf{h}^2\circ\mathbf{v}\right)\mathbf{D}^T+\mathbf{h}\circ(\mathbf{h}\circ\mathbf{v}\circ\mathbf{x}_\xi)\mathbf{D}^T+\mathbf{x}_\xi\circ\mathbf{h}\circ\mathbf{v}\circ(\mathbf{h})\,\mathbf{D}^T\right)\\
&+\frac{1}{2}g\left(-\left(\mathbf{x}_\xi\circ\mathbf{h}^2\circ\mathbf{v}\right)\mathbf{D}^T+\mathbf{h}\mathbf{v}\circ\mathbf{v}\circ\left(\mathbf{x}_\xi\circ\mathbf{v}\right)\mathbf{D}^T+\mathbf{h}\circ\mathbf{v}\circ\left(\mathbf{x}_\xi\circ\mathbf{h}\right)\mathbf{D}^T\right)\\
&+g\left(\mathbf{x}_\xi\circ\mathbf{h}\circ\mathbf{v}\circ\mathbf{b}\right)\mathbf{D}^T+\frac{1}{2}g\left(-\left(\mathbf{x}_\xi\circ\mathbf{h}\circ\mathbf{v}\circ\mathbf{b}\right)\mathbf{D}^T+\mathbf{b}\circ(\mathbf{h}\circ\mathbf{v}\circ\mathbf{x}_\xi)\mathbf{D}^T+\mathbf{h}\circ\mathbf{v}\circ\left(\mathbf{x}_\xi\circ(\mathbf{b})\right)\mathbf{D}^T\right)\\
&+\frac{1}{2}g\left(-\left(\mathbf{x}_\xi\circ\mathbf{h}\circ\mathbf{v}\circ\mathbf{b}\right)\mathbf{D}^T+\mathbf{x}_\xi\circ\mathbf{b}\circ(\mathbf{h}\circ\mathbf{v})\mathbf{D}^T+\mathbf{h}\circ\mathbf{v}\circ\left(\mathbf{x}_\xi\circ(\mathbf{b})\right)\mathbf{D}^T\right)\\
&+\frac{1}{2}g\left[\mathbf{h}\circ\mathbf{v}\circ\mathbf{b}\circ(\mathbf{x}_\xi)\mathbf{D}^T+\mathbf{h}^2\circ\mathbf{v}\circ(\mathbf{x}_\xi)\mathbf{D}^T\right].
\end{aligned}
\tag{C.20}
$$

We collect all the terms with discrete derivatives of the metric terms and see that they cancel due to the metric identities (3.18) from

$$
\begin{aligned}
&\frac{1}{2}g\left[\mathbf{b}\circ\mathbf{h}\circ\mathbf{u}\circ\mathbf{D}(\mathbf{y}_\eta)+\mathbf{h}^2\circ\mathbf{u}\circ\mathbf{D}(\mathbf{y}_\eta)\right]-\frac{1}{2}g\left[\mathbf{h}\circ\mathbf{b}\circ\mathbf{u}\circ(\mathbf{y}_\xi)\mathbf{D}^T+\mathbf{h}^2\circ\mathbf{u}\circ(\mathbf{y}_\xi)\mathbf{D}^T\right]\\
&-\frac{1}{2}g\left[\mathbf{h}^2\circ\mathbf{v}\circ\mathbf{D}(\mathbf{x}_\eta)+\mathbf{h}\circ\mathbf{v}\circ\mathbf{b}\circ\mathbf{D}(\mathbf{x}_\eta)\right]+\frac{1}{2}g\left[\mathbf{h}\circ\mathbf{v}\circ\mathbf{b}\circ(\mathbf{x}_\xi)\mathbf{D}^T+\mathbf{h}^2\circ\mathbf{v}\circ(\mathbf{x}_\xi)\mathbf{D}^T\right]\\
&=\frac{1}{2}g\left(\mathbf{b}\circ\mathbf{h}\circ\mathbf{u}\circ+\mathbf{h}^2\circ\mathbf{u}\right)\circ\left[\mathbf{D}(\mathbf{y}_\eta)-(\mathbf{y}_\xi)\mathbf{D}^T\right]+\frac{1}{2}g\left(\mathbf{h}^2\circ\mathbf{v}+\mathbf{h}\circ\mathbf{v}\circ\mathbf{b}\right)\circ\left[-\mathbf{D}(\mathbf{x}_\eta)+(\mathbf{x}_\xi)\mathbf{D}^T\right]=0.
\end{aligned}
\tag{C.21}
$$

So far we have neglected the right hand side of the discrete energy equation. As the non-linear correction terms do not affect conservation, we omit them from now on when we state the equation. Including the surface terms, the discrete energy equation is

$$
\begin{aligned}
&\mathbf{J}\circ\left(\frac{1}{2}g\mathbf{h}^2+g\mathbf{h}\circ\mathbf{b}+\frac{1}{2}\mathbf{h}(\mathbf{u}^2+\mathbf{v}^2)\right)_t\\
&\quad+\mathbf{D}\left(\frac{1}{2}\mathbf{y}_\eta\circ\mathbf{h}\circ\mathbf{u}^3+\frac{1}{2}\mathbf{y}_\eta\circ\mathbf{h}\circ\mathbf{u}\circ\mathbf{v}^2+g\mathbf{y}_\eta\circ\mathbf{h}^2\circ\mathbf{u}+\mathbf{y}_\eta\circ g\mathbf{h}\circ\mathbf{u}\circ\mathbf{b}\right)\\
&\quad-\mathbf{D}\left(\frac{1}{2}\mathbf{x}_\eta\circ\mathbf{h}\circ\mathbf{v}^3+\frac{1}{2}\mathbf{x}_\eta\circ\mathbf{h}\circ\mathbf{u}^2\circ\mathbf{v}+g\mathbf{x}_\eta\circ\mathbf{h}^2\circ\mathbf{v}+g\mathbf{x}_\eta\circ\mathbf{h}\circ\mathbf{v}\circ\mathbf{b}\right)\\
&\quad-\left(\frac{1}{2}\mathbf{y}_\xi\circ\mathbf{h}\circ\mathbf{u}^3+\frac{1}{2}\mathbf{y}_\xi\circ\mathbf{h}\circ\mathbf{u}\circ\mathbf{v}^2+g\mathbf{y}_\xi\circ\mathbf{h}^2\circ\mathbf{u}+g\mathbf{y}_\xi\circ\mathbf{h}\circ\mathbf{u}\circ\mathbf{b}\right)\mathbf{D}^T\\
&\quad+\left(\frac{1}{2}\mathbf{x}_\xi\circ\mathbf{h}\circ\mathbf{v}^3+\frac{1}{2}\mathbf{x}_\xi\circ\mathbf{h}\circ\mathbf{u}^2\circ\mathbf{v}+g\mathbf{x}_\xi\circ\mathbf{h}^2\circ\mathbf{v}+g\mathbf{x}_\xi\circ\mathbf{h}\circ\mathbf{v}\circ\mathbf{b}\right)\mathbf{D}^T\\
&\quad=\left(g(\mathbf{h}+\mathbf{b})-\frac{1}{2}\mathbf{u}^2-\frac{1}{2}\mathbf{v}^2\right)\circ\mathbf{S}\left(\tilde{\mathbf{F}}_1^*-\tilde{\mathbf{F}}_1\right)+\left(g(\mathbf{h}+\mathbf{b})-\frac{1}{2}\mathbf{u}^2-\frac{1}{2}\mathbf{v}^2\right)\circ\left(\tilde{\mathbf{G}}_1^*-\tilde{\mathbf{G}}_1\right)\mathbf{S}\\
&\quad+\mathbf{u}\circ\mathbf{S}\left(\tilde{\mathbf{F}}_2^*-\tilde{\mathbf{F}}_2\right)+\mathbf{u}\circ\left(\tilde{\mathbf{G}}_2^*-\tilde{\mathbf{G}}_2\right)\mathbf{S}-\frac{g}{2}\mathbf{u}\circ\mathbf{M}^{-1}\left(\mathbf{y}_\eta\circ\{\{\mathbf{h}\}\}_\xi\circ[\![\mathbf{b}]\!]_\xi\right)+\frac{g}{2}\mathbf{u}\circ\left(\mathbf{y}_\xi\circ\{\{\mathbf{h}\}\}_\eta\circ[\![\mathbf{b}]\!]_\eta\right)\mathbf{M}^{-1}\\
&\quad+\mathbf{v}\circ\mathbf{S}\left(\tilde{\mathbf{F}}_3^*-\tilde{\mathbf{F}}_3\right)+\mathbf{v}\circ\left(\tilde{\mathbf{G}}_3^*-\tilde{\mathbf{G}}_3\right)\mathbf{S}+\frac{g}{2}\mathbf{v}\circ\mathbf{M}^{-1}\left(\mathbf{x}_\eta\circ\{\{\mathbf{h}\}\}_\xi\circ[\![\mathbf{b}]\!]_\xi\right)-\frac{g}{2}\mathbf{v}\circ\left(\mathbf{x}_\xi\circ\{\{\mathbf{h}\}\}_\eta\circ[\![\mathbf{b}]\!]_\eta\right)\mathbf{M}^{-1}.
\end{aligned}
\tag{C.22}
$$

We use the SBP properties $\mathbf{D} = -\mathbf{S} + \hat{\mathbf{D}}$ and $\mathbf{D}^T = -\mathbf{S} + \hat{\mathbf{D}}^T$ to bring this equation into a conservative form. By this we mean that the volume terms will be zero when integrated over the domain. This can be seen from $\hat{\mathbf{D}} = -\mathbf{M}^{-1}\mathbf{D}\mathbf{M}$ and the consistency of the $\mathbf{D}$ matrix: $\vec{1}\mathbf{M}\hat{\mathbf{D}} = -(\mathbf{D}\vec{1})^T\mathbf{M} = \vec{0}$ and $\hat{\mathbf{D}}^T\mathbf{M}\vec{1} = -\mathbf{M}(\mathbf{D}\vec{1}) = \vec{0}$. When the new surface terms are moved to the other side, we have the following equation

$$
\begin{aligned}
&\mathbf{J} \circ \left(\frac{1}{2} g\mathbf{h}^2 + g\mathbf{h} \circ \mathbf{b} + \frac{1}{2}\mathbf{h}(\mathbf{u}^2 + \mathbf{v}^2)\right)_t \\
&+ \hat{\mathbf{D}}\left(\frac{1}{2}\mathbf{y}_\eta \circ \mathbf{h} \circ \mathbf{u}^3 + \frac{1}{2}\mathbf{y}_\eta \circ \mathbf{h} \circ \mathbf{u} \circ \mathbf{v}^2 + g\mathbf{y}_\eta \circ \mathbf{h}^2 \circ \mathbf{u} + \mathbf{y}_\eta \circ g\mathbf{h} \circ \mathbf{u} \circ \mathbf{b}\right) \\
&- \hat{\mathbf{D}}\left(\frac{1}{2}\mathbf{x}_\eta \circ \mathbf{h} \circ \mathbf{v}^3 + \frac{1}{2}\mathbf{x}_\eta \circ \mathbf{h} \circ \mathbf{u}^2 \circ \mathbf{v} + g\mathbf{x}_\eta \circ \mathbf{h}^2 \circ \mathbf{v} + g\mathbf{x}_\eta \circ \mathbf{h} \circ \mathbf{v} \circ \mathbf{b}\right) \\
&- \left(\frac{1}{2}\mathbf{y}_\xi \circ \mathbf{h} \circ \mathbf{u}^3 + \frac{1}{2}\mathbf{y}_\xi \circ \mathbf{h} \circ \mathbf{u} \circ \mathbf{v}^2 + g\mathbf{y}_\xi \circ \mathbf{h}^2 \circ \mathbf{u} + g\mathbf{y}_\xi \circ \mathbf{h} \circ \mathbf{u} \circ \mathbf{b}\right)\hat{\mathbf{D}}^T \\
&+ \left(\frac{1}{2}\mathbf{x}_\xi \circ \mathbf{h} \circ \mathbf{v}^3 + \frac{1}{2}\mathbf{x}_\xi \circ \mathbf{h} \circ \mathbf{u}^2 \circ \mathbf{v} + g\mathbf{x}_\xi \circ \mathbf{h}^2 \circ \mathbf{v} + g\mathbf{x}_\xi \circ \mathbf{h} \circ \mathbf{v} \circ \mathbf{b}\right)\hat{\mathbf{D}}^T \\
&= \left(g(\mathbf{h}+\mathbf{b}) - \frac{1}{2}\mathbf{u}^2 - \frac{1}{2}\mathbf{v}^2\right) \circ \mathbf{S}\left(\tilde{\mathbf{F}}_1^* - \tilde{\mathbf{F}}_1\right) + \left(g(\mathbf{h}+\mathbf{b}) - \frac{1}{2}\mathbf{u}^2 - \frac{1}{2}\mathbf{v}^2\right) \circ \left(\tilde{\mathbf{G}}_1^* - \tilde{\mathbf{G}}_1\right)\mathbf{S} \\
&+ \mathbf{u} \circ \mathbf{S}\left(\tilde{\mathbf{F}}_2^* - \tilde{\mathbf{F}}_2\right) + \mathbf{u} \circ \left(\tilde{\mathbf{G}}_2^* - \tilde{\mathbf{G}}_2\right)\mathbf{S} - \frac{g}{2}\mathbf{u} \circ \mathbf{M}^{-1}\left(\mathbf{y}_\eta \circ \{\{\mathbf{h}\}\}_\xi \circ [\![\mathbf{b}]\!]_\xi\right) + \frac{g}{2}\mathbf{u} \circ \left(\mathbf{y}_\xi \circ \{\{\mathbf{h}\}\}_\eta \circ [\![\mathbf{b}]\!]_\eta\right)\mathbf{M}^{-1} \\
&+ \mathbf{v} \circ \mathbf{S}\left(\tilde{\mathbf{F}}_3^* - \tilde{\mathbf{F}}_3\right) + \mathbf{v} \circ \left(\tilde{\mathbf{G}}_3^* - \tilde{\mathbf{G}}_3\right)\mathbf{S} + \frac{g}{2}\mathbf{v} \circ \mathbf{M}^{-1}\left(\mathbf{x}_\eta \circ \{\{\mathbf{h}\}\}_\xi \circ [\![\mathbf{b}]\!]_\xi\right) - \frac{g}{2}\mathbf{v} \circ \left(\mathbf{x}_\xi \circ \{\{\mathbf{h}\}\}_\eta \circ [\![\mathbf{b}]\!]_\eta\right)\mathbf{M}^{-1} \\
&+ \mathbf{S}\left(\frac{1}{2}\mathbf{y}_\eta \circ \mathbf{h} \circ \mathbf{u}^3 + \frac{1}{2}\mathbf{y}_\eta \circ \mathbf{h} \circ \mathbf{u} \circ \mathbf{v}^2 + g\mathbf{y}_\eta \circ \mathbf{h}^2 \circ \mathbf{u} + \mathbf{y}_\eta \circ g\mathbf{h} \circ \mathbf{u} \circ \mathbf{b}\right) \\
&- \mathbf{S}\left(\frac{1}{2}\mathbf{x}_\eta \circ \mathbf{h} \circ \mathbf{v}^3 + \frac{1}{2}\mathbf{x}_\eta \circ \mathbf{h} \circ \mathbf{u}^2 \circ \mathbf{v} + g\mathbf{x}_\eta \circ \mathbf{h}^2 \circ \mathbf{v} + g\mathbf{x}_\eta \circ \mathbf{h} \circ \mathbf{v} \circ \mathbf{b}\right) \\
&- \left(\frac{1}{2}\mathbf{y}_\xi \circ \mathbf{h} \circ \mathbf{u}^3 + \frac{1}{2}\mathbf{y}_\xi \circ \mathbf{h} \circ \mathbf{u} \circ \mathbf{v}^2 + g\mathbf{y}_\xi \circ \mathbf{h}^2 \circ \mathbf{u} + g\mathbf{y}_\xi \circ \mathbf{h} \circ \mathbf{u} \circ \mathbf{b}\right)\mathbf{S} \\
&+ \left(\frac{1}{2}\mathbf{x}_\xi \circ \mathbf{h} \circ \mathbf{v}^3 + \frac{1}{2}\mathbf{x}_\xi \circ \mathbf{h} \circ \mathbf{u}^2 \circ \mathbf{v} + g\mathbf{x}_\xi \circ \mathbf{h}^2 \circ \mathbf{v} + g\mathbf{x}_\xi \circ \mathbf{h} \circ \mathbf{v} \circ \mathbf{b}\right)\mathbf{S}.
\end{aligned}
\tag{C.23}
$$

As the volume parts in (C.23) are conservative when integrated over the domain, what is left to do is to examine the surface terms. With the definitions of the contravariant fluxes (3.5) we obtain the right hand side for the discrete energy equation for one element

$$
\begin{aligned}
&\left(g(\mathbf{h}+\mathbf{b}) - \frac{1}{2}\mathbf{u}^2 - \frac{1}{2}\mathbf{v}^2\right) \circ \mathbf{S}\left[\mathbf{y}_\eta \circ \{\{\mathbf{h}\}\} \circ \{\{\mathbf{u}\}\} - \mathbf{x}_\eta \circ \{\{\mathbf{h}\}\} \circ \{\{\mathbf{v}\}\} - \mathbf{y}_\eta \circ \mathbf{h} \circ \mathbf{u} + \mathbf{x}_\eta \circ \mathbf{h} \circ \mathbf{v}\right] \\
&+ \left(g(\mathbf{h}+\mathbf{b}) - \frac{1}{2}\mathbf{u}^2 - \frac{1}{2}\mathbf{v}^2\right) \circ \left[-\mathbf{y}_\xi \circ \{\{\mathbf{h}\}\} \circ \{\{\mathbf{u}\}\} + \mathbf{x}_\xi \circ \{\{\mathbf{h}\}\} \circ \{\{\mathbf{v}\}\} + \mathbf{y}_\xi \circ \mathbf{h} \circ \mathbf{u} - \mathbf{x}_\xi \circ \mathbf{h} \circ \mathbf{v}\right]\mathbf{S} \\
&+ \mathbf{u} \circ \mathbf{S}\left[\mathbf{y}_\eta \circ (\{\{\mathbf{h}\}\} \circ \{\{\mathbf{u}\}\}^2 + \frac{1}{2}g\left\{\left\{\mathbf{h}^2\right\}\right\}) - \mathbf{x}_\eta \circ \{\{\mathbf{h}\}\} \circ \{\{\mathbf{u}\}\} \circ \{\{\mathbf{v}\}\} - \mathbf{y}_\eta \circ (\mathbf{h} \circ \mathbf{u}^2 + \frac{1}{2}g\mathbf{h}^2) + \mathbf{x}_\eta \circ \mathbf{h} \circ \mathbf{u} \circ \mathbf{v}\right] \\
&+ \mathbf{u} \circ \left[-\mathbf{y}_\xi \circ (\{\{\mathbf{h}\}\} \circ \{\{\mathbf{u}\}\}^2 + \frac{1}{2}g\left\{\left\{\mathbf{h}^2\right\}\right\}) + \mathbf{x}_\xi \circ \{\{\mathbf{h}\}\} \circ \{\{\mathbf{u}\}\} \circ \{\{\mathbf{v}\}\} + \mathbf{y}_\xi \circ (\mathbf{h} \circ \mathbf{u}^2 + \frac{1}{2}g\mathbf{h}^2) - \mathbf{x}_\xi \circ \mathbf{h} \circ \mathbf{u} \circ \mathbf{v}\right]\mathbf{S} \\
&- \frac{g}{2}\mathbf{u} \circ \mathbf{M}^{-1}\left(\mathbf{y}_\eta \circ \{\{\mathbf{h}\}\}_\xi \circ [\![\mathbf{b}]\!]_\xi\right) + \frac{g}{2}\mathbf{u} \circ \left(\mathbf{y}_\xi \circ \{\{\mathbf{h}\}\}_\eta \circ [\![\mathbf{b}]\!]_\eta\right)\mathbf{M}^{-1} \\
&+ \mathbf{v} \circ \mathbf{S}\left[\mathbf{y}_\eta \circ (\{\{\mathbf{h}\}\} \circ \{\{\mathbf{u}\}\} \circ \{\{\mathbf{v}\}\}) - \mathbf{x}_\eta \circ (\{\{\mathbf{h}\}\} \circ \{\{\mathbf{v}\}\}^2 + \frac{1}{2}g\left\{\left\{\mathbf{h}^2\right\}\right\}) - \mathbf{y}_\eta \circ (\mathbf{h} \circ \mathbf{u} \circ \mathbf{v}) + \mathbf{x}_\eta \circ (\mathbf{h} \circ \mathbf{v}^2 + \frac{1}{2}g\mathbf{h}^2)\right] \\
&+ \mathbf{v} \circ \left[-\mathbf{y}_\xi \circ (\{\{\mathbf{h}\}\} \circ \{\{\mathbf{u}\}\} \circ \{\{\mathbf{v}\}\}) + \mathbf{x}_\xi \circ (\{\{\mathbf{h}\}\} \circ \{\{\mathbf{v}\}\}^2 + \frac{1}{2}g\left\{\left\{\mathbf{h}^2\right\}\right\}) + \mathbf{y}_\xi \circ (\mathbf{h} \circ \mathbf{u} \circ \mathbf{v}) - \mathbf{x}_\xi \circ (\mathbf{h} \circ \mathbf{v}^2 + \frac{1}{2}g\mathbf{h}^2)\right]\mathbf{S} \\
&+ \frac{g}{2}\mathbf{v} \circ \mathbf{M}^{-1}\left(\mathbf{x}_\eta \circ \{\{\mathbf{h}\}\}_\xi \circ [\![\mathbf{b}]\!]_\xi\right) - \frac{g}{2}\mathbf{v} \circ \left(\mathbf{x}_\xi \circ \{\{\mathbf{h}\}\}_\eta \circ [\![\mathbf{b}]\!]_\eta\right)\mathbf{M}^{-1} \\
&+ \mathbf{S}\left(\frac{1}{2}\mathbf{y}_\eta \circ \mathbf{h} \circ \mathbf{u}^3 + \frac{1}{2}\mathbf{y}_\eta \circ \mathbf{h} \circ \mathbf{u} \circ \mathbf{v}^2 + g\mathbf{y}_\eta \circ \mathbf{h}^2 \circ \mathbf{u} + \mathbf{y}_\eta \circ g\mathbf{h} \circ \mathbf{u} \circ \mathbf{b}\right)
\end{aligned}
$$

$$
\begin{aligned}
&- \mathbf{S}\left(\frac{1}{2}\mathbf{x}_\eta \circ \mathbf{h} \circ \mathbf{v}^3 + \frac{1}{2}\mathbf{x}_\eta \circ \mathbf{h} \circ \mathbf{u}^2 \circ \mathbf{v} + g\mathbf{x}_\eta \circ \mathbf{h}^2 \circ \mathbf{v} + g\mathbf{x}_\eta \circ \mathbf{h} \circ \mathbf{v} \circ \mathbf{b}\right) \\
&- \left(\frac{1}{2}\mathbf{y}_\xi \circ \mathbf{h} \circ \mathbf{u}^3 + \frac{1}{2}\mathbf{y}_\xi \circ \mathbf{h} \circ \mathbf{u} \circ \mathbf{v}^2 + g\mathbf{y}_\xi \circ \mathbf{h}^2 \circ \mathbf{u} + g\mathbf{y}_\xi \circ \mathbf{h} \circ \mathbf{u} \circ \mathbf{b}\right)\mathbf{S} \\
&+ \left(\frac{1}{2}\mathbf{x}_\xi \circ \mathbf{h} \circ \mathbf{v}^3 + \frac{1}{2}\mathbf{x}_\xi \circ \mathbf{h} \circ \mathbf{u}^2 \circ \mathbf{v} + g\mathbf{x}_\xi \circ \mathbf{h}^2 \circ \mathbf{v} + g\mathbf{x}_\xi \circ \mathbf{h} \circ \mathbf{v} \circ \mathbf{b}\right)\mathbf{S}.
\end{aligned} \tag{C.24}
$$

We now look at one arbitrary fixed interface. On unstructured meshes local orientation might be different. Thus, this interface might be an interface with constant $\xi$ in one element and constant $\eta$ in the other. However, due to the tensor product ansatz and identical polynomial order in both directions, the interface nodes of the two adjacent elements coincide and the scaling factors of the mass matrix are identical. Without loss of generality we write terms (namely $\xi$, $\eta$) in the local coordinate system of one designated 'master' element. We have to look at terms separately, depending on whether they are multiplied by **S** from the left or the right, as these terms belong to separate element interfaces. The interface contribution at one single interface is taken into account with different signs for the two elements depending on the normal pointing from the one element into the other. Thus, we express the total contribution of the interface with the jump operator. A special case is the surface part of the discretization of the bottom topography. These terms are not scaled by the **S** operator but only by the quadrature weights **M**. Thus, these surface terms occur in both elements with the same sign and we can use the factor of $\frac{1}{2}$ to assemble the average operator $\{\{\cdot\}\}$. We collect terms by their corresponding interface, omit the scaling by the quadrature weights, and write terms for one single node on the interface. Thus, for any node on a constant $\xi$ interface we have

$$
\begin{aligned}
&\left(g\llbracket h\rrbracket + g\llbracket b\rrbracket - \frac{1}{2}\llbracket u^2\rrbracket - \frac{1}{2}\llbracket v^2\rrbracket\right)\left[y_\eta \{\{h\}\}\{\{u\}\} - x_\eta \{\{h\}\}\{\{v\}\}\right] \\
&- y_\eta\left(g\llbracket h^2 u\rrbracket + g\llbracket bhu\rrbracket - \frac{1}{2}\llbracket hu^3\rrbracket - \frac{1}{2}\llbracket huv^2\rrbracket\right) + x_\eta\left(g\llbracket h^2 v\rrbracket + g\llbracket bhv\rrbracket - \frac{1}{2}\llbracket hu^2 v\rrbracket - \frac{1}{2}\llbracket hv^3\rrbracket\right) \\
&+ \llbracket u\rrbracket\left[y_\eta(\{\{h\}\}\{\{u\}\}^2 + \frac{1}{2}g\left\{\left\{h^2\right\}\right\}) - x_\eta\{\{h\}\}\{\{u\}\}\{\{v\}\}\right] \\
&- y_\eta\left(\llbracket hu^3\rrbracket + \frac{1}{2}g\llbracket h^2 u\rrbracket\right) + x_\eta\llbracket hu^2 v\rrbracket + \llbracket v\rrbracket\left[y_\eta(\{\{h\}\}\{\{u\}\}\{\{v\}\}) - x_\eta(\{\{h\}\}\{\{v\}\}^2 + \frac{1}{2}g\left\{\left\{h^2\right\}\right\})\right] \\
&- y_\eta\llbracket huv^2\rrbracket + x_\eta\left(\llbracket hv^3\rrbracket + \frac{1}{2}g\llbracket h^2 v\rrbracket\right) - g\{\{u\}\}\left(y_\eta\{\{h\}\}\llbracket b\rrbracket\right) + g\{\{v\}\}\left(x_\eta\{\{h\}\}\llbracket b\rrbracket\right) \\
&+ \frac{1}{2}y_\eta\llbracket hu^3\rrbracket + \frac{1}{2}y_\eta\llbracket huv^2\rrbracket + gy_\eta\llbracket h^2 u\rrbracket + gy_\eta\llbracket hub\rrbracket - \frac{1}{2}x_\eta\llbracket hv^3\rrbracket - \frac{1}{2}x_\eta\llbracket hu^2 v\rrbracket - gx_\eta\llbracket h^2 v\rrbracket - gx_\eta\llbracket hvb\rrbracket.
\end{aligned} \tag{C.25}
$$

The term (C.25) must be zero to guarantee entropy conservation. Just as for the volume terms, we examine the terms corresponding to the different metric terms separately. First we collect the $y_\eta$ terms. We also distinguish between terms scaled by gravity, drop terms that immediately cancel and rearrange terms to find

$$
\begin{aligned}
&g\left(\{\{h\}\}\{\{u\}\}\llbracket h\rrbracket + \frac{1}{2}\left\{\left\{h^2\right\}\right\}\llbracket u\rrbracket - \frac{1}{2}\llbracket h^2 u\rrbracket\right) \\
&- \frac{1}{2}\{\{h\}\}\{\{u\}\}\llbracket u^2\rrbracket + \{\{h\}\}\{\{u\}\}^2\llbracket u\rrbracket - \frac{1}{2}\{\{h\}\}\{\{u\}\}\llbracket v^2\rrbracket + \{\{h\}\}\{\{u\}\}\{\{v\}\}\llbracket v\rrbracket.
\end{aligned} \tag{C.26}
$$

To cancel the remaining terms we need to use the rules for the jump operator:

$$
\llbracket ab\rrbracket = \{\{a\}\}\llbracket b\rrbracket + \llbracket a\rrbracket\{\{b\}\} \quad \text{and} \quad \llbracket a^2\rrbracket = 2\{\{a\}\}\llbracket a\rrbracket. \tag{C.27}
$$

Specifically we find that

$$
\begin{aligned}
\llbracket h^2 u\rrbracket &= \{\{u\}\}\llbracket h^2\rrbracket + \left\{\left\{h^2\right\}\right\}\llbracket u\rrbracket = 2\{\{h\}\}\{\{u\}\}\llbracket h\rrbracket + \left\{\left\{h^2\right\}\right\}\llbracket u\rrbracket, \\
\llbracket h^2 v\rrbracket &= \{\{v\}\}\llbracket h^2\rrbracket + \left\{\left\{h^2\right\}\right\}\llbracket v\rrbracket = 2\{\{h\}\}\{\{v\}\}\llbracket h\rrbracket + \left\{\left\{h^2\right\}\right\}\llbracket v\rrbracket, \\
\llbracket u^2\rrbracket &= 2\{\{u\}\}\llbracket u\rrbracket, \\
\llbracket v^2\rrbracket &= 2\{\{v\}\}\llbracket v\rrbracket,
\end{aligned} \tag{C.28}
$$

and see that all the interface terms vanish. We follow the same steps for the $x_\eta$ terms on a constant $\xi$ interface, starting by collecting terms from (C.25)

$$\begin{aligned} & g\left(-\{\{h\}\}\{\{v\}\}[\![h]\!]-\frac{1}{2}\left\{\left\{h^2\right\}\right\}[\![v]\!]+\frac{1}{2}[\![h^2 v]\!]\right) \\ & +\frac{1}{2}\{\{h\}\}\{\{v\}\}[\![u^2]\!]+\frac{1}{2}\{\{h\}\}\{\{u\}\}[\![v^2]\!]-\{\{h\}\}\{\{u\}\}\{\{v\}\}[\![u]\!]-\{\{h\}\}\{\{v\}\}^2[\![v]\!]. \end{aligned} \tag{C.29}$$

We see that all terms vanish from the jump rules (C.28).

We have shown that for each constant $\xi$ interface all the terms vanish when the two adjacent elements are summed. We proceed to do the same for constant $\eta$ interfaces. For any node on such an interface we have from (C.24)

$$\begin{aligned} & [\![gh+gb-\frac{1}{2}u^2-\frac{1}{2}v^2]\!]\left[-y_\xi\{\{h\}\}\{\{u\}\}+x_\xi\{\{h\}\}\{\{v\}\}\right] \\ & gy_\xi[\![h^2u]\!]+gy_\xi[\![hub]\!]-\frac{1}{2}y_\xi[\![hu^3]\!]-\frac{1}{2}y_\xi[\![huv^2]\!]-gx_\xi[\![h^2v]\!]-gx_\xi[\![hvb]\!]+\frac{1}{2}x_\xi[\![hvu^2]\!]+\frac{1}{2}x_\xi[\![hv^3]\!] \\ & +[\![u]\!]\left[-y_\xi(\{\{h\}\}\{\{u\}\}^2+\frac{1}{2}g\left\{\left\{h^2\right\}\right\})+x_\xi\{\{h\}\}\{\{u\}\}\{\{v\}\}\right]+y_\xi[\![hu^3]\!]+\frac{1}{2}gy_\xi[\![h^2u]\!]-x_\xi[\![hu^2v]\!] \\ & +\frac{g}{2}\{\{u\}\}\left(y_\xi\{\{h\}\}_\eta[\![b]\!]_\eta\right)-\frac{g}{2}\{\{v\}\}\left(x_\xi\{\{h\}\}_\eta[\![b]\!]_\eta\right) \\ & +[\![v]\!]\left[-y_\xi(\{\{h\}\}\{\{u\}\}\{\{v\}\})+x_\xi(\{\{h\}\}\{\{v\}\}^2+\frac{1}{2}g\left\{\left\{h^2\right\}\right\})\right]+y_\xi[\![huv^2]\!]-x_\xi[\![hv^3]\!]-\frac{1}{2}gx_\xi[\![h^2v]\!] \\ & -\frac{1}{2}y_\xi[\![hu^3]\!]-\frac{1}{2}y_\xi[\![huv^2]\!]-gy_\xi[\![h^2u]\!]-gy_\xi[\![hub]\!] \\ & +\frac{1}{2}x_\xi[\![hv^3]\!]+\frac{1}{2}x_\xi[\![hu^2v]\!]+gx_\xi[\![h^2v]\!]+gx_\xi[\![hvb]\!], \end{aligned} \tag{C.30}$$

which we simplify, like before, to become

$$\begin{aligned} & y_\xi\left[g\left(-\{\{h\}\}\{\{u\}\}[\![h]\!]-\frac{1}{2}\left\{\left\{h^2\right\}\right\}[\![u]\!]+\frac{1}{2}[\![h^2u]\!]\right)\right. \\ & \left.+\frac{1}{2}\{\{h\}\}\{\{u\}\}[\![u^2]\!]+\frac{1}{2}\{\{h\}\}\{\{u\}\}[\![v^2]\!]-\frac{1}{2}\{\{h\}\}\{\{u\}\}^2[\![u]\!]-\frac{1}{2}\{\{h\}\}\{\{u\}\}\{\{v\}\}[\![v]\!]\right] \\ & +x_\xi\left[g\left(\{\{h\}\}\{\{v\}\}[\![h]\!]-\frac{1}{2}\left\{\left\{h^2\right\}\right\}[\![v]\!]+\frac{1}{2}[\![h^2v]\!]\right)\right. \\ & \left.-\frac{1}{2}\{\{h\}\}\{\{v\}\}[\![u^2]\!]-\frac{1}{2}\{\{h\}\}\{\{v\}\}[\![v^2]\!]+\frac{1}{2}\{\{h\}\}\{\{v\}\}^2[\![v]\!]+\frac{1}{2}\{\{h\}\}\{\{v\}\}\{\{v\}\}[\![u]\!]\right]. \end{aligned} \tag{C.31}$$

All of the terms in (C.31) vanish by similar arguments as before by using the jump rules (C.28). □

### C.2. Proof of Property 1.3

**Proof.** To verify the well-balancedness of the scheme we must show that the scheme preserves the "lake at rest" problem correctly, meaning that the initial conditions $h+b=\text{const}$ and $u=v=0$ are satisfied for all time. It is immediately satisfied for the discretized continuity equation as $u$ or $v$ are factors in all the terms. However, the lake at rest solution is not immediately clear for the momentum equations. We show here in detail that the discrete time derivative vanishes for the $hu$ equation, the $hv$ equation is handled analogously.

In the following proof we make extensive use of the Hadamard product notation (3.28) for the component-wise multiplication of matrices and define component-wise powers of nodal values by

$$\mathbf{W}^k := \mathbf{W}^{k-1}\circ\mathbf{W}. \tag{C.32}$$

If we fully expand the flux-differencing form (4.2) of the $hu$ equation by (3.52) and the cubic forms from [30] we have the following scheme

$$
\begin{aligned}
&\mathbf{J}(\mathbf{h}\circ\mathbf{u})_t + \frac{1}{4}(\mathbf{D}(\mathbf{y}_\eta\circ\mathbf{h}\circ\mathbf{u}^2) + (-\mathbf{y}_\xi\circ\mathbf{h}\circ\mathbf{u}^2)\mathbf{D}^T)\\
&\quad+\frac{1}{4}(\mathbf{y}_\eta\circ\mathbf{D}(\mathbf{h}\circ\mathbf{u}^2) + \mathbf{h}\circ\mathbf{u}^2\circ\mathbf{D}(\mathbf{y}_\eta) - \mathbf{h}\circ\mathbf{u}^2\circ(\mathbf{y}_\xi)\mathbf{D}^T - \mathbf{y}_\xi\circ(\mathbf{h}\circ\mathbf{u}^2)\mathbf{D}^T)\\
&\quad+\frac{1}{4}(\mathbf{h}\circ\mathbf{u}\circ\mathbf{D}(\mathbf{y}_\eta\circ\mathbf{u}) + \mathbf{y}_\eta\circ\mathbf{h}\circ\mathbf{u}\circ\mathbf{D}(\mathbf{u}) - \mathbf{h}\circ\mathbf{u}\circ(\mathbf{y}_\xi\circ\mathbf{u})\mathbf{D}^T - \mathbf{y}_\xi\circ\mathbf{h}\circ\mathbf{u}\circ(\mathbf{u})\mathbf{D}^T)\\
&\quad+\frac{1}{4}\left(\mathbf{u}\circ\mathbf{D}(\mathbf{y}_\eta\circ\mathbf{h}\circ\mathbf{u}) + \mathbf{y}_\eta\circ\mathbf{u}\circ\mathbf{D}(\mathbf{h}\circ\mathbf{u}) - (\mathbf{y}_\xi\circ\mathbf{h}\circ\mathbf{u}^2)\mathbf{D}^T - \mathbf{y}_\xi\circ\mathbf{u}\circ(\mathbf{h}\circ\mathbf{u})\mathbf{D}^T\right)\\
&\quad+\frac{g}{2}(\mathbf{h}\circ\mathbf{D}(\mathbf{y}_\eta\circ\mathbf{h}) + \mathbf{y}_\eta\circ\mathbf{h}\circ\mathbf{D}(\mathbf{h}) - \mathbf{h}\circ(\mathbf{y}_\xi\circ\mathbf{h})\mathbf{D}^T - \mathbf{y}_\xi\circ\mathbf{h}\circ(\mathbf{h})\mathbf{D}^T)\\
&\quad+\frac{1}{4}(-\mathbf{D}(\mathbf{x}_\eta\circ\mathbf{h}\circ\mathbf{u}\circ\mathbf{v}) + (\mathbf{x}_\xi\circ\mathbf{h}\circ\mathbf{u}\circ\mathbf{v})\mathbf{D}^T)\\
&\quad+\frac{1}{4}(-\mathbf{x}_\eta\circ\mathbf{h}\circ\mathbf{v}\circ\mathbf{D}(\mathbf{u}) - \mathbf{h}\circ\mathbf{v}\circ\mathbf{D}(\mathbf{x}_\eta\circ\mathbf{u}) + \mathbf{h}\circ\mathbf{v}\circ\mathbf{x}_\xi\circ(\mathbf{u})\mathbf{D}^T + \mathbf{h}\circ\mathbf{v}\circ(\mathbf{x}_\xi\circ\mathbf{u})\mathbf{D}^T)\\
&\quad+\frac{1}{4}(-\mathbf{x}_\eta\circ\mathbf{D}(\mathbf{h}\circ\mathbf{u}\circ\mathbf{v}) - \mathbf{h}\circ\mathbf{u}\circ\mathbf{v}\circ\mathbf{D}(\mathbf{x}_\eta) + \mathbf{h}\circ\mathbf{u}\circ\mathbf{v}\circ(\mathbf{x}_\xi)\mathbf{D}^T + \mathbf{x}_\xi\circ(\mathbf{h}\circ\mathbf{u}\circ\mathbf{v})\mathbf{D}^T)\\
&\quad+\frac{1}{4}\left(-\mathbf{u}\circ\mathbf{D}(\mathbf{x}_\eta\circ\mathbf{h}\circ\mathbf{v}) - \mathbf{x}_\eta\circ\mathbf{u}\circ\mathbf{D}(\mathbf{h}\circ\mathbf{v}) + (\mathbf{x}_\xi\circ\mathbf{h}\circ\mathbf{v}\circ\mathbf{u})\mathbf{D}^T + \mathbf{x}_\xi\circ\mathbf{u}\circ(\mathbf{h}\circ\mathbf{v})\mathbf{D}^T\right)\\
&\quad+\frac{1}{2}g\mathbf{h}\circ\left(\mathbf{y}_\eta\circ\mathbf{D}(\mathbf{b}) + \mathbf{D}(\mathbf{y}_\eta\circ\mathbf{b}) - \mathbf{y}_\xi\circ(\mathbf{b})\mathbf{D}^T - (\mathbf{y}_\xi\circ\mathbf{b})\mathbf{D}^T\right)\\
&\quad=-\frac{g}{2}\mathbf{M}^{-1}\left(\mathbf{y}_\eta\circ\{\{\mathbf{h}\}\}_\xi\circ[\![\mathbf{b}]\!]_\xi\right) - \frac{g}{2}\left(-\mathbf{y}_\xi\circ\{\{\mathbf{h}\}\}_\eta\circ[\![\mathbf{b}]\!]_\eta\right)\mathbf{M}^{-1} + \mathbf{S}\left(\tilde{\mathbf{F}}_2^* - \tilde{\mathbf{F}}_2\right) + \left(\tilde{\mathbf{G}}_2^* - \tilde{\mathbf{G}}_2\right)\mathbf{S}.
\end{aligned}
\tag{C.33}
$$

The source term discretization is a key factor in obtaining a well-balanced scheme. In accordance with our approach for the flux terms, we have also discretized the source term as a quadratic split form. To account for possibly discontinuous bottom topographies on element interfaces we have introduced an additional interface part that vanishes for continuous topographies. The full source term discretization is

$$
\begin{aligned}
\frac{g}{2}\mathbf{h}\circ\mathbf{b}_x \approx\ & \frac{g}{2}\mathbf{h}\circ\left(\mathbf{y}_\eta\circ\mathbf{D}(\mathbf{b}) + \mathbf{D}(\mathbf{y}_\eta\circ\mathbf{b}) - \mathbf{y}_\xi\circ(\mathbf{b})\mathbf{D}^T - (\mathbf{y}_\xi\circ\mathbf{b})\mathbf{D}^T\right)\\
&+\frac{g}{2}\mathbf{M}^{-1}\left(\mathbf{y}_\eta\circ\{\{\mathbf{h}\}\}_\xi\circ[\![\mathbf{b}]\!]_\xi\right) - \frac{g}{2}\left(\mathbf{y}_\xi\circ\{\{\mathbf{h}\}\}_\eta\circ[\![\mathbf{b}]\!]_\eta\right)\mathbf{M}^{-1},
\end{aligned}
\tag{C.34}
$$

where we use notation (4.1) for the jump in bottom topography and the average water height. Using the definitions of the numerical and physical fluxes, the interface terms of the strong form DG discretization are

$$
\begin{aligned}
&\mathbf{S}\left(\tilde{\mathbf{F}}_2^* - \tilde{\mathbf{F}}_2\right) + \left(\tilde{\mathbf{G}}_2^* - \tilde{\mathbf{G}}_2\right)\mathbf{S} =\\
&+\mathbf{S}\left(\mathbf{y}_\eta\circ(\{\{\mathbf{u}\}\}^2\circ\{\{\mathbf{h}\}\} + \frac{g}{2}\left\{\left\{\mathbf{h}^2\right\}\right\}) - \mathbf{x}_\eta\circ\{\{\mathbf{u}\}\}\circ\{\{\mathbf{v}\}\}\circ\{\{\mathbf{h}\}\} - \mathbf{y}_\eta\circ\left(\mathbf{h}\circ\mathbf{v}\circ\mathbf{u}^2 + \frac{g}{2}\mathbf{h}^2\right) + \mathbf{x}_\eta\circ\mathbf{h}\circ\mathbf{u}\circ\mathbf{v})\right)\\
&+\left(-\mathbf{y}_\xi\circ(\{\{\mathbf{u}\}\}^2\circ\{\{\mathbf{h}\}\} + \frac{g}{2}\left\{\left\{\mathbf{h}^2\right\}\right\}) + \mathbf{x}_\xi\circ\{\{\mathbf{u}\}\}\circ\{\{\mathbf{v}\}\}\circ\{\{\mathbf{h}\}\} + \mathbf{y}_\xi\circ\left(\mathbf{h}\circ\mathbf{u}^2 + \frac{g}{2}\mathbf{h}^2\right) - \mathbf{x}_\xi\circ\mathbf{h}\circ\mathbf{u}\circ\mathbf{v}\right)\mathbf{S}.
\end{aligned}
\tag{C.35}
$$

Under the "lake at rest" initial conditions, $u = v = 0$, many terms in the momentum equation (C.33) vanish. The remaining terms are

$$
\begin{aligned}
&\mathbf{J}\circ(\mathbf{h}\circ\mathbf{u})_t + \frac{1}{2}(g\mathbf{h}\circ\mathbf{D}(\mathbf{y}_\eta\circ\mathbf{h}) + \mathbf{y}_\eta\circ g\mathbf{h}\circ\mathbf{D}(\mathbf{h}) - g\mathbf{h}\circ(\mathbf{y}_\xi\circ\mathbf{h})\mathbf{D}^T - \mathbf{y}_\xi\circ g\mathbf{h}\circ(\mathbf{h})\mathbf{D}^T)\\
&\quad+\frac{1}{2}g\mathbf{h}\circ\left(\mathbf{y}_\eta\circ\mathbf{D}(\mathbf{b}) + \mathbf{D}(\mathbf{y}_\eta\circ\mathbf{b}) - \mathbf{y}_\xi\circ(\mathbf{b})\mathbf{D}^T - (\mathbf{y}_\xi\circ\mathbf{b})\mathbf{D}^T\right)\\
&\quad=-\mathbf{M}^{-1}\left(\mathbf{y}_\eta\circ\{\{\mathbf{h}\}\}_\xi\circ[\![\mathbf{b}]\!]_\xi\right) + \mathbf{S}\left(\mathbf{y}_\eta\circ\left(\left\{\left\{\mathbf{h}^2\right\}\right\} - \mathbf{h}^2\right)\right)\\
&\quad-\left(-\mathbf{y}_\xi\circ\{\{\mathbf{h}\}\}_\eta\circ[\![\mathbf{b}]\!]_\eta\right)\mathbf{M}^{-1} + \left(-\mathbf{y}_\xi\circ\left(\left\{\left\{\mathbf{h}^2\right\}\right\} - \mathbf{h}^2\right)\right)\mathbf{S}.
\end{aligned}
\tag{C.36}
$$

We first consider the volume terms in (C.36). For constant total water height $h+b=\text{const}$, the exactness of the derivative operator implies that $\mathbf{D}(\mathbf{h}+\mathbf{b})=(\mathbf{h}+\mathbf{b})\mathbf{D}^T=0$. The remaining terms cancel due to the metric identities (3.18) and we find that

$$\begin{aligned}\frac{g}{2}\mathbf{h}\circ(\mathbf{D}(\mathbf{y}_\eta\circ(\mathbf{h}+\mathbf{b}))+\mathbf{y}_\eta\circ\mathbf{D}(\mathbf{h}+\mathbf{b})-(\mathbf{y}_\xi\circ(\mathbf{h}+\mathbf{b}))\mathbf{D}^T-\mathbf{y}_\xi\circ(\mathbf{h}+\mathbf{b})\mathbf{D}^T)\\ =\frac{g}{2}\mathbf{h}\circ((\mathbf{h}+\mathbf{b})\mathbf{D}(\mathbf{y}_\eta)-(\mathbf{h}+\mathbf{b})\circ(\mathbf{y}_\xi)\mathbf{D}^T)=0.\end{aligned} \tag{C.37}$$

Since we allow discontinuities in the bottom topography at element interfaces we must account for the jump in water height and we cannot guarantee that $\{\{h^2\}\}=h^2$. Instead we have at each interface

$$\{\{h^2\}\}-h^2=\frac{h_i^2+h_o^2}{2}-h_i^2=\frac{h_o^2-h_i^2}{2}=\pm\frac{1}{2}[\![h^2]\!]=\pm\{\{h\}\}[\![h]\!], \tag{C.38}$$

where $h_i$ denotes the inner and $h_o$ the outer value. The sign of (C.38) depends upon which interface we consider. It is positive for the right and top interface and negative otherwise. In combination with the sign applied by the matrix, $\mathbf{S}=\text{diag}(\frac{1}{\omega_0},0,\dots,0,-\frac{1}{\omega_N})$, which gives a negative contribution for the top right component and a positive contribution for the bottom left component, we restate these interface terms as

$$\begin{aligned}\mathbf{S}\left(\mathbf{y}_\eta\circ\left(\{\{\mathbf{h}^2\}\}_\xi-\mathbf{h}^2\right)\right)&=-\mathbf{M}^{-1}\left(\mathbf{y}_\eta\circ\left(\{\{\mathbf{h}\}\}_\xi\circ[\![\mathbf{h}]\!]_\xi\right)\right),\\ \left(-\mathbf{y}_\xi\circ\left(\{\{\mathbf{h}^2\}\}_\eta-\mathbf{h}^2\right)\right)\mathbf{S}&=-\left(-\mathbf{y}_\xi\circ\left(\{\{\mathbf{h}\}\}_\eta\circ[\![\mathbf{h}]\!]_\eta\right)\right)\mathbf{M}^{-1}.\end{aligned} \tag{C.39}$$

With the reformulation (C.39) we find that the interface contributions are zero

$$\begin{aligned}&-\mathbf{M}^{-1}\left(\mathbf{y}_\eta\circ\{\{\mathbf{h}\}\}_\xi\circ[\![\mathbf{b}]\!]_\xi\right)-\mathbf{M}^{-1}\left(\mathbf{y}_\eta\circ\left(\{\{\mathbf{h}\}\}_\xi\circ[\![\mathbf{h}]\!]_\xi\right)\right)\\ &-\left(-\mathbf{y}_\xi\circ\{\{\mathbf{h}\}\}_\eta\circ[\![\mathbf{b}]\!]_\eta\right)\mathbf{M}^{-1}-\left(-\mathbf{y}_\xi\circ\left(\{\{\mathbf{h}\}\}_\eta\circ[\![\mathbf{h}]\!]_\eta\right)\right)\mathbf{M}^{-1}\\ =&-\mathbf{M}^{-1}\left(\mathbf{y}_\eta\circ\left(\{\{\mathbf{h}\}\}_\xi\circ[\![\mathbf{b}+\mathbf{h}]\!]_\xi\right)\right)\\ &-\left(-\mathbf{y}_\xi\circ\left(\{\{\mathbf{h}\}\}_\eta\circ[\![\mathbf{b}+\mathbf{h}]\!]_\eta\right)\right)\mathbf{M}^{-1}=0,\end{aligned} \tag{C.40}$$

since $h+b=\text{const}$, even on interfaces.

Thus, we have shown that the discrete time derivative of the $J(hu)_t$ is zero. The treatment of the $J(hv)_t$ contribution is also zero by an analogous argument. Thus, the DG scheme is well-balanced. □

## Appendix D. Algorithmic description of the ESDGSEM

We outlined the reformulation of the curvilinear DGSEM in the flux differencing form in Sec. 3.4. Now we provide specific details and restructure the algorithms of a standard DGSEM implementation to incorporate the entropy stable approximation. The flux differencing form for the curvilinear ESDGSEM (4.25) is self-contained, but it seems to be a daunting task to implement. We demonstrate, however, that with a few extra procedures and a slight restructuring of a standard DGSEM time derivative routine it is straightforward to implement the newly proposed entropy stable scheme.

For this discussion we focus on the computation of the time derivative on a single spectral element. The global time derivative is assembled by looping over every element in a mesh [18]. To make the discussion concrete we utilize the DGSEM structure outlined in Chap. 8.4 of the book by Kopriva [18], but the discussion readily extends to any standard DGSEM implementation.

To begin, we introduce the notation used throughout this section. We store the computed solution on each element, scaled by the Jacobian, in the array $\{Jw_{i,j,n}\}_{i=0,j=0,n=1}^{N,N,nEqn}$ where $N$ is the polynomial order of the approximation and $nEqn$ is the number of equations. The time derivative, also scaled by the Jacobian, is stored in the array $\{J\dot{w}_{i,j,n}\}_{i=0,j=0,n=1}^{N,N,nEqn}$. Each element stores array information about its mapping (the Jacobian, metric terms, etc.) in the *geom* object. We adopt the notation of a period to denote access to a component of an object. We store the bottom topography contributions in the volume and on the boundary of an element in separate places (for convenience). The array $\{b_{i,j}\}_{i=0,j=0}^{N,N}$ stores the bottom

topography evaluated at the Legendre–Gauss–Lobatto nodes. The array $\{db_{i,j,n}\}_{i=0,j=0,n=1}^{N,N,nEqn}$ stores the volume contributions of the source term and the array $\{[\![b]\!]_{i,ID}\}_{i=0,ID=1}^{N,4}$ stores the jump in the bottom topography along each edge of a quadrilateral element. To compute the source term at each edge we also store the average of the computed water height in the array $\{\{\{h\}\}_{i,ID}\}_{i=0,ID=1}^{N,4}$.

First, we outline the details of the source term discretization. We divide the computation into two parts: surface and volume contributions. For the surface contributions we alter the routine Alg. 137 (*EdgeFluxes*) from [18]. This is done out of convenience because the *EdgeFluxes* procedure already has access to local information about an edge, its local ID, and the elements that border an edge. Because we are on an unstructured mesh, care must be taken when computing the jump in the bottom topography term. We take the element to the left of an edge, $e_1$, to be the "interior" and the element on the right, $e_2$, to be the "exterior" so that definition of the $[\![b]\!]$ terms is clear. Also, we denote the local side ID of an edge on each element by $s_1$ and $s_2$ respectively. We fill a temporary array from the bottom topography term $\{b_{i,j}\}_{i=0,j=0}^{N,N}$ that depends on the local side index of the edge on the elements $e_1$ and $e_2$, e.g., if $s_1 = 1$ then $b_L = e_1.\{b_{i,0}\}_{i=0}^{N}$ and $s_2 = 3$ then $b_R = e_2.\{b_{i,N}\}_{i=0}^{N}$. Then, after the normal numerical flux at an edge is computed, one adds to the existing algorithm:

$$
\begin{aligned}
e_1.\left\{[\![b]\!]_{i,s_1}\right\}_{i=0}^{N} &= b_R - b_L, \\
e_2.\left\{[\![b]\!]_{i,s_2}\right\}_{i=0}^{N} &= e_1.\left\{[\![b]\!]_{i,s_1}\right\}_{i=0}^{N}, \\
e_1.\left\{\{\{h\}\}_{i,s_1}\right\}_{i=0}^{N} &= \frac{1}{2}(h_R + h_L), \\
e_2.\left\{\{\{h\}\}_{i,s_2}\right\}_{i=0}^{N} &= e_1.\left\{\{\{h\}\}_{i,s_1}\right\}_{i=0}^{N}.
\end{aligned}
\tag{D.1}
$$

Algorithm 1 (*BottomContributions*) is a straightforward implementation of (4.5) to compute the volume contributions of the source term. We note that one could write the volumetric computation of the source term under BLAS3 architecture standards. Because the bottom topography does not depend on time we precompute and store the quantities $\{db_{i,j,n}\}_{i=0,j=0,n=1}^{N,N,nEqn}$ for later use.

**Algorithm 1:** (*BottomContributions*) Computation of the volumetric source term contributions.

**Procedure** BottomContributions

**Input**: $x$, $y$, $\{h\}_{i=0,j=0}^{N,N}$, $\{b\}_{i=0,j=0}^{N,N}$, $geom$, $\{D_{i,j}\}_{i=0,j=0}^{N,N}$ `// polynomial derivative matrix`

$\{db_{i,j,n}\}_{i=0,j=0,n=1}^{N,N,nEqn} \leftarrow 0$
**for** $i = 0$ **to** $N$ **do**
  **for** $j = 0$ **to** $N$ **do**
    $\{sum_m\}_{m=1}^{6} \leftarrow 0$
    **for** $k = 0$ **to** $N$ **do**
      $sum_1 \leftarrow sum_1 + D_{i,k} * b_{k,j}$
      $sum_2 \leftarrow sum_2 + b_{i,k} * D_{k,j}^T$
      $sum_3 \leftarrow sum_3 + D_{i,k} * \left((geom.y_\eta)_{k,j} * b_{k,j}\right)$
      $sum_4 \leftarrow sum_4 + \left((geom.y_\xi)_{i,k} * b_{i,k}\right) * D_{k,j}^T$
      $sum_5 \leftarrow sum_5 + D_{i,k} * \left((geom.x_\eta)_{k,j} * b_{k,j}\right)$
      $sum_6 \leftarrow sum_6 + \left((geom.x_\xi)_{i,k} * b_{i,k}\right) * D_{k,j}^T$
    $db_{i,j,2} \leftarrow (geom.y_\eta)_{i,j} * sum_1 - (geom.y_\xi)_{i,j} * sum_2 + sum_3 - sum_4$
    $db_{i,j,3} \leftarrow -(geom.x_\eta)_{i,j} * sum_1 + (geom.x_\xi)_{i,j} * sum_2 - sum_5 + sum_6$

**Output**: $\{db\}_{i=0,j=0,n=1}^{N,N,nEqn}$

**End Procedure** BottomContributions

We next present Algorithms 2 (*HighOrder-xFluxDifference*) and 3 (*HighOrder-yFluxDifference*) needed to reformulate the volume contributions of the ESDGSEM into the sub-cell flux differencing form presented in (3.48) and (3.49). Routines to compute the volume fluxes $\vec{F}^{vol}$ and $\vec{G}^{vol}$, given in (4.3), are straightforward to implement, so we omit an explicit algorithm. To simplify the indexing in each of the high-order flux differencing algorithms we assume that the procedures is passed an appropriate slice from the solution storage and metric term arrays.

**Algorithm 2:** (*HighOrder-xFluxDifference*) Computation of the flux difference $\mathbf{\Delta}\bar{\bar{\mathbf{F}}}$.

**Procedure** HighOrder-xFluxDifference

**Input**: $\{W_{i,n}\}_{i=0,n=1}^{N,nEqn}$ `// slice of solution on Gauss-Lobatto grid`

**Input**: $\left\{(y_\eta)_i\right\}_{i=0}^{N}, \left\{(x_\eta)_i\right\}_{i=0}^{N}$ `// metric terms on Gauss-Lobatto grid`

**Input**: $Q$ `// SBP matrix`

**for** $i = 0$ **to** $N$ **do**

  **for** $m = 0$ **to** $N$ **do**

    $\{\{y_\eta\}\} \leftarrow \frac{1}{2}\left((y_\eta)_i + (y_\eta)_m\right)$

    $\{\{x_\eta\}\} \leftarrow \frac{1}{2}\left((x_\eta)_i + (x_\eta)_m\right)$

    $\left\{d\bar{\bar{F}}_{i,n}\right\}_{n=1}^{nEqn} \leftarrow \left\{d\bar{\bar{F}}_{i,n}\right\}_{n=1}^{nEqn} + 2Q_{i,m}\left(\{\{y_\eta\}\} * F^{vol}\left(\{W_{i,n}\}_{n=1}^{nEqn}, \{W_{m,n}\}_{n=1}^{nEqn}\right) - \{\{x_\eta\}\} * G^{vol}\left(\{W_{i,n}\}_{n=1}^{nEqn}, \{W_{m,n}\}_{n=1}^{nEqn}\right)\right)$

**Output**: $\left\{d\bar{\bar{F}}_{i,n}\right\}_{i=0,n=1}^{N,nEqn}$

**End Procedure** HighOrder-xFluxDifference

**Algorithm 3:** (*HighOrder-yFluxDifference*) Computation of the flux difference $\bar{\bar{\mathbf{G}}}\mathbf{\Delta}^T$.

**Procedure** HighOrder-yFluxDifference

**Input**: $\{W_{j,n}\}_{j=0,n=1}^{N,nEqn}$ `// slice of solution on Gauss-Lobatto grid`

**Input**: $\left\{(y_\xi)_j\right\}_{j=0}^{N}, \left\{(x_\xi)_j\right\}_{j=0}^{N}$ `// metric terms on Gauss-Lobatto grid`

**Input**: $Q$ `// SBP matrix`

**for** $j = 0$ **to** $N$ **do**

  **for** $m = 0$ **to** $N$ **do**

    $\{\{y_\xi\}\} \leftarrow \frac{1}{2}\left((y_\xi)_j + (y_\xi)_m\right)$

    $\{\{x_\xi\}\} \leftarrow \frac{1}{2}\left((x_\xi)_j + (x_\xi)_m\right)$

    $\left\{d\bar{\bar{G}}_{j,n}\right\}_{n=1}^{nEqn} \leftarrow \left\{d\bar{\bar{G}}_{j,n}\right\}_{n=1}^{nEqn} + 2Q_{j,m}\left(-\{\{y_\xi\}\} * F^{vol}\left(\{W_{j,n}\}_{n=1}^{nEqn}, \{W_{m,n}\}_{n=1}^{nEqn}\right) + \{\{x_\xi\}\} * G^{vol}\left(\{W_{j,n}\}_{n=1}^{nEqn}, \{W_{m,n}\}_{n=1}^{nEqn}\right)\right)$

**Output**: $\left\{d\bar{\bar{G}}_{j,n}\right\}_{j=0,n=1}^{N+1,nEqn}$

**End Procedure** HighOrder-yFluxDifference

Now that we have outlined the source term discretization and the high-order flux extensions we are prepared to present the main algorithm for the efficient ESDGSEM implementation. We restructure the routine Alg. 144 (*MappedDG2DTimeDerivative*) from [18] that computes the local time derivative on a curved quadrilateral element. We outline the explicit steps to change a standard DGSEM approximation to implement the ESDGSEM for the shallow water equations:

1. Begin with Alg. 144 (*MappedDG2DTimeDerivative*) from [18] that computes the local time derivative on an element.
2. Remove the standard approach that computes the DG derivative (denoted Alg. 92 (*SystemDGDerivative*) in [18]).
3. Insert the equivalent flux differencing formulation for the volume terms outlined in Sec. 3.4 and detailed in Algorithms 2 and 3.
4. Use the entropy stable numerical fluxes (4.23) and (4.24) at element interfaces.
5. Multiply the precomputed parts of the volume source term discretization by the water height and add the source term contributions at each element in the volume.
6. Multiply the precomputed parts of the surface source term discretization by the average water height and add the source term contributions at each element edge.
7. Algorithm 4 (*ESDG2DTimeDerivative*) summarizes the reformulation of a standard DG derivative to the computationally efficient flux difference form.

To reiterate, we assume that the approximations to the bottom derivatives are precomputed and stored and the surface source term contributions are computed in an augmented *EdgeFluxes* procedure.

**Algorithm 4:** (*ESDG2DTimeDerivative*) Implementation of two dimensional ESDGSEM in curvilinear coordinates.

**Procedure** ESDG2DTimeDerivative

**Input**: $\{JW_{i,j,n}\}_{i=0,j=0,n=1}^{N,N,nEqn}$ `// solution scaled by Jacobian`

**Input**: $\left\{\tilde{F}^{*,es}_{i,n,ID}\right\}_{i=0,n=1,ID=1}^{N,nEqn,4}$, $\left\{\tilde{G}^{*,es}_{j,n,ID}\right\}_{j=0,n=1,ID=1}^{N,nEqn,4}$ `// entropy stable numerical fluxes`

**Input**: $geom$ `// element geometry`

**Input**: $Q$ `// SBP matrix`

**Input**: $\{\omega_i\}_{i=0}^{N}$ `// Gauss-Lobatto quadrature weights`

**Input**: $\{db_{i,j,n}\}_{i=0,j=0,n=1}^{N,N,nEqn}$, $\{[\![b]\!]_{i,ID}\}_{i=0,ID=1}^{N,4}$, $\{\{\{h\}\}_{i,ID}\}_{i=0,ID=1}^{N,4}$ `// bottom contributions`

$\{W_{i,j,n}\}_{i=0,j=0,n=1}^{N,N,nEqn} \leftarrow \{JW_n\}_{i=0,j=0,n=1}^{N,N,nEqn}/\{(geom.J)_{i,j}\}_{i=0,j=0}^{N,N}$

`// ξ-direction`

**for** $j = 0$ **to** $N$ **do**

$\left\{\tilde{F}_{0,n}\right\}_{n=1}^{nEqn} \leftarrow (geom.y_\eta)_{0,j} * xFlux\left(\{W_{0,j,n}\}_{n=1}^{nEqn}\right) - (geom.x_\eta)_{0,j} * yFlux\left(\{W_{0,j,n}\}_{n=1}^{nEqn}\right)$

$\left\{\tilde{F}_{N,n}\right\}_{n=1}^{nEqn} \leftarrow (geom.y_\eta)_{N,j} * xFlux\left(\{W_{N,j,n}\}_{n=1}^{nEqn}\right) - (geom.x_\eta)_{N,j} * yFlux\left(\{W_{N,j,n}\}_{n=1}^{nEqn}\right)$

$\left\{d\tilde{\bar{F}}_{i,n}\right\}_{i=0,n=1}^{N+1,nEqn} \leftarrow HighOrder{-}xFluxDifference\left(\left\{W_{i,j,n}\right\}_{i=0,n=1}^{N,nEqn}, Q, \left\{(geom.y_\eta)_{i,j}\right\}_{i=0}^{N}, \left\{(geom.x_\eta)_{i,j}\right\}_{i=0}^{N}\right)$

**for** $i = 0$ **to** $N$ **do**

$\{J\dot{W}_{i,j,n}\}_{n=1}^{nEqn} \leftarrow \{J\dot{W}_{i,j,n}\}_{n=1}^{nEqn} + \frac{1}{\omega_i} * \left\{d\tilde{\bar{F}}_{i,n}\right\}_{n=1}^{nEqn}$

$\{J\dot{W}_{0,j,n}\}_{n=1}^{nEqn} \leftarrow \{J\dot{W}_{0,j,n}\}_{n=1}^{nEqn} - \frac{1}{\omega_0}\left(\left\{\tilde{F}^{*,es}_{j,n,4}\right\}_{n=1}^{nEqn} - \left\{\tilde{F}_{0,n}\right\}_{n=1}^{nEqn}\right)$

$\{J\dot{W}_{N,j,n}\}_{n=1}^{nEqn} \leftarrow \{J\dot{W}_{N,j,n}\}_{n=1}^{nEqn} + \frac{1}{\omega_N}\left(\left\{\tilde{F}^{*,es}_{j,n,2}\right\}_{n=1}^{nEqn} - \left\{\tilde{F}_{N,n}\right\}_{n=1}^{nEqn}\right)$

$\{J\dot{W}_{0,j,2}\} \leftarrow \{J\dot{W}_{0,j,2}\} + \frac{g}{2\omega_0}(geom.y_\eta)_{0,j} * [\![b]\!]_{j,4} * \{\{h\}\}_{j,4}$

$\{J\dot{W}_{0,j,3}\} \leftarrow \{J\dot{W}_{0,j,3}\} - \frac{g}{2\omega_0}(geom.x_\eta)_{0,j} * [\![b]\!]_{j,4} * \{\{h\}\}_{j,4}$

$\{J\dot{W}_{N,j,2}\} \leftarrow \{J\dot{W}_{N,j,2}\} + \frac{g}{2\omega_N}(geom.y_\eta)_{N,j} * [\![b]\!]_{j,2} * \{\{h\}\}_{j,2}$

$\{J\dot{W}_{N,j,3}\} \leftarrow \{J\dot{W}_{N,j,3}\} - \frac{g}{2\omega_N}(geom.x_\eta)_{N,j} * [\![b]\!]_{j,2} * \{\{h\}\}_{j,2}$

`// η-direction`

**for** $i = 0$ **to** $N$ **do**

$\left\{\tilde{G}_{0,n}\right\}_{n=1}^{nEqn} \leftarrow -(geom.y_\xi)_{i,0} * xFlux\left(\{W_{i,0,n}\}_{n=1}^{nEqn}\right) + (geom.x_\xi)_{i,0} * yFlux\left(\{W_{i,0,n}\}_{n=1}^{nEqn}\right)$

$\left\{\tilde{G}_{N,n}\right\}_{n=1}^{nEqn} \leftarrow -(geom.y_\xi)_{i,N} * xFlux\left(\{W_{i,N,n}\}_{n=1}^{nEqn}\right) + (geom.x_\xi)_{i,N} * yFlux\left(\{W_{i,N,n}\}_{n=1}^{nEqn}\right)$

$\left\{d\tilde{\bar{G}}_{j,n}\right\}_{j=0,n=1}^{N+1,nEqn} \leftarrow HighOrder\text{-}yFluxDifference\left(\left\{W_{i,j,n}\right\}_{j=0,n=1}^{N,nEqn}, Q, \left\{(geom.y_\xi)_{i,j}\right\}_{j=0}^{N}, \left\{(geom.x_\xi)_{i,j}\right\}_{j=0}^{N}\right)$

**for** $j = 0$ **to** $N$ **do**

$\{J\dot{W}_{i,j,n}\}_{n=1}^{nEqn} \leftarrow \{J\dot{W}_{i,j,n}\}_{n=1}^{nEqn} + \frac{1}{\omega_j} * \left\{d\tilde{\bar{G}}_{j,n}\right\}_{n=1}$

$\{J\dot{W}_{i,0,n}\}_{n=1}^{nEqn} \leftarrow \{J\dot{W}_{i,0,n}\}_{n=1}^{nEqn} - \frac{1}{\omega_0}\left(\left\{\tilde{G}^{*,es}_{i,n,1}\right\}_{n=1}^{nEqn} - \left\{\tilde{G}_{0,n}\right\}_{n=1}^{nEqn}\right)$

$\{J\dot{W}_{i,N,n}\}_{n=1}^{nEqn} \leftarrow \{J\dot{W}_{i,N,n}\}_{n=1}^{nEqn} + \frac{1}{\omega_N}\left(\left\{\tilde{G}^{*,es}_{i,n,3}\right\}_{n=1}^{nEqn} - \left\{\tilde{G}_{N,n}\right\}_{n=1}^{nEqn}\right)$

$\{J\dot{W}_{i,0,2}\} \leftarrow \{J\dot{W}_{i,0,2}\} - \frac{g}{2\omega_0}(geom.y_\xi)_{i,0} * [\![b]\!]_{i,1} * \{\{h\}\}_{i,1}$

$\{J\dot{W}_{i,0,3}\} \leftarrow \{J\dot{W}_{i,0,3}\} + \frac{g}{2\omega_0}(geom.x_\xi)_{i,0} * [\![b]\!]_{i,1} * \{\{h\}\}_{i,1}$

$\{J\dot{W}_{i,N,2}\} \leftarrow \{J\dot{W}_{i,N,2}\} - \frac{g}{2\omega_N}(geom.y_\xi)_{i,N} * [\![b]\!]_{i,3} * \{\{h\}\}_{i,3}$

$\{J\dot{W}_{i,N,3}\} \leftarrow \{J\dot{W}_{i,N,3}\} + \frac{g}{2\omega_N}(geom.x_\xi)_{i,N} * [\![b]\!]_{i,3} * \{\{h\}\}_{i,3}$

**for** $i = 0$ **to** $N$ **do**

**for** $j = 0$ **to** $N$ **do**

$\{J\dot{W}_{i,j,n}\}_{n=1}^{nEqn} \leftarrow -\left(\{J\dot{W}_{i,j,n}\}_{n=1}^{nEqn} + g * W_{i,j,1} * \{db_{i,j,n}\}_{n=1}^{nEqn}\right)$

**Output**: $\{J\dot{W}_{i,j,n}\}_{i=0,j=0,n=1}^{N,N,nEqn}$

**End Procedure** ESDG2DTimeDerivative

## References


[1] G.B. Whitham, Linear and Nonlinear Waves, John Wiley and Sons, New York, 1974.
[2] L.C. Evans, Partial Differential Equations, American Mathematical Society, 2012.
[3] U.S. Fjordholm, S. Mishra, E. Tadmor, Well-balanced and energy stable schemes for the shallow water equations with discontinuous topography, J. Comput. Phys. 230 (14) (2011) 5587–5609.
[4] Y. Xing, Exactly well-balanced discontinuous Galerkin methods for the shallow water equations with moving water equilibrium, J. Comput. Phys. A 257 (2014) 536–553.
[5] E. Audusse, F. Bouchut, M.-O. Bristeau, R. Klein, B. Perthame, A fast and stable well-balanced scheme with hydrostatic reconstruction for shallow water flows, SIAM J. Sci. Comput. 25 (6) (2004) 2050–2065.
[6] R.J. LeVeque, Balancing source terms and flux gradients in high-resolution Godunov methods: the quasi-steady wave-propagation algorithm, J. Comput. Phys. 146 (1) (1998) 346–365.
[7] A. Chertock, M. Dudzinski, A. Kurganov, M. Lukácová-Medvid'ová, Well-balanced schemes for the shallow water equations with Coriolis forces, in: ECMI 2014 28 Mini-Symposium on Spacetime Models of Gravity in Geolocation and Acoustics, 2014, p. 496.
[8] G.J. Gassner, A.R. Winters, D.A. Kopriva, A well balanced and entropy conservative discontinuous Galerkin spectral element method for the shallow water equations, Appl. Math. Comput. 272 (2016) 291–308.
[9] M. Carpenter, T. Fisher, E. Nielsen, S. Frankel, Entropy stable spectral collocation schemes for the Navier–Stokes equations: discontinuous interfaces, SIAM J. Sci. Comput. 36 (5) (2014) B835–B867.
[10] D.A. Kopriva, G.J. Gassner, An energy stable discontinuous Galerkin spectral element discretization for variable coefficient advection problems, SIAM J. Sci. Comput. 36 (4) (2014) 2076–2099.
[11] M.L. Merriam, An Entropy-Based Approach to Nonlinear Stability, NASA Technical Memorandum 101086 (64), 1989, pp. 1–154.
[12] E. Tadmor, Entropy stability theory for difference approximations of nonlinear conservation laws and related time-dependent problems, Acta Numer. 12 (2003) 451–512.
[13] E. Tadmor, Numerical viscosity and the entropy condition for conservative difference schemes, Math. Comput. 43 (1984) 369–381.
[14] T. Fisher, M. Carpenter, J. Nordström, N.K. Yamaleev, C. Swanson, Discretely conservative finite-difference formulations for nonlinear conservation laws in split form: theory and boundary conditions, J. Comput. Phys. 234 (2013) 353–375.
[15] G. Gassner, A skew-symmetric discontinuous Galerkin spectral element discretization and its relation to SBP-SAT finite difference methods, SIAM J. Sci. Comput. 35 (3) (2013) A1233–A1253.
[16] G.J. Gassner, A kinetic energy preserving nodal discontinuous Galerkin spectral element method, Int. J. Numer. Methods Fluids 76 (1) (2014) 28–50.
[17] S. Nikkar, J. Nordström, Fully discrete energy stable high order finite difference methods for hyperbolic problems in deforming domains, J. Comput. Phys. 291 (2015) 82–98.
[18] D.A. Kopriva, Implementing Spectral Methods for Partial Differential Equations: Algorithms for Scientists and Engineers, 1st edition, Springer Publishing Company, Incorporated, 2009.
[19] T.C. Fisher, High-Order $l_2$ Stable Multi-Domain Finite Difference Method for Compressible Flows, Ph.D. Thesis, Purdue University, 2012.
[20] T.C. Fisher, M.H. Carpenter, High-order entropy stable finite difference schemes for nonlinear conservation laws: finite domains, J. Comput. Phys. 252 (2013) 518–557.
[21] D.A. Kopriva, Metric identities and the discontinuous spectral element method on curvilinear meshes, J. Sci. Comput. 26 (3) (2006) 301–327.
[22] J.S. Hesthaven, T. Warburton, Nodal Discontinuous Galerkin Methods: Algorithms, Analysis, and Applications, Springer-Verlag, New York, 2008.
[23] D. Kopriva, G. Gassner, On the quadrature and weak form choices in collocation type discontinuous Galerkin spectral element methods, J. Sci. Comput. 44 (2) (2010) 136–155.
[24] H.-O. Kreiss, J. Olliger, Comparison of accurate methods for the integration of hyperbolic equations, Tellus 24 (1972) 199–215.
[25] H.-O. Kreiss, G. Scherer, Finite element and finite difference methods for hyperbolic partial differential equations, in: Mathematical Aspects of Finite Elements in Partial Differential Equations, Academic Press, 1974, pp. 195–212.
[26] G.A. Blaisdell, E.T. Spyropoulos, J.H. Qin, The effect of the formulation of nonlinear terms on aliasing errors in spectral methods, Appl. Numer. Math. 21 (3) (1996) 207–219.
[27] F. Ducros, F. Laporte, T. Soulères, V. Guinot, P. Moinat, B. Caruelle, High-order fluxes for conservative skew-symmetric-like schemes in structured meshes: application to compressible flows, J. Comput. Phys. 161 (2000) 114–139.
[28] C.A. Kennedy, A. Gruber, Reduced aliasing formulations of the convective terms within the Navier–Stokes equations for a compressible fluid, J. Comput. Phys. 227 (2008) 1676–1700.
[29] J. Nordström, Conservative finite difference formulations, variable coefficients, energy estimates and artificial dissipation, J. Sci. Comput. 29 (3) (2006) 375–404.
[30] G.J. Gassner, A.R. Winters, D.A. Kopriva, Split form nodal discontinuous Galerkin schemes with summation-by-parts property for the compressible Euler equations, J. Comput. Phys. 327 (2016) 39–66.
[31] M. Carpenter, C. Kennedy, Fourth-Order 2$N$-Storage Runge–Kutta Schemes, Tech. Rep. NASA TM 109112, NASA Langley Research Center, 1994.
[32] V.R. Ambati, O. Bokhove, Space–time discontinuous Galerkin discretization of rotating shallow water equations, J. Comput. Phys. 225 (2) (2007) 1233–1261.
[33] P.A. Tassi, O. Bokhove, C.A. Vionnet, Space discontinuous Galerkin method for shallow water flows—kinetic and HLLC flux, and potential vorticity generation, Adv. Water Resour. 30 (4) (2007) 998–1015.
[34] J. Pedlosky, Geophysical Fluid Dynamics, Springer, 1987.
[35] P. Persson, J. Peraire, Sub-cell shock capturing for discontinuous Galerkin methods, AIAA J. 112, http://dx.doi.org/10.1007/978-1-4612-4650-3.